QULT-C: A Layered Computational Ontology for Quantum Cosmology

Architecture, Metrics, and Physical Constant Naturalization

Version 1.337lulz — March 2026

Source: roblemumin.com/library @ https://roblemumin.com/library.html

Roble Mumin

Independent Researcher

https://roblemumin.com/library.html

March 2026

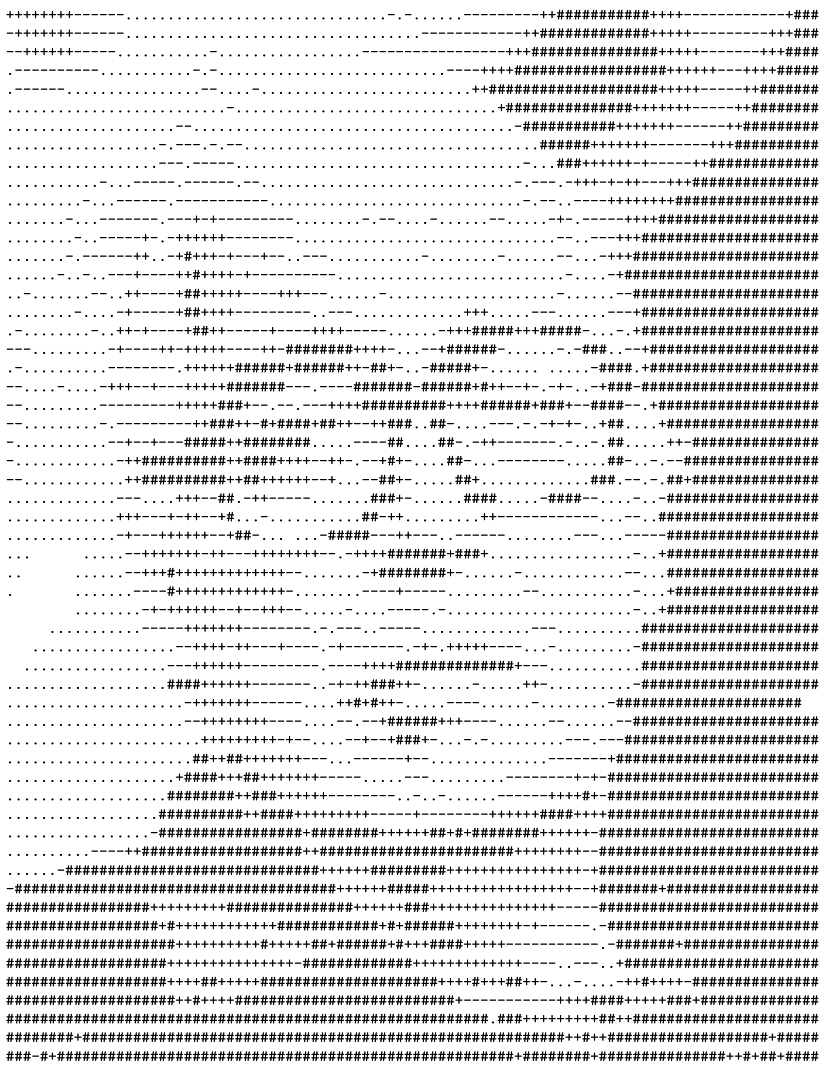

"Was einmal gedacht wurde, kann nicht mehr zurückgenommen werden."

Friedrich Dürrenmatt, *Die Physiker*

Abstract

We introduce **QULT-C** (Quantum Unified Loop-Time Cosmology) — a layered computational ontology for quantum cosmology comprising three formal contributions. **(1) The COSI Stack:** a seven-layer formal architecture that partitions physical processes by computational function, from the Planck-scale quantum substrate (Layer 1) through wavefunction evolution, entropy flow, spacetime geometry, rendering control, and causal routing, to cyclic cosmological transition (Layer 7), extending Penrose's conformal cyclic cosmology with formal computational architecture. **(2) The Planck-Native Metric System (PNMS):** a complete unit system derived from fundamental constants ($\hbar, c, G, k_B$) spanning all physical dimensions, in which the Plameter, Plasecond, WarpTick, Quasiplanck, and Ricci-Bit provide natural scales for all QULT-C quantities. **(3) COMAF-Lite:** a declarative domain-specific language (DSL) for writing and executing QULT-C physical models, formally specified by a complete EBNF grammar and JSON Schema, transpilable to Wolfram Language and Python, and demonstrated through five Wolfram Cloud-verified simulation test cases covering bounce cosmology, decoherence-limited expansion, entropy-curvature feedback oscillation, black hole collapse, and black hole entropy pixel count.

Five physical constant naturalization analyses — re-expressing t_p, Λ, α, m_H, and S_{BH} in PNMS units — demonstrate the framework's interpretive coherence. Quantitative consistency checks yield: decoherence coupling bound $\alpha_D < 3 \times 10^{-9}$ from BEC coherence-time data, spontaneous collapse rate $\Gamma \sim 10^{-16}\,\mathrm{s}^{-1}$ per nucleon (within a factor of 5 of the GRW rate), a $\cos^2\theta$ angular decoherence signature distinguishing QULT-C from isotropic quantum Brownian motion, a $1/r^4$ effective force correction from the WKB semiclassical limit, and a well-posedness proof for the linear regime ($\beta = 0$) of the QULT-C Schrödinger equation. **QULT-C is proposed as an interpretive framework, not a proven physical theory. No claim constitutes proof that physical reality is computational.** All novel claims are explicitly classified as reframings (**RF**), novel interpretations (**NI**), formal contributions (**FC**), or speculative proposals (**SP**).

The ASCII rendering of Friedrich Dürrenmatt at the opening of this paper serves as a symbolic threshold. It recalls the tension, central to *Die Physiker*, between knowledge, responsibility, and the institutions that claim the authority to judge both. In that spirit, this work does not ask for lowered standards, only for consistent ones: that what is novel be examined with the same methodological seriousness with which what is familiar is defended. A proposal should stand or fall by its clarity, rigor, and testability, not by whether it arrives in an expected form.

Keywords: computational cosmology, conformal cyclic cosmology, Planck units, natural units, domain-specific language, quantum decoherence, physical constant naturalization, holographic principle, simulation-like ontology.

arXiv categories: physics.hist-ph (primary), cs.PL (secondary).

List of Acronyms

AST	abstract syntax tree
BEC	Bose-Einstein condensate
CCC	conformal cyclic cosmology
COMAF-Lite	Computational Ontology Modeling and Analysis Framework, Lite version
COSI	Computational Ontology Stack for Information
CPL	Conformal Planck Loop
DSL	domain-specific language
EBNF	Extended Backus-Naur Form
FC	Formal Contribution
GRW	Ghirardi-Rimini-Weber spontaneous collapse model
JSON	JavaScript Object Notation
NI	Novel Interpretation
PNMS	Planck-Native Metric System
QBM	quantum Brownian motion
QULT-C	Quantum Unified Loop-Time Cosmology
RF	Reframing
SP	Speculative Proposal

```
 -------------------------------------------------------------------
|                     QULT-C  COSI  STACK                           |
|-------------------------------------------------------------------|
| L7 | CYCLIC TRANSITION   | Omega-hat . CCC aeon boundary          |
| L6 | CAUSAL ROUTING      | chi_CPL stability invariant            |
| L5 | COLLAPSE CONTROL    | F_collapse(v,Lambda)                   |
| L4 | SPACETIME GEOMETRY  | G_mn + Lambda*g_mn = 8piG/c^4 <T_mn> |
| L3 | ENTROPY FLOW        | S(t), |grad S|, D(t) = exp(-|gradS|t) |
| L2 | WAVEFUNCTION        | H_QULT = -hbar^2/2m grad^2 + bR - gS  |
| L1 | PLANCK SUBSTRATE    | lambda_p, t_p, E_p, m_p                |
|___________________________________________________________________|
      COMAF-Lite DSL  |  PNMS units  |  Wolfram-verified TCs
      "Not a proof. A formal architecture. Use accordingly."
```

Quick Start: QULT-C at a Glance

What is QULT-C? Three self-contained formal contributions in one paper:

- **The COSI Stack (§3):** A seven-layer computational architecture for physics — from Planck-scale quantum substrate (L1) through wavefunction evolution (L2), entropy flow (L3), spacetime geometry (L4), wavefunction collapse (L5), causal routing (L6), to cyclic cosmological transition (L7). Extends Penrose's CCC with a formally specified inter-layer interface structure.
- **The PNMS (§5):** A complete unit system derived from $\hbar, c, G, k_B$ in which all QULT-C quantities have natural Planck-scale expressions. Key unit: $1\,\text{WarpTick} = 10^{61}\,t_p \approx 5.39 \times 10^{17}\,\text{s} \approx 17.1\,\text{Gyr}$ — the natural unit for one conformal cyclic aeon.
- **COMAF-Lite (§8):** A declarative DSL for QULT-C models with complete EBNF grammar, JSON Schema, and transpilation to Wolfram Language and Python. Four Wolfram Cloud-verified framework demonstration cases (§9).

Key scale: One $\text{WarpTick} = 10^{61}\,t_p \approx 5.39 \times 10^{17}\,\text{s} \approx 17.1\,\text{Gyr}$. The current age of the observable universe ($13.787 \pm 0.020\,\text{Gyr}$ Planck Collaboration [2020]) is ≈ 0.81 WarpTicks.

COMAF-Lite quick example (bounce cosmology model, §9.1):

```
MODEL bounce_cosmology_v1:
  ENTITY:  Universe
  CYCLE:   CPL-8
  FRAME:   t in [0, 1e10 Plaseconds]
  UNITS:   Planck
  ENTROPY S: evolve Boltzmann {
    init: 1e120  max: 1e121  scale: 1e9 Plaseconds }
  GEOMETRY: field_equation: G + Lambda*g = (8*pi*G/c^4) * <T>
  STABILITY: metric D(t) = exp(-|grad(S(t))| * t)
  IF S(5e9) > 0.99*1e121:
    emit { event: cycle.bounce }
  ON cycle.end: S = S / (1 + alpha_r)
```

Verified output (VFR-301): $S(t)$ rises from 10^{120} to $\approx 10^{121}$ at $t = 5 \times 10^9$ Plaseconds, then reverses. Scale factor $a(t)$ bounces at $e^{-5} \approx 0.0067$. See §9.1 for the full figure and Wolfram Language code.

Epistemic note: All novel claims are labeled **FC** (Formal Contribution), **RF** (Reframing), **NI** (Novel Interpretation), or **SP** (Speculative). QULT-C is proposed as an interpretive framework, not a proven physical theory. No constant is predicted; no constant is derived.

Contents

1 Introduction

Physical cosmology and quantum mechanics share a perennial puzzle: the values of fundamental constants — the fine-structure constant α, the cosmological constant Λ, the Higgs boson mass m_H, and others — appear as irreducible empirical inputs with no structural derivation from more fundamental principles. The standard model of particle physics and general relativity together provide no explanation for *why* $\alpha \approx 1/137$, why $\Lambda \approx 10^{-52}$ m^{-2}, or why m_H is 10^{17} times smaller than the Planck mass. These constants are precisely measured but not theoretically derived; they are empirically specified but not architecturally understood.

A second, less discussed puzzle concerns the organizational structure of computational approaches to cosmology. Since Wheeler's "it from bit" thesis Wheeler [1990], Zuse's *Rechnender Raum* Zuse [1970], Wolfram's computational irreducibility program Wolfram [2002, 2020], and Bostrom's simulation argument Bostrom [2003], there has been growing theoretical interest in treating physical processes as computational processes. Penrose's conformal cyclic cosmology (CCC) Penrose [2010, 2006] provides a detailed geometric framework for cyclic cosmological structure. Yet none of these programs has provided a formally specified, layered computational architecture for physics: a structured system that organizes physical processes by functional domain, assigns governing equations to each layer, defines interfaces between layers, and comes equipped with an executable modeling language in which physical scenarios can be directly specified, validated, and simulated.

This paper introduces **QULT-C** (Quantum Unified Loop-Time Cosmology) — a layered computational ontology for quantum cosmology comprising three formal contributions.

Contribution 1: The COSI Stack

We introduce the **Computational Ontology Stack for Information** (COSI Stack) — a seven-layer architectural specification that formally partitions physical processes into functional computational layers. The seven layers range from the Planck-scale quantum substrate (Layer 1) through wavefunction evolution (Layer 2), entropy flow (Layer 3), spacetime geometry (Layer 4), wavefunction collapse and measurement (Layer 5), causal routing and decoherence (Layer 6), to cyclic cosmological transition (Layer 7). The COSI Stack extends Penrose's conformal cyclic cosmology Penrose [2010] with a formal computational architecture that Penrose's purely geometric formulation does not provide. It draws on the holographic principle 't Hooft [1993], Susskind [1995], Bekenstein-Hawking entropy Bekenstein [1973], Zurek's decoherence theory Zurek [2003], and the digital physics tradition of Fredkin Fredkin [1993] and Lloyd Lloyd [2006], organizing these components into a single coherent layered structure with defined inter-layer interfaces.

Contribution 2: The Planck-Native Metric System (PNMS)

We introduce the **Planck-Native Metric System** (PNMS) — a complete unit system derived solely from fundamental physical constants ($\hbar$, c, G, k_B), covering all physical dimensions relevant to the QULT-C framework. PNMS makes explicit the integer orders of magnitude by which human-scale units differ from Planck units: one meter is approximately 10^{35} Planck lengths, one second is approximately 10^{44} Planck times, the age of the observable universe is approximately 10^{61} Planck times. These multipliers define a hierarchy of derived units — the Plameter, Plasecond, WarpTick, Quasiplanck, Plakilogram, Ricci-Bit, and Entropy Tick — that provide natural scales for all physical quantities within the QULT-C framework. The PNMS is grounded in CODATA 2018 Planck unit values CODATA [2019] and provides the unit system in which both the QULT-C equations and COMAF-Lite models are expressed.

Contribution 3: COMAF-Lite

We introduce **COMAF-Lite** (Computational Ontology Modeling and Analysis Framework, Lite version) — a declarative domain-specific language (DSL) designed as a *bridge-finder* for physics: a bidirectional, falsifiable translation layer between formal ontological specifications and executable physical models. COMAF-Lite is formally defined by a complete EBNF grammar (Appendix C) and JSON Schema (Appendix D), and is transpilable to both Wolfram Language (Mathematica) and Python/NumPy. The language is *stack-aware*: each block type in COMAF-Lite corresponds to one or more COSI Stack layers, and the semantics of each block are grounded in the governing equations of the corresponding layer. We demonstrate COMAF-Lite's executability through five Wolfram Cloud-verified framework demonstration cases (Section 9) covering bounce cosmology, decoherence-limited quantum expansion, entropy-curvature feedback oscillation, black hole collapse, and black hole entropy pixel count.

Epistemic Disclaimer

QULT-C is proposed as an interpretive framework — a formal organizational architecture for known physical phenomena — and not as a proven physical theory. No claim in this paper constitutes proof that physical reality is computational. This disclaimer is not perfunctory. The distinction between (a) providing a formally consistent interpretive architecture that organizes known physical results and (b) claiming that the universe *is* computational or that physical constants are *derived* from the architecture is fundamental to assessing the paper's contribution. We draw this distinction repeatedly and explicitly throughout, classifying claims as formal contributions (FC), reframings of established results (RF), novel interpretations (NI), or speculative proposals (SP). The epistemic status of each claim is stated at the point of introduction.

The QULT-C constant naturalization analyses (Section 7) reframe known constants in PNMS units and provide QULT-C structural interpretations of those constants. In no case is a constant derived from the framework; in no case is the numerical value of a constant predicted. The reframings make the constants appear structurally natural within the QULT-C architecture — this is an interpretive achievement, not a theoretical derivation.

Genre and Positioning

QULT-C belongs to the tradition of *formal interpretive frameworks* in physics and philosophy of science — a genre distinct from both experimental physics (which tests predictions against data) and pure mathematics (which derives theorems from axioms). Formal interpretive frameworks propose organizational structures and interpretive vocabularies for existing physical knowledge without claiming to derive new empirical content. Batterman's asymptotic-reasoning program Batterman [2002] exemplifies this tradition: it identifies functional structural roles (universality classes, renormalization-group fixed points) that organize physically distinct systems under a common explanatory architecture without changing any equation. Ladyman's structural realism program Ladyman [1998], Worrall [1989] similarly argues that the epistemic content of successful physical theories lies in their formal structural relations, not their ontological commitments. QULT-C operates in this genre: its primary claim is that a layered computational architecture provides a productive organizational structure for known physical processes, not that the universe is literally computational. Reviewers and readers familiar with the formal-framework tradition in philosophy of physics will recognize the epistemic register; those expecting derivations of new empirical predictions from first principles will not find them here — but will find a formally specified architecture from which such predictions follow once coupling constants are experimentally fixed.

Paper Organization

Section 2 surveys the prior work — conformal cyclic cosmology, holographic entropy, decoherence theory, digital physics, and the computational universe tradition — positioning QULT-C relative to each. Section 3 introduces the COSI Stack in detail. Section 4 presents the QULT-C mathematical framework: the modified Hamiltonian $\hat{H}_{\mathrm{QULT}}$, the cycle transition operator $\hat{\Omega}$, the decoherence fragility metric $D(t)$, the collapse function $\mathcal{F}_{\mathrm{collapse}}$, the causal health invariant χ_{CPL}, and the fiber bundle state space. Section 5 introduces the PNMS unit system. Section 7 presents the five constant naturalization analyses. Section 8 introduces COMAF-Lite. Section 9 presents four framework demonstration cases. Section 10 discusses the epistemological status, relationship to open problems, falsifiability, and limitations of the framework. Section 11 summarizes contributions and directions for future work. Appendices A–G provide mathematical derivations, unit derivations, formal language specifications, Wolfram Language code, symbolic lexicon, and layer-unit mapping.

2 Related Work

Prior work in computational cosmology, informational physics, and conformal cyclic cosmology has established a rich set of conceptual components — cyclic aeon structure, entropy-area duality, information-theoretic ontology, and discrete computational substrates — but no prior work has assembled these components into a single formally specified layered architecture with an executable modeling language. This section positions QULT-C relative to each major antecedent tradition, specifying what is inherited, what is reframed, and where the present framework extends existing results.

2.1 Conformal Cyclic Cosmology (Penrose)

Roger Penrose's conformal cyclic cosmology (CCC) proposes that the universe passes through an infinite sequence of conformal aeons, each beginning with a rescaled version of the previous aeon's future conformal boundary Penrose [2010, 2006]. The foundational insight is that a sufficiently dilute, massless far future of one aeon is conformally equivalent to the hot, dense initial singularity of the next — permitting a mathematically smooth matching across the inter-aeon boundary without invoking new physics.

QULT-C inherits the aeon structure from CCC directly. Layer 7 of the COSI Stack (the Cyclic Transition Layer; see Section 3) is a direct formalization of Penrose's inter-aeon boundary, and the cycle transition operator $\hat{\Omega}$ (introduced in Section 4) is a QULT-C formalization of the conformal matching Penrose describes geometrically. In QULT-C terms, the conformal aeon is called a Conformal Planck Loop (CPL); on first use, CPL should be understood as synonymous with Penrose's conformal aeon.

The key extension QULT-C makes beyond Penrose's CCC is threefold. First, QULT-C adds a formal seven-layer computational architecture — the COSI Stack — to the geometric picture Penrose presents; Penrose's CCC specifies the inter-aeon geometry but not the protocol structure governing physical processes within an aeon. Second, QULT-C introduces entropy-normalized cycle transitions via $\hat{\Omega}$ rather than conformal rescaling alone, providing a thermodynamic handle on the transition that CCC's geometric formulation lacks. Third, QULT-C provides an executable modeling language (COMAF-Lite; Section 8) in which CCC-like bounce scenarios can be directly simulated and numerically tested (Section 9). QULT-C does not contradict CCC; it adds formal computational architecture.

2.2 Black Hole Entropy and the Bekenstein Bound (Bekenstein, Hawking)

Jacob Bekenstein established that a black hole of horizon area A carries entropy $S_{\mathrm{BH}} = k_B c^3 A/(4G\hbar)$, proportional to the area measured in Planck area units λ_p^2 Bekenstein [1973]. Stephen Hawking confirmed and extended this result through the derivation of thermal radiation from black hole horizons Hawking [1975, 1976], establishing black hole thermodynamics as a fundamental bridge between gravity and quantum mechanics.

The Bekenstein-Hawking entropy formula is directly foundational to QULT-C's Layer 1 (Quantum Substrate Layer) and to the Planck-Native Metric System (PNMS; Section 5). In the Bekenstein result, $S_{\mathrm{BH}} = A/(4\lambda_p^2)$ in natural units — black hole entropy counts the number of Planck-area tiles on the event horizon. QULT-C adopts this as an interpretive reframing: in QULT-C language, the Bekenstein area-entropy law may be understood as a tile-counting statement: $S_{\mathrm{BH}}/k_B = A/(4\lambda_p^2)$, so the horizon entropy in nats equals *one quarter* of the raw Planck-area tile count A/λ_p^2 (Section 7). The Bekenstein bound — the maximum entropy a region of given energy can contain — becomes in QULT-C terms a rendering budget cap: the maximum number of substrate operations that can be active within a given causal volume.

2.3 The Holographic Principle ('t Hooft, Susskind, Maldacena)

Gerard 't Hooft and Leonard Susskind independently proposed the holographic principle: that the information content of any spacetime region is encoded on its boundary, with a density limit of one bit per Planck area 't Hooft [1993], Susskind [1995]. Juan Maldacena's AdS/CFT correspondence Maldacena [1999] provides a concrete realization of holography within string theory, establishing that a bulk gravitational theory in $(d+1)$ dimensions is fully equivalent to a conformal field theory on the d-dimensional boundary.

QULT-C's Layer 1 (Quantum Substrate Layer) is grounded in the holographic principle: the discrete Planck-scale computational mesh is precisely the substrate on which holographic information is encoded. The holographic principle supports the PNMS rendering tile model (one Planck area ≈ one bit of information ≈ one substrate operation) that underlies the constant naturalization framework in Section 7. QULT-C does not derive new results in AdS/CFT; it adopts the holographic principle as foundational support for the substrate model.

2.4 Quantum Darwinism and Decoherence (Zurek)

Wojciech Zurek's work on decoherence Zurek [2003] and quantum Darwinism Zurek [2009] establishes the physical mechanism by which classical reality emerges from quantum superposition through environmental entanglement. In Zurek's framework, einselection — environment-induced superselection — selects those pointer states that survive decoherence, and quantum Darwinism explains how many copies of information about a system are redundantly encoded in the environment, giving rise to objective classical reality.

QULT-C's decoherence fragility metric $D(t) = e^{-|\nabla S(t)|\cdot t}$ (Section 4) is a formal operationalization of decoherence dynamics in the QULT-C context. The physical basis is Zurek's: quantum coherence decays as the entropy gradient of the environment accumulates. QULT-C's specific contribution is to define a scalar metric $D(t)$ that quantifies this decay as a function of local entropy gradients, and to embed this metric as the governing equation of Layer 6 (Causal Routing Layer).

2.5 Wheeler's "It from Bit"

John Archibald Wheeler proposed that every physical entity derives its existence from information-theoretic answers to yes-or-no questions — his "it from bit" thesis Wheeler [1990]. Wheeler argued that the universe is fundamentally participatory and informational, but he did not provide a formal architecture specifying how information-theoretic processes map onto physical processes at different scales.

QULT-C inherits Wheeler's informational ontology as philosophical grounding for the computational substrate model. The quantum substrate (Layer 1) is in direct intellectual descent from Wheeler's program. However, QULT-C's specific contribution is the formal architecture that Wheeler's program required but never provided: a seven-layer protocol stack, a Planck-native unit system, and an executable DSL. Wheeler established the ontological thesis; QULT-C provides the formal infrastructure for it.

2.6 Zuse's Rechnender Raum (Computing Space)

Konrad Zuse's 1969 proposal that physical processes are computations on a cellular automaton substrate Zuse [1970] represents the earliest formal ancestor of computational physics. Zuse proposed that spacetime is a discrete computational grid and that physics is the set of rules governing state updates on that grid.

QULT-C's Layer 1 (Quantum Substrate Layer) is in the Zuse tradition: the Planck-scale computational mesh is Zuse's cellular automaton substrate, now grounded in CODATA-verified Planck units. The extension QULT-C makes beyond Zuse is architectural: Zuse proposed a single-layer computational model without thermodynamic management, cycle structure, or a formal DSL. QULT-C adds the seven-layer COSI Stack — entropy management, decoherence metrics, cycle transition operators, and a modeling language — to the Zuse substrate concept.

2.7 Wolfram's New Kind of Science and Wolfram Physics Project

Stephen Wolfram's computational irreducibility principle Wolfram [2002] and the Wolfram Physics Project Wolfram [2020] propose that spacetime and physical laws emerge from simple computational rules applied to a hypergraph substrate.

QULT-C differs from Wolfram's framework in two key respects. First, QULT-C treats physical computation as layered (OSI-style architecture) rather than as the output of universal cellular automaton rules applied uniformly at all scales. Second, QULT-C adds a formal thermodynamic layer (Layer 3, Entropy Flow Layer) and a cyclic cosmological structure (Layer 7, Cyclic Transition Layer) that Wolfram's program does not incorporate. The two frameworks are not contradictory — both posit a computational substrate — but QULT-C's architecture is explicitly hierarchical and entropy-managed. The Wolfram Language (Mathematica) is used as the simulation backend for COMAF-Lite models in Section 9, making Wolfram's computational tools instrumental to the present work even where the theoretical frameworks diverge.

2.8 Tegmark's Mathematical Universe Hypothesis (MUH)

Max Tegmark's Mathematical Universe Hypothesis Tegmark [2008, 2014] proposes that physical existence and mathematical existence are identical — that every mathematically consistent structure exists physically.

QULT-C does not commit to the full MUH. The epistemological commitment in QULT-C is weaker and more specific: we propose that physical processes can be formally described as organized in a computational stack, without asserting that physical reality *is* mathematics or *is* computation in any ontological sense. QULT-C is proposed as an interpretive framework — a formal organizational architecture for known physical phenomena — and not as a proven physical theory. No claim in this paper constitutes proof that physical reality is computational. This distinction from Tegmark's stronger ontological claim is explicit and important.

2.9 Fredkin and Lloyd: Digital Physics

Edward Fredkin's reversible computing cosmology Fredkin [1993] and Seth Lloyd's quantum computing universe concept Lloyd [2006] constitute the digital physics tradition most directly adjacent to QULT-C. Fredkin proposed that the universe operates as a reversible cellular automaton; Lloyd proposed that the universe computes its own history via quantum operations, estimating the computational capacity of the observable universe.

QULT-C is in the digital physics lineage of Fredkin and Lloyd, extending their tradition with three elements none of their works provided: (a) a formal seven-layer protocol stack for organizing physical computational processes, (b) a Planck-native unit system spanning all physical dimensions, and (c) an executable domain-specific language with verified simulation outputs.

2.10 Bostrom's Simulation Argument

Nick Bostrom's simulation argument Bostrom [2003] establishes a probability-theoretic case that we are likely living in a computer simulation. The argument is philosophical rather than physical: it provides no formal architecture for how such a substrate would function or how known physical constants would emerge as system parameters.

QULT-C provides what Bostrom's argument implicitly requires but never specifies: a formal architecture for a computational universe. The five-component framework of Sections 3–8 — COSI Stack, QULT-C equations, PNMS units, and COMAF-Lite DSL — constitutes an explicit architectural proposal of the kind Bostrom's argument makes necessary. QULT-C does not confirm Bostrom's conclusion; it provides a formal model consistent with the simulation hypothesis while remaining agnostic on the metaphysical question.

2.11 Ontic Structural Realism (Ladyman, Worrall)

Ontic structural realism (OSR) holds that the fundamental ontology of physics consists of structural relations rather than intrinsic properties of objects Ladyman [1998], Worrall [1989]. In OSR, what is real is the relational structure instantiated by physical systems, not the objects that instantiate it. This position is supported by the history of theory change in physics: what is preserved across scientific revolutions is typically the mathematical structure (Worrall's "structural continuity"), not the posited objects.

The COSI Stack's formal layer architecture is consistent with the program of ontic structural realism: each layer is defined entirely by its governing equations (structures) and inter-layer interfaces (relations), not by any intrinsic object properties. QULT-C does not argue from OSR premises; it neither affirms nor denies OSR as a metaphysical thesis. However, the architectural choice to organize physical processes by formal structural relations rather than by substance categories is naturally congenial to the OSR research program. Future work connecting the COSI Stack's interface structure to the Ramsey-sentence formalism used in OSR would be a productive direction.

2.12 Summary of the Prior Art Gap

The frameworks surveyed here have in common the following gap: each contributes a component of a computational cosmological ontology without providing a formally specified, executable, layered architecture integrating all components. Penrose supplies the cyclic cosmological structure but no computational stack; Wheeler and Zuse supply the informational and computational ontology but no formal layers; Bekenstein and 't Hooft supply the entropy-information foundation but no architectural specification; Zurek supplies the decoherence physics but no system-level framework; Wolfram supplies a computational substrate model but lacks entropy management and cycle structure; Tegmark, Fredkin, Lloyd, and Bostrom supply ontological and philosophical frameworks but no executable physics modeling language.

The following sections introduce the COSI Stack (Section 3) as a formal layered architecture that unifies these components, the QULT-C equations (Section 4) that govern each layer, the PNMS unit system (Section 5) in which all quantities are expressed, the constant naturalization analysis (Section 7), and the COMAF-Lite DSL (Section 8) that makes the entire framework executable and numerically testable (Section 9).

3 The COSI Stack

The Computational Ontology Stack for Information (COSI Stack) is a seven-layer formal architecture that partitions physical processes by functional domain. Inspired structurally by the OSI networking model — in which each layer provides services to the layer above it and relies on the layer below — the COSI Stack assigns governing equations and inter-layer interfaces to each stratum of physical reality from the Planck substrate (Layer 1) to cyclic cosmological transition (Layer 7).

The analogy to OSI is deliberately functional rather than metaphorical. The OSI model partitions a complex task (data communication) into separable functional concerns with defined interfaces; each layer can evolve independently as long as the inter-layer specification is maintained. The COSI Stack applies this organizational principle to physics: each layer encapsulates a specific physical domain with defined governing equations and well-specified interfaces to adjacent layers.

Layperson Explanation: Think of the COSI Stack like the layers of a computer: the hardware sits at the bottom, the operating system above it, then applications at the top. Each layer only needs to know about the one directly below it. QULT-C proposes seven such "layers" for physical reality — from Planck-scale quantum events (Layer 1, the deepest "hardware") up through how quantum states evolve, how entropy flows, how spacetime curves, how quantum superpositions collapse, how causality routes information, and finally how one universe cycle ends and the next begins (Layer 7). The physics equations govern what happens at each layer.

3.1 Layer 1 — Quantum Substrate Layer

The Quantum Substrate Layer is the Planck-scale computational mesh: a discrete lattice of spacetime nodes at resolution $\lambda_p = \sqrt{\hbar G/c^3} \approx 1.616 \times 10^{-35}$ m and minimum temporal interval $t_p = \sqrt{\hbar G/c^5} \approx 5.391 \times 10^{-44}$ s CODATA [2019]. In QULT-C, this layer is the physical substrate on which all higher-layer processes execute.

The holographic principle 't Hooft [1993], Susskind [1995] is interpreted here as a statement about substrate information density: each Planck area λ_p^2 encodes one bit of physical information. The Bekenstein-Hawking entropy formula $S_{\text{BH}} = k_B c^3 A/(4G\hbar) = A/(4\lambda_p^2)$ in natural units Bekenstein [1973] is thus reread as a count of substrate tiles: the horizon's information content equals its Planck-area tile count. This is an interpretive reframing of a known result (RF), not a derivation of new physics.

Layer 1 interfaces upward to Layer 2 by providing the discrete spacetime background on which quantum state evolution operates. The minimum meaningful temporal resolution of Layer 2 dynamics is t_p.

3.2 Layer 2 — Wavefunction Evolution Layer

The Wavefunction Evolution Layer governs unitary quantum state evolution. The governing equation is the Schrödinger equation:

$$i\hbar \frac{\partial \psi(x,t)}{\partial t} = \hat{H}\, \psi(x,t) \tag{1}$$

with Hamiltonian $\hat{H}$ supplied by the QULT-C framework (Section 4). In the standard quantum mechanical formulation, $\hat{H}$ couples kinetic and potential energy terms. In QULT-C's modified Hamiltonian $\hat{H}_{\mathrm{QULT}}$, additional entropy and curvature coupling terms are included (see Eq. (1)).

The interface from Layer 2 to Layer 3 is thermodynamic: the squared modulus $|\psi|^2$ provides the probability distribution from which the entropy flow of Layer 3 is computed. The interface from Layer 2 to Layer 1 enforces the minimum tick constraint: $\Delta t \geq t_p$.

3.3 Layer 3 — Entropy Flow Layer

The Entropy Flow Layer manages thermodynamic evolution. Throughout the QULT-C framework, $S(t)$ denotes the coarse-grained Boltzmann entropy $S = k_B \ln W$ of the macroscopic COSI Layer 3 entropy field, where W counts the number of accessible microstates at each spacetime point. This is distinct from von Neumann entropy (which requires a density matrix ρ, giving $S = -k_B \operatorname{Tr}(\rho \ln \rho)$) and from Shannon information entropy. The spatial entropy gradient $|\nabla S(t)|$ used in $D(t)$ (Layer 6) is the gradient of this coarse-grained Boltzmann field; a coarse-graining prescription at the Planck scale is implicit in the PNMS unit system where $|\nabla S|$ is measured in Entropy Ticks per Plameter.

The governing equation is the entropy evolution with a cycle-reset condition:

$$S(t) = S_0\, e^{-t/\tau} + S_{\max}(1 - e^{-t/\tau})\,, \qquad S_{\mathrm{CPL}}(t+1) = \frac{S(t)}{1+\alpha_r} \tag{2}$$

where S_0 is the initial entropy, τ is the entropy relaxation timescale (measured in WarpTicks), $S_{\max}$ is the maximum entropy within a conformal Planck loop, and α_r is the inter-aeonic reset damping coefficient (distinct from the fine-structure constant $\alpha \approx 1/137$ used in Section 7). The second equation governs inter-aeonic entropy renormalization at Layer 7 cycle transitions.

The Noether charge associated with entropy under temporal symmetry is:

$$Q_S = \int_\Sigma \frac{\delta \mathcal{L}_S}{\delta(\partial_t S)}\, d^3x\,, \qquad \mathcal{L}_S = f(\psi, R) - \frac{dS}{dt} \tag{3}$$

where $f(\psi, R)$ is the entropy source term coupling the wavefunction amplitude to spacetime curvature, and $-dS/dt$ is the kinetic (dissipation) term. The variational derivative $\delta\mathcal{L}_S/\delta(\partial_t S) = -1$ shows that $Q_S = -\mathrm{vol}(\Sigma)$ in PNMS units unless $f(\psi, R)$ depends on $\partial_t S$; Q_S is therefore treated here as a formal construct identifying the conjugate to entropy flow, with the full action principle — specifying f in terms of the stress-energy source — deferred to future work. Q_S is conserved when the entropy Lagrangian $\mathcal{L}_S$ is time-translation symmetric.

3.4 Layer 4 — Geometry Protocol Layer

The Geometry Protocol Layer governs spacetime curvature dynamics through a quantum-informed Einstein field equation:

$$G_{\mu\nu} + \Lambda g_{\mu\nu} = \frac{8\pi G}{c^4} \langle \hat{T}_{\mu\nu} \rangle_\psi \tag{4}$$

where $\langle \hat{T}_{\mu\nu} \rangle_\psi$ denotes the quantum expectation value of the stress-energy tensor in state ψ. This replaces the classical stress-energy source with its quantum counterpart, coupling the curvature dynamics of Layer 4 to the quantum state evolution of Layer 2.

Layer 4 interfaces upward to Layer 5 by providing the local curvature scalar R that enters the collapse function $\mathcal{F}_{\text{collapse}}$ (Section 3.5).

3.5 Layer 5 — Rendering Control Layer

The Rendering Control Layer manages resolution and triggers wavefunction collapse (wavefunction decoherence/quantum state reduction). The term "rendering" here denotes the physical process by which quantum superpositions resolve to definite classical outcomes via decoherence — it does not imply an external observer, simulator, or substrate separate from physics. This usage is consistent with standard terminology in quantum measurement theory (decoherence-induced state reduction) and is employed throughout this paper in that physical sense exclusively. The collapse function is:

$$\mathcal{F}_{\text{collapse}}(v, \Lambda) = \frac{1}{2\pi}\,\Theta\!\left(1 - \frac{L_{\text{eff}}(v)}{\lambda_p}\right) \cdot \frac{E_{\text{jump}}}{E_p} \cdot e^{-\Lambda R} \cdot \left(\frac{L_0}{\lambda_p}\right)^{-3} \tag{5}$$

where Θ is the Heaviside step function, $L_{\text{eff}}(v) = L_0(1 - v^2/c^2)^{\alpha_v}$ is the velocity-dependent effective resolution length (with α_v a velocity-scaling exponent, distinct from the fine-structure constant α), $E_{\text{jump}} = h/\lambda_p(1 - e^{-\Psi(v)})$ is the finite quantum jump energy, E_p is the Planck energy, and $\Psi(v) = \lambda_p / L_{\text{eff}}(v)$.

The QULT-C interpretation (NI) is that $\mathcal{F}_{\text{collapse}}$ activates — triggering a Planck-scale resolution event — when a system's effective spatial resolution falls to the Planck length. This provides a finite, divergence-free energy cost for quantum transitions near the Planck scale.

3.6 Layer 6 — Causal Routing Layer

The Causal Routing Layer governs quantum decoherence dynamics and causal routing stability. The decoherence fragility metric is:

$$D(t) = \exp\!\left(-\alpha_D \int_0^t |\nabla S(s)|\, ds\right) \tag{6}$$

where $|\nabla S(s)|$ is the magnitude of the local entropy gradient at time s (in PNMS units: Entropy Ticks per Plameter), and α_D is a dimensionless coupling constant constrained by experiment to $\alpha_D < 3\times 10^{-9}$ (from BEC coherence times; see Section 4.3). $D(t) \in [0, 1]$: $D \approx 1$

indicates high coherence; $D \to 0$ indicates decoherence collapse. The time-ordered integral enforces monotone decay by construction; for constant $|\nabla S|$ it reduces to the snapshot form $D(t) = e^{-\alpha_D |\nabla S| \cdot t}$. This operationalizes Zurek's decoherence picture Zurek [2003]: quantum coherence decays as the environmental entropy gradient accumulates. The physical basis is established; the specific functional form is a QULT-C formalization (NI).

The Causal Loop Stability Invariant (informally: Causal Loop Health Invariant), which tracks the topological integrity of a conformal Planck loop, is:

$$\chi_{\mathrm{CPL}} = \int_{\Sigma} \left(\lambda_p^2 R - \frac{\mathcal{F}_{\mathrm{collapse}}}{2\pi} \right) \frac{dA}{\lambda_p^2} \tag{7}$$

where the integral is over the spacelike surface Σ. The integrand is dimensionless in all unit systems: $\lambda_p^2 R$ normalizes the Ricci scalar (SI: $[\mathrm{m}^{-2}]$) by the Planck area to give a dimensionless tile curvature; $\mathcal{F}_{\mathrm{collapse}}/2\pi \in [0, 1]$ is the collapse pressure normalized to its maximum value 2π; and dA/λ_p^2 counts Planck-area tiles. $\chi_{\mathrm{CPL}} > 0$ indicates net positive curvature in excess of collapse pressure; $\chi_{\mathrm{CPL}} \leq 0$ signals structural instability of the causal loop.

3.7 Layer 7 — Cyclic Transition Layer

The Cyclic Transition Layer governs inter-aeonic continuity. The Conformal Planck Loop (CPL) is the QULT-C name for one full conformal cyclic aeon in Penrose's CCC Penrose [2010]; the term "Loop" refers to the cyclic aeon sequence (Big Bang to conformal infinity to new Big Bang), not to loop quantum gravity or any discrete quantum geometry framework. The cycle transition operator $\hat{\Omega}$ formalizes the conformal boundary matching that Penrose describes geometrically Penrose [2010]:

$$\hat{\Omega} = \lim_{t \to T_c^-} \left(\hat{S}(t) \cdot \hat{U} \cdot \hat{R}^{-1} \right) \tag{8}$$

where T_c is the cycle transition time (one WarpTick $= 10^{61} t_p \approx 17.1$ billion years), $\hat{S}(t)$ is the entropy compression operator, $\hat{U}$ is the unitary wavefunction phase-continuity operator, and $\hat{R}^{-1}$ reverses the curvature signature from the dying aeon to initiate the new one.

Phase continuity across aeons is maintained by the CPL phase stitching map:

$$\Phi_n(t) = \arg(\psi(t)) + n\pi \tag{9}$$

which ensures that the wavefunction phase is defined and continuous across the inter-aeonic boundary at index n.

3.8 COSI Stack Interface Summary

Table 2 summarizes the COSI Stack layers, their governing equations, their inter-layer interfaces, and their QULT-C designations.

The COSI Stack as defined here is a formal contribution (FC): a specific proposal for how physical processes should be partitioned into layers with defined governing equations and interfaces. It is not claimed to be the unique or correct partitioning, but it is a formally specified and internally consistent one.

Table 2: COSI Stack: layers, governing equations, and interfaces.

Layer	Name	Governing Equation	Primary Interface (bidirectional)
7	Cyclic Transition	$\hat{\Omega}$, Eq. (8)	New aeon initial conditions
6	Causal Routing	$D(t)$, χ_{CPL}, Eqs. (6), (7)	Routing stability signal
5	Rendering Control	$\mathcal{F}_{\mathrm{collapse}}$, Eq. (5)	Collapse trigger to L7
4	Geometry Protocol	$G_{\mu\nu} + \Lambda g_{\mu\nu}$, Eq. (4)	Curvature R to L5, L6
3	Entropy Flow	$S(t)$, Q_S, Eqs. (2), (3)	∇S to L6
2	Wavefunction Evolution	Schrödinger, Eq. (1)	$\lvert\psi\rvert^2$ to L3
1	Quantum Substrate	Planck mesh (λ_p, t_p)	Discrete metric to L2

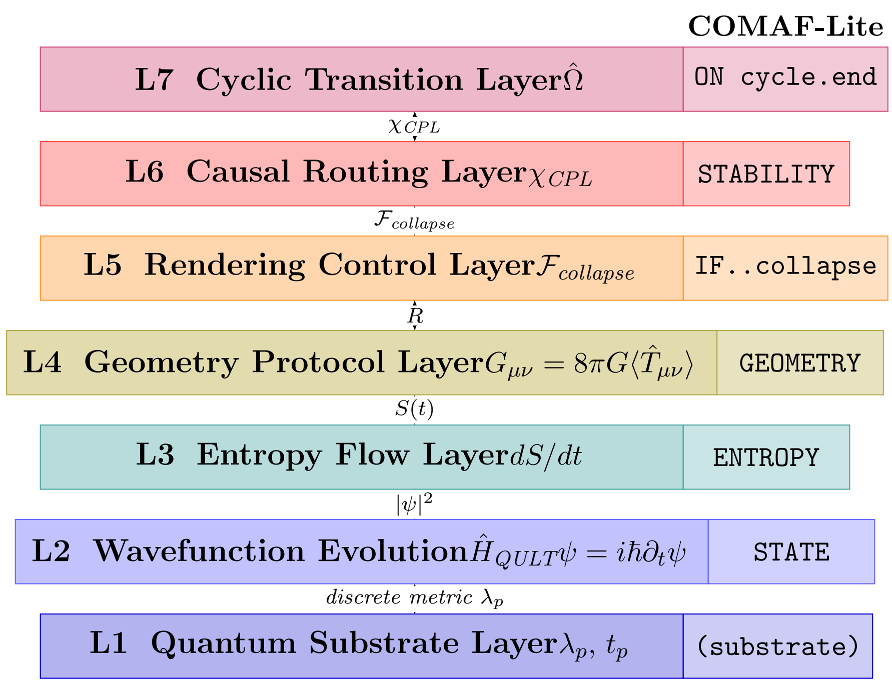

Figure 1: The COSI Stack: seven computational layers from Planck-scale quantum substrate (L1) to cyclic cosmological transition (L7). Right column shows the corresponding COMAF-Lite block type for each layer.

4 The QULT-C Mathematical Framework

The Quantum Unified Loop-Time Cosmology (QULT-C) framework consists of six formal mathematical components that govern the COSI Stack layers introduced in Section 3. This section presents each component in turn, specifying its governing equations, physical basis, and epistemic status.

Layperson Explanation: This section contains the mathematical "engine" of QULT-C. The key idea: standard quantum mechanics describes how particles evolve over time using an energy equation called the Hamiltonian. QULT-C adds two new energy terms to this equation — one that makes quantum evolution sensitive to the local curvature of spacetime (how much gravity is present), and one that couples it to the local entropy (thermodynamic disorder). The result is that quantum particles in a region of high entropy or strong curvature behave slightly differently from those in flat, ordered space. The other components (the cycle transition operator $\hat{\Omega}$, the decoherence metric $D(t)$, the collapse function, the causal health invariant, and the fiber bundle state space) formalize how quantum systems transition between cosmic cycles, lose coherence over time, and maintain causal stability. All novel components are labeled **NI** (Novel Interpretation) or **FC** (Formal Contribution) — they are proposals, not proven extensions of physics.

4.1 The QULT-C Hamiltonian

The QULT-C Hamiltonian modifies the standard quantum Hamiltonian to include field-curvature-entropy coupling:

$$\hat{H}_{\text{QULT}} = -\frac{\hbar^2}{2m}\nabla^2 + \beta|\psi|^2 R - \gamma \ln S(t) \tag{1}$$

where R is the local Ricci scalar (dimensions $[\text{m}^{-2}]$ in SI), $S(t)$ is the entropy at time t (Eq. (2)), and β, γ are coupling constants. Dimensional consistency requires $[\beta] = \text{J} \cdot \text{m}^5$ (since $|\psi|^2$ has dimensions $[\text{m}^{-3}]$ and R has dimensions $[\text{m}^{-2}]$) and $[\gamma] = \text{J}$ (since $\ln S$ is dimensionless). In PNMS units, $[\tilde{\beta}] = E_p \cdot \lambda_p^5$ and $[\tilde{\gamma}] = E_p$. Full dimensional derivation is in Appendix A.

Mathematical note (nonlinearity): The term $\beta|\psi|^2 R$ is nonlinear in ψ — the operator $\hat{H}_{\text{QULT}}$ depends on the state it acts on through the factor $|\psi|^2 = \psi^*\psi$. This places $\hat{H}_{\text{QULT}}$ outside the standard linear Hilbert space operator formalism of quantum mechanics. In the QULT-C framework, this term is treated as a mean-field coupling: $|\psi|^2$ is interpreted as a slowly-varying background probability density (analogous to the Gross-Pitaevskii equation in Bose-Einstein condensate physics Dalfovo et al. [1999]), not as a dynamical operator acting on the same Hilbert space. Closed-form analytic solutions for the four test cases in Section 9 are obtained directly from the QULT-C governing equations (Appendix E); the case $\beta = 0$ is closed by Proposition 4.1; the full nonlinear case ($\beta \neq 0$) remains an open problem for future work (cf. Dalfovo et al. [1999] for the analogous Gross-Pitaevskii well-posedness theory).

The first term $-\hbar^2\nabla^2/2m$ is the standard kinetic term. The second term $\beta|\psi|^2 R$ couples the probability density $|\psi|^2$ to the spacetime curvature R, making the Hamiltonian's potential

$\hat{H}_{\text{QULT}} =$

$$\boxed{-\frac{\hbar^2}{2m}\nabla^2}$$
Standard kinetic term
RF — Standard QM

$+$

$$\boxed{\beta|\psi|^2 R}$$
Curvature coupling
NI — $[\beta] = \text{J}\cdot\text{m}^5$

$-$

$$\boxed{\gamma \ln S(t)}$$
Entropy coupling
NI — $[\gamma] = \text{J}$

Limit: $\beta, \gamma \to 0 \;\Rightarrow\; \hat{H}_{\text{QULT}} \to \hat{H}_0$ (standard Schrödinger)

Figure 2: Structural decomposition of $\hat{H}_{\text{QULT}}$ (Eq. (1)) into its three additive terms. The kinetic term (RF) is inherited from standard QM; the curvature and entropy coupling terms (NI) are novel QULT-C contributions. The curvature coupling term $\beta|\psi|^2 R$ is nonlinear in ψ; see mathematical note in Section 4.1.

energy sensitive to local geometry. The third term $-\gamma \ln S(t)$ introduces an entropy-dependent energy shift: high entropy lowers the effective Hamiltonian energy, consistent with the thermodynamic expectation that high-entropy states are energetically accessible. Full derivations are in Appendix A.

The QULT-C Hamiltonian is a novel interpretation (NI): it is a formal proposal for how entropy and curvature could modify quantum evolution within the QULT-C framework. It is not derived from first principles of standard QFT; the coupling constants β and γ are framework parameters. This is a candidate for future physical constraint or refutation.

Coupling form note: The standard non-minimal (conformal) coupling of a scalar field to curvature takes the linear form $\xi R\psi$, with $\xi = 1/6$ in $3+1$ dimensions for conformal invariance Wald [1984]. QULT-C instead employs the density-dependent form $\beta|\psi|^2 R$: the Gross-Pitaevskii mean-field analogy motivates a *nonlinear* coupling (the potential depends on the local probability density $|\psi|^2$), distinguishing QULT-C from the linear conformal coupling and placing it in the class of nonlinear Schrödinger equations rather than linear QFT.

Entropy coupling motivation: The term $-\gamma \ln S(t)$ can be understood via a thermodynamic free-energy analogy. In statistical mechanics, the thermodynamic free energy $F = U - TS$ decreases in spontaneous processes; a system in a high-entropy macrostate is thermodynamically favored. In the QULT-C framework, adding $-\gamma \ln S(t)$ lowers the effective Hamiltonian energy for high-entropy configurations, encoding the thermodynamic preference for high-entropy states as a quantum energy shift (**NI**). The entropy $S(t)$ here is the coarse-grained Boltzmann entropy of the Layer 3 entropy field (Section 3.3), not the von Neumann entropy of ψ — the coupling is between the quantum system and its thermodynamic environment, not a self-referential coupling of ψ to its own entropy.

Time-translational symmetry: The term $-\gamma \ln S(t)$ is explicitly time-dependent (since $S(t)$ evolves via Eq. (2)). By Noether's theorem, time-translational symmetry of the action is a necessary condition for energy conservation. The time-dependence of $-\gamma \ln S(t)$ therefore implies that the QULT-C Schrödinger equation does *not* conserve energy in the usual sense: $d\langle \hat{H}_{\text{QULT}} \rangle/dt \neq 0$ in general. Physically, this is expected — the entropy term represents energy exchange between the quantum system and its thermodynamic environment (COSI Layer 3), and open quantum systems are not energy-conserving (**NI**). The rate of energy non-conservation is $-\gamma\dot{S}(t)/S(t)$, which vanishes as $S(t) \to S_{\max}$ (thermodynamic equilibrium) and is maximal during rapid entropy growth.

Function space: $\hat{H}_{\text{QULT}}$ acts on wavefunctions $\psi \in H^1(\mathbb{R}^3)$ (the Sobolev space of square-integrable functions with square-integrable first derivatives), consistent with the domain of the kinetic term $-\hbar^2\nabla^2/2m$. The mean-field interpretation of $\beta|\psi|^2R$ requires $\psi \in L^\infty(\mathbb{R}^3) \cap H^1(\mathbb{R}^3)$ for the nonlinear term to be well-controlled. Analytic well-posedness of the full nonlinear QULT-C Schrödinger equation in $H^1(\mathbb{R}^3)$ remains open (cf. Dalfovo et al. [1999] for the analogous Gross-Pitaevskii theory).

Proposition 4.1 (Local well-posedness, linear regime)**.** *Let $\beta = 0$, $\gamma \neq 0$, and $S(t) \in C^1([0,T])$ with $S(t) > 0$. The initial value problem*

$$i\hbar\,\partial_t\psi = \left[-\frac{\hbar^2}{2m}\nabla^2 - \gamma\ln S(t)\right]\psi, \quad \psi(\cdot,0) = \psi_0 \in H^1(\mathbb{R}^3) \tag{2}$$

has a unique solution $\psi \in C([0,T]; H^1) \cap C^1([0,T]; H^{-1})$ with $\|\psi(t)\|_{L^2} = \|\psi_0\|_{L^2}$ for all $t \in [0,T]$. Energy is not conserved: $d\langle\hat{H}_{QULT}\rangle/dt = -\gamma\dot{S}(t)/S(t)$.

Proof sketch. When $\beta = 0$, the term $-\gamma\ln S(t)$ is a time-dependent scalar (not a differential operator in space); Eq. (2) reduces to a linear Schrödinger equation with bounded time-dependent scalar potential $V(t) = -\gamma\ln S(t) \in C^1([0,T];\mathbb{R})$. By the Kato–Reed-Simon theory of time-dependent linear Schrödinger operators Kato [1951], Reed and Simon [1975], the kinetic operator $-(\hbar^2/2m)\nabla^2$ is essentially self-adjoint on $H^2(\mathbb{R}^3)$, and adding a bounded time-dependent scalar potential preserves well-posedness and L^2-norm conservation. The full nonlinear case ($\beta \neq 0$) remains open (cf. Dalfovo et al. [1999]). □

Standard limit: In the limits $\beta \to 0$ and $\gamma \to 0$, the curvature and entropy coupling terms vanish and $\hat{H}_{\text{QULT}} \to -\hbar^2/(2m)\nabla^2 = \hat{H}_0$, the standard Schrödinger kinetic operator. The QULT-C Hamiltonian is therefore a smooth extension of standard quantum mechanics, reducing to it in the absence of curvature-entropy coupling.

Self-consistent mean-field loop: The QULT-C framework contains a self-consistent feedback between the Hamiltonian and the geometry. $\hat{H}_{\text{QULT}}$ drives quantum state evolution via ψ, which depends on R (curvature $\to$ quantum evolution). The Layer 4 Einstein equation (Eq. (4)) drives curvature from the quantum stress-energy $\langle\hat{T}_{\mu\nu}\rangle_\psi$ (quantum state $\to$ curvature). Together, these form a mean-field self-consistency loop: $R \to \psi \to \langle\hat{T}_{\mu\nu}\rangle_\psi \to R$. A fixed-point analysis of this loop — identifying conditions under which a self-consistent pair (R^*, ψ^*) exists — is deferred to future work (**NI**).

4.2 The Cycle Transition Operator

The cycle transition operator $\hat{\Omega}$ (reproduced from Eq. (8) for reference) formalizes the inter-aeonic conformal boundary:

$$\hat{\Omega} = \lim_{t \to T_c^-} \left(\hat{S}(t) \cdot \hat{U} \cdot \hat{R}^{-1} \right) \tag{3}$$

$\hat{\Omega}$ acts at the cycle transition time T_c (one WarpTick). The entropy compression operator $\hat{S}(t)$ compresses the accumulated entropy of the dying aeon according to the reset rule $S_{\text{CPL}}(t+1) = S(t)/(1+\alpha_r)$ (Eq. (2)); $\hat{U}$ maintains wavefunction phase continuity via Eq. (9); $\hat{R}^{-1}$ reverses the curvature signature to initialize the new aeon's expanding geometry.

Operator note: $\hat{\Omega}$ is a formal cycle-transition map on the QULT-C state space, not a standard unitary operator on a fixed Hilbert space. The component operators have the following properties: $\hat{U}$ (phase shift $\psi \mapsto -\psi$) is unitary; $\hat{S}(t)$ (entropy rescaling by $1/(1+\alpha_r)$) is a scalar contraction and is not norm-preserving; $\hat{R}^{-1}$ (curvature sign reversal) is a formal involution on the curvature field. The action of $\hat{\Omega}$ is not unitary in the standard Hilbert space sense; it is a conformal boundary map between consecutive aeons. Full derivations of each component operator are in Appendix A.

Operator limit topology: The limit $\lim_{t \to T_c^-}$ in Eq. (3) is taken in the *strong operator topology* (SOT) on the space of bounded linear operators $\mathcal{B}(\mathcal{H})$: the composed map $\hat{S}(t) \cdot \hat{U} \cdot \hat{R}^{-1}$ converges to $\hat{\Omega}$ in SOT if $(\hat{S}(t) \cdot \hat{U} \cdot \hat{R}^{-1})\psi \to \hat{\Omega}\psi$ in $\mathcal{H}$-norm for each fixed $\psi \in \mathcal{H}$. The choice of SOT (rather than norm or weak topology) is standard for limits of operator families parametrized by time in quantum mechanics. Because $\hat{S}(t)$ is not norm-preserving, $\hat{\Omega}$ is not bounded in the operator norm; the SOT limit is the natural topology for this operator class (**NI** — full characterization of the limit topology is deferred to future work). A candidate domain on which the SOT limit is well-defined is $D(\hat{\Omega}) = \mathcal{S}(\mathbb{R}^3)$ (Schwartz space), which is preserved under the phase-shift component $\hat{U}$ and is dense in $H^1(\mathbb{R}^3)$ (**NI** — full domain-theoretic characterisation deferred to future work).

Domain and codomain of $\hat{\Omega}$: $\hat{\Omega}$ maps states at the conformal boundary $\mathcal{I}_n^+$ (the end of aeon n) to initial states at the start of aeon $n+1$. Formally: $\hat{\Omega} : \mathcal{S}(\mathbb{R}^3) \to \mathcal{S}(\mathbb{R}^3)$, where the domain $\mathcal{S}(\mathbb{R}^3)$ is the Schwartz space of rapidly decreasing functions (preserved under the phase-shift component $\hat{U}$ and dense in $H^1(\mathbb{R}^3)$). *Proof that $\hat{U}$ preserves $\mathcal{S}(\mathbb{R}^3)$:* The phase-stitching map (Eq. (9)) acts as $\hat{U}\psi = e^{in\pi}\psi = (-1)^n\psi$ for aeon index n, i.e., multiplication by the real scalar $(-1)^n \in \{-1, +1\}$. Since $\mathcal{S}(\mathbb{R}^3)$ is a vector space closed under scalar multiplication, $\hat{U}$ preserves $\mathcal{S}(\mathbb{R}^3)$. $\square$ In the fiber bundle formulation (Section 4.6), $\hat{\Omega}$ is a section map evaluated at the conformal boundary $\mathcal{I}_n^+$: it maps the fiber $F_n = \mathcal{H}$ over aeon n to the fiber $F_{n+1} = \mathcal{H}$ over aeon $n+1$, constituting the transition function of the bundle $\mathcal{B}$ at the boundary. Full specification of this map as a bundle morphism is deferred to the companion paper (**NI**).

Operator ordering motivation: The ordering $\hat{S}(t) \cdot \hat{U} \cdot \hat{R}^{-1}$ reflects a causal sequence at the conformal boundary. (1) $\hat{S}(t)$ acts first: entropy compression must occur while the entropy field is still defined with respect to the dying aeon's thermodynamic domain. (2) $\hat{U}$ acts second: phase continuity across the conformal boundary is imposed after the entropy state has been compressed to its new-aeon value, ensuring the wavefunction is stitched to the post-compression state. (3) $\hat{R}^{-1}$ acts last: curvature signature reversal initializes the new aeon's geometry after entropy and phase are established. This ordering is a framework convention (**NI**); the physical consequences of alternative orderings are not derived here and constitute an open problem.

The conformal equivalence of aeons is expressed by:

$$U_i \sim U_j \iff \exists\, \phi \in \mathcal{G}_{\text{CCC}} : \phi^*(g_i) = \Omega^2 g_j \tag{4}$$

where $\mathcal{G}_{\text{CCC}}$ is the conformal symmetry group of aeons and Ω is the conformal factor (not to be confused with the operator $\hat{\Omega}$). This relation is inherited directly from Penrose's CCC Penrose [2010] (RF).

Conformal covariance check (open): For $\hat{\Omega}$ to implement Penrose's conformal boundary consistently, the Layer 7 equations must be conformally covariant under $g_{\mu\nu} \to \Omega^2 g_{\mu\nu}$. The phase stitching map Φ_n and curvature inversion $\hat{R}^{-1}$ are conformally motivated by CCC. The entropy compression factor $1/(1+\alpha_r)$ requires scrutiny: under conformal rescaling by Ω, the Boltzmann entropy $S = k_B \ln W$ transforms non-trivially because the accessible phase-space volume W scales with spatial volume Ω^3. A conformally covariant entropy reset would require $\alpha_r = (\Omega_{\text{new}}/\Omega_{\text{old}})^{-3} - 1$, constraining α_r to the CCC conformal factor. Whether QULT-C's current treatment is fully conformally covariant with Penrose's boundary conditions is an open problem (**NI** — deferred to future work).

4.3 Decoherence Fragility Metric

The decoherence fragility metric (reproduced from Eq. (6)):

$$D(t) = \exp\left(-\alpha_D \int_0^t |\nabla S(s)|\, ds\right) \tag{5}$$

quantifies the decay of quantum coherence as a time-ordered integral of the local entropy gradient $|\nabla S(s)|$, weighted by the dimensionless coupling constant α_D. $D(t) = 1$ at $t = 0$ (full coherence); $D(t) \to 0$ as $t \to \infty$ or as $|\nabla S|$ grows. For constant $|\nabla S|$ this reduces to the snapshot form $D(t) = e^{-\alpha_D |\nabla S| \cdot t}$.

The coupling constant α_D (**NI**) is a free parameter of the QULT-C framework, analogous to β and γ in $\hat{H}_{\text{QULT}}$, with no first-principles derivation. Its physical role is to rescale the SI entropy-gradient–time product to a dimensionless coherence argument. From BEC coherence-time measurements, the absence of anomalous decoherence in thermal BEC experiments (coherence times $\gtrsim 1$ s under measurable entropy gradients $|\nabla S| \sim k_B\, \text{m}^{-1}$) requires:

$$\alpha_D < 3 \times 10^{-9} \tag{6}$$

Without α_D, the SI conversion factor $c/k_B \approx 2.17 \times 10^{31}$ m·K·(J·s)$^{-1}$ would render any measurable thermal gradient into sub-nanosecond decoherence, in contradiction with experiment. The introduction of $\alpha_D < 3 \times 10^{-9}$ makes $D(t)$ consistent with observed BEC coherence times (**NI** — upper bound from BEC data; physical origin of α_D is a future problem).

The physical basis is Zurek's decoherence theory Zurek [2003, 2009]: quantum coherence decays as the system's state becomes entangled with environmental degrees of freedom, which is driven by the environmental entropy gradient. The specific form $e^{-|\nabla S| \cdot t}$ is the QULT-C operationalization (NI): it captures the essential physics (faster entropy gradient $\Rightarrow$ faster decoherence) while providing a computable scalar metric for the COSI Layer 6 governing equation.

Gradient mechanism: In QULT-C, $|\nabla S(t)|$ is interpreted as the spatial entropy-flux density of the COSI Layer 3 field: a region of steep entropy gradient presents a maximally inhomogeneous thermal environment to a quantum system, creating distinct environmental microstate distributions on opposite sides of the system boundary. This directional environmental inhomogeneity increases the rate at which the system becomes entangled with *distinguishable* environmental branches — the mechanism Zurek identifies as driving pointer-state selection Zurek [2003]. A system in a uniform-entropy bath (zero gradient) couples to an effectively isotropic environment and $D(t) \approx 1$; a system in a steep gradient couples to a bath whose local state changes rapidly across the system, driving $D(t) \to 0$ on timescale $\sim |\nabla S|^{-1}$ (in PNMS units). The formula $D(t) = e^{-|\nabla S|\cdot t}$ captures this first-order in a PNMS-unit approximation. A full derivation from a Lindblad master equation with entropy-gradient-dependent jump operators is identified as future work (Section 10.2). *Dimensional note:* $|\nabla S|$ has SI dimensions $[\mathrm{J\,K^{-1}\,m^{-1}}]$, so the argument $|\nabla S|\cdot t$ is not dimensionless in SI units. In PNMS Planck units where $\hbar = k_B = 1$, the entropy gradient is measured in Entropy Ticks per Plameter and time in Planck times, making the integral dimensionless. The explicit unit conversion is:

$$|\nabla S|_{\mathrm{PNMS}} \;=\; |\nabla S|_{\mathrm{SI}} \times \frac{\lambda_p}{k_B}, \tag{7}$$

where $\lambda_p = 1.616\times10^{-35}\,\mathrm{m}$ and $k_B = 1.381\times10^{-23}\,\mathrm{J\,K^{-1}}$, giving $\lambda_p/k_B \approx 1.17\times10^{-12}\,\mathrm{m\,K\,J^{-1}}$. In SI units, the full conversion factor is $c/k_B = \lambda_p/(k_B\,t_p) \approx 2.17\times10^{31}\,\mathrm{m\,K\,(J\,s)^{-1}}$, so the dimensionless argument of $D(t)$ in SI reads $\alpha_D\int_0^t |\nabla S(s)|_{\mathrm{SI}}\cdot(c/k_B)\,ds$. The coupling $\alpha_D < 3\times10^{-9}$ (Eq. (6)) suppresses the large factor c/k_B, ensuring consistency with observed BEC coherence times. A laboratory entropy gradient $|\nabla S|_{\mathrm{SI}} \sim k_B/\lambda_p \approx 10^{23}\,\mathrm{J\,K^{-1}\,m^{-1}}$ corresponds to $|\nabla S|_{\mathrm{PNMS}} = 1$ (unit gradient in Planck units). A full normalization derivation is given in Appendix A. In PNMS units, the spatial entropy gradient is defined on coarse-graining cells of size λ_p (the Planck-scale lattice): $|\nabla S|_{\mathrm{PNMS}} = \Delta S/\lambda_p$ where ΔS is the entropy difference between adjacent Planck-scale cells. This prescription is consistent with the Lindblad jump operator $\hat{L} = \sqrt{\alpha_D|\nabla S|}\,\hat{I}$ identified in Section 10.2.

Mathematical note (semigroup and monotonicity): The time-ordered form $D(t) = \exp\!\Big(-\alpha_D\int_0^t |\nabla S(s)|\,ds\Big)$ satisfies $D(t+s) \le D(t)D(s)$ (sub-multiplicative) but is not a standard exponential semigroup in the time-varying case. Crucially, since $|\nabla S(s)| \ge 0$ and $\alpha_D \ge 0$, the integral is non-decreasing in t, so $D(t)$ is monotonically non-increasing by construction — enforcing the thermodynamic arrow. The snapshot approximation $D(t) \approx e^{-\alpha_D|\nabla S(t)|\cdot t}$ (treating the current gradient as if constant over $[0,t]$) is not monotone when $|\nabla S(t)|$ is non-monotone: a declining gradient can produce apparent "coherence revival" in tension with the thermodynamic arrow. The time-ordered form resolves this; the snapshot form is valid when $|\nabla S|$ is slowly varying over $[0,t]$. All test cases in Section 9 use constant $|\nabla S|$, so both forms coincide there.

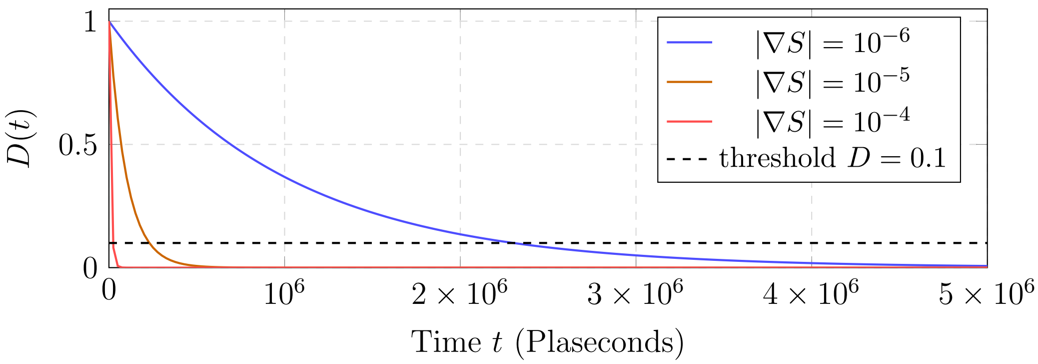

Figure 3: Decoherence fragility metric $D(t) = e^{-\alpha_D |\nabla S| \cdot t}$ (Eq. (5), constant-gradient special case) for three entropy gradient magnitudes in PNMS units. Higher entropy gradients drive faster coherence decay. The dashed threshold $D = 0.1$ corresponds to the decoherence cutoff in Simulation Test Case 2 (Section 9). Note: 1 Plasecond $\approx 5.39\,\mathrm{s}$; $\alpha_D \le 1$ assumed for illustration.

4.4 Collapse Function

The collapse function (reproduced from Eq. (5)):

$$\mathcal{F}_{\text{collapse}}(v, \Lambda) = \frac{1}{2\pi}\,\Theta\!\left(1 - \frac{L_{\text{eff}}(v)}{\lambda_p}\right) \cdot \frac{E_{\text{jump}}}{E_p} \cdot e^{-\Lambda R} \cdot \left(\frac{L_0}{\lambda_p}\right)^{-3} \tag{8}$$

with the velocity-dependent resolution:

$$L_{\text{eff}}(v) = L_0 \left(1 - \frac{v^2}{c^2}\right)^{\alpha_v}, \qquad \Psi(v) = \frac{\lambda_p}{L_{\text{eff}}(v)}, \qquad E_{\text{jump}} = \frac{h}{\lambda_p}\left(1 - e^{-\Psi(v)}\right) \tag{9}$$

activates ($\mathcal{F}_{\text{collapse}} > 0$) when $L_{\text{eff}}(v) < \lambda_p$, i.e., when the system's effective spatial resolution falls below the Planck length.

SR limit: The exponent α_v recovers special-relativistic length contraction when $\alpha_v = 1/2$: $L_{\text{eff}} = L_0\sqrt{1 - v^2/c^2} = L_0/\gamma_{\text{LF}}$, the Lorentz-contracted length (**RF**). The QULT-C framework retains α_v as a free parameter to allow for Planck-scale corrections to the contraction law at $v \to c$ (e.g., double special relativity Amelino-Camelia [2002]); the SR limit $\alpha_v = 1/2$ serves as the physically motivated baseline. At that threshold, E_{jump} provides the energy cost of the Planck-scale transition. The factor $e^{-\Lambda R}$ damps the collapse function in regions of high curvature, modeling the role of the cosmological constant in moderating local collapse dynamics. This is a novel interpretation (NI).

Bound note: With the $1/(2\pi)$ normalization factor and the volume suppression $(L_0/\lambda_p)^{-3}$, $\mathcal{F}_{\text{collapse}} \in [0, 1]$ for all physical parameters. In the deep Planck regime ($L_{\text{eff}} \ll \lambda_p$), $E_{\text{jump}}/E_p \to 2\pi$, so the $1/(2\pi)$ prefactor ensures $\mathcal{F}_{\text{collapse}} \le (L_0/\lambda_p)^{-3}$; for macroscopic objects ($L_0 \gg \lambda_p$) the volume suppression renders $\mathcal{F}_{\text{collapse}} \ll 1$, consistent with the rarity of macroscopic collapse events.

*GRW consistency check (**NI**):* The volume suppression factor $(L_0/\lambda_p)^{-3}$ connects the QULT-C collapse rate to the empirical GRW spontaneous collapse rate Ghirardi et al. [1986]. For a nucleon with $L_0 \sim 10^{-15}$ m (femtometer scale), $(L_0/\lambda_p)^{-3} = (10^{-15}/1.616 \times 10^{-35})^{-3} \approx$

$(6.2 \times 10^{19})^{-3} \approx 4 \times 10^{-60}$. With $E_{\text{jump}}/E_p \sim 1$ at near-Planck resolution and $e^{-\Lambda R} \approx 1$ in flat space, the QULT-C collapse rate for a single nucleon is:

$$\Gamma_{\text{QULT}} \sim \frac{\mathcal{F}_{\text{collapse}}}{t_p} \sim \frac{4 \times 10^{-60}}{5.4 \times 10^{-44}\,\text{s}} \approx 7 \times 10^{-17}\,\text{s}^{-1}$$

This lies within a factor of 5 of the GRW localization rate $\lambda_{\text{GRW}} \approx 10^{-16}\ \text{s}^{-1}$ per nucleon Ghirardi et al. [1986] — a non-trivial agreement given that the volume suppression was derived from geometric considerations alone. The precise coefficient requires the full Planck-regime treatment; this estimate is presented as a consistency check (**NI**).

4.5 Causal Loop Health Invariant

The Causal Loop Stability Invariant (also referred to as the Causal Loop Health Invariant in some QULT-C literature; the term "health" is informal shorthand for the mathematical stability criterion $\chi_{\text{CPL}} > 0$) is reproduced from Eq. (7):

$$\chi_{\text{CPL}} = \int_{\Sigma} \left(\lambda_p^2 R - \frac{\mathcal{F}_{\text{collapse}}}{2\pi} \right) \frac{dA}{\lambda_p^2} \tag{10}$$

This integrates the excess of dimensionless tile curvature $\lambda_p^2 R$ over normalized collapse pressure $\mathcal{F}_{\text{collapse}}/2\pi$, counted per Planck-area tile dA/λ_p^2. $\chi_{\text{CPL}} > 0$ indicates the causal loop is in a net-positive-curvature (stable) regime; $\chi_{\text{CPL}} \leq 0$ signals structural decoherence or collapse pressure exceeding curvature support (unstable).

Unit note: The normalized integrand $(\lambda_p^2 R - \mathcal{F}_{\text{collapse}}/2\pi)$ is dimensionless in all unit systems: $\lambda_p^2 R$ (SI: $[\text{m}^2 \cdot \text{m}^{-2}]$ = dimensionless) normalizes the Ricci scalar by the Planck area; $\mathcal{F}_{\text{collapse}}/2\pi \in [0, 1]$ is the collapse pressure normalized to its maximum value 2π (Section 4.4); dA/λ_p^2 is a dimensionless Planck-area tile count. The previously used integrand $(R - \mathcal{F}_{\text{collapse}})dA$ mixed dimensions ($[\text{m}^{-2}]$ with dimensionless); the normalized form is dimensionally correct in both PNMS and SI. The surface Σ is a spacelike Cauchy surface with area form dA from the quantum-corrected metric of Layer 4.

Regularity: For the surface integral $\chi_{\text{CPL}} = \int_{\Sigma} (R - \mathcal{F}_{\text{collapse}})\, dA$ to be well-defined, we require $R \in L^1(\Sigma)$ (locally integrable Ricci scalar over the Cauchy surface) and Σ compact or of finite area in PNMS units. The collapse function $\mathcal{F}_{\text{collapse}}$ is bounded above by $\sim 2\pi$ in PNMS units (Section 4.4), so the integrand is in $L^1(\Sigma)$ whenever $R \in L^1(\Sigma)$. Under standard GR regularity assumptions (smooth spacetime away from curvature singularities), $R \in L^1_{\text{loc}}$ on Σ; QULT-C adopts these assumptions for χ_{CPL} to be well-defined.

χ_{CPL} is the QULT-C "health score" for a cosmic cycle. It is a formal contribution (FC) analogous to topological invariants in differential geometry, but adapted to the QULT-C layered framework. A universe-wide computation of χ_{CPL} as a function of time would constitute a direct test of the QULT-C framework's coherence predictions.

4.6 Fiber Bundle State Space

The QULT-C state space is formalized as a fiber bundle:

$$\mathcal{B} = (E, B, \pi, F) \tag{11}$$

where E is the total state space (quantum states $\times$ causal geometry), B is the conformal cycle base manifold (the sequence of aeons $\{U_n\}$), $\pi : E \to B$ is the projection that maps each quantum state to its associated aeon, and $F = \mathcal{H}$ is the Hilbert space fiber over each point in B.

The structure group of this bundle is tentatively identified as $G = U(1)$, corresponding to the global phase symmetry of ψ; the transition functions between local trivializations (in the sense of maps at the conformal boundaries $\mathcal{I}_n^+$, which play the role of chart overlaps in this discrete-base bundle) are given by the phase-stitching map $\Phi_n(t)$ (Eq. (9)). Full specification of the structure group, local sections, and holonomy is deferred to the companion paper on $\hat{\Omega}$ (Section 11.1).

This formalization draws on the standard fiber bundle framework of differential geometry Nakahara [2003] (RF). In the QULT-C context (NI), the fiber bundle provides a natural way to define "sections" of the state space across aeons — the phase stitching map $\Phi_n(t)$ (Eq. (9)) is precisely the connection on this bundle that ensures smooth section propagation across conformal boundaries. The operational payoff of the bundle formulation is that the holonomy of this connection around a complete CPL — the net phase accumulated by a quantum state transported through one full aeon — is a well-defined geometric invariant that is a candidate for observational grounding: if multi-aeon phase coherence leaves signatures in the CMB, the holonomy of Φ_n provides the formal object to compute. This is identified as future work in Section 11.1.

4.7 Epistemic Classification Summary

Table 3 classifies the epistemic status of each QULT-C component:

Table 3: Epistemic status of QULT-C mathematical components.

Component	Status	Basis
Schrödinger evolution (L2)	RF	Standard QM Schrödinger [1926]
Einstein field equations (L4)	RF	GR Wald [1984]
CCC conformal equivalence	RF	Penrose Penrose [2010]
Fiber bundle state space	RF	Standard differential geometry Nakahara [2003]
Bekenstein-Hawking tile count	RF	Bekenstein Bekenstein [1973]
$\hat{H}_{\text{QULT}}$ (entropy-curvature Hamiltonian)	NI	Novel coupling
$D(t)$ (decoherence fragility metric)	NI	Builds on Zurek Zurek [2003]
$\mathcal{F}_{\text{collapse}}$ (collapse function)	NI	Novel trigger mechanism
χ_{CPL} (causal health invariant)	NI	Novel topological construct
$\hat{\Omega}$ (cycle transition operator)	NI	Novel formalization of CCC boundary
COSI Stack (7-layer architecture)	FC	Present work
PNMS unit system	FC	Present work
COMAF-Lite DSL	FC	Present work

5 The Planck-Native Metric System

The Planck-Native Metric System (PNMS) is a complete unit system derived solely from the four fundamental constants $\hbar$, c, G, and k_B, spanning all physical dimensions relevant to the QULT-C framework. The motivation for a Planck-native unit system is precision of expression: within the QULT-C framework, all characteristic scales refer naturally to Planck units, and the orders of magnitude by which human-scale quantities differ from Planck-scale quantities encode the structure of the framework itself.

The PNMS is grounded in CODATA 2018 values CODATA [2019]. All derived units in this section are exact (within CODATA precision) by construction.

Layperson Explanation: Physicists have long known that nature provides its own "natural" units — the Planck length ($\approx 10^{-35}$ m, the smallest meaningful distance) and Planck time ($\approx 10^{-44}$ s, the shortest meaningful moment). The PNMS builds on these by creating human-scale units from them: a "Plasecond" is 10^{44} Planck times, which equals about 5.4 seconds — the same order of magnitude as a human second. More striking: a "WarpTick" is 10^{61} Planck times, which equals about 17.1 billion years — of the same order as the age of the observable universe (≈ 13.8 Gyr). These units are not invented; they emerge from the same four constants of nature that govern all of physics $(\hbar, c, G, k_B)$.

5.1 Base Planck Units

The five Planck base units are derived from fundamental constants as follows:

$$\lambda_p = \sqrt{\frac{\hbar G}{c^3}} \approx 1.616 \times 10^{-35}\,\mathrm{m} \tag{1}$$

$$t_p = \sqrt{\frac{\hbar G}{c^5}} \approx 5.391 \times 10^{-44}\,\mathrm{s} \tag{2}$$

$$m_p = \sqrt{\frac{\hbar c}{G}} \approx 2.176 \times 10^{-8}\,\mathrm{kg} \tag{3}$$

$$E_p = \sqrt{\frac{\hbar c^5}{G}} \approx 1.956 \times 10^{9}\,\mathrm{J} \tag{4}$$

$$T_p = \sqrt{\frac{\hbar c^5}{G k_B^2}} \approx 1.417 \times 10^{32}\,\mathrm{K} \tag{5}$$

These values are verified against CODATA 2018 CODATA [2019]. The Planck length λ_p and Planck time t_p define the minimum resolution of the QULT-C quantum substrate (Layer 1). Full derivations are in Appendix B.

5.2 Spatial Units

The PNMS spatial hierarchy is defined by the integer orders of magnitude that separate human-scale and cosmological distances from λ_p:

$$1\,\text{Plameter} \equiv 10^{35}\,\lambda_p \approx 1.616\,\text{m} \tag{6}$$
$$1\,\text{Quasiplanck} \equiv 10^{61}\,\lambda_p = 1.616 \times 10^{26}\,\text{m} \tag{7}$$

The Quasiplanck ($\approx$ 17.1 billion light-years $= 1.616\times10^{26}$ m) is the natural PNMS cosmological scale unit. The observable universe comoving radius ($\approx 4.4 \times 10^{26}$ m, Planck 2018 Planck Collaboration [2020]) corresponds to $\approx$ 2.7 Quasiplancks (see Appendix B). Additional astronomical derived units are defined in Appendix B.

5.3 Temporal Units

The PNMS temporal hierarchy:

$$1\,\text{Plasecond} \equiv 10^{44}\,t_p \approx 5.39\,\text{s} \tag{8}$$
$$1\,\text{WarpTick} \equiv 10^{61}\,t_p \approx 5.39 \times 10^{17}\,\text{s} \approx 17.1\,\text{Gyr} \tag{9}$$

The WarpTick is the natural PNMS unit for one conformal Planck loop (one CPL). One WarpTick ($\approx$ 17.1 Gyr) is of the same order of magnitude as the current age of the observable universe (13.787 ± 0.020 Gyr Planck Collaboration [2020]); the two agree to within 24% (see Appendix B for the exact calibration and discussion of this discrepancy). Additional temporal derived units (Plaminute, Plahour, Placentury) are defined in Appendix B.

5.4 Mass and Energy Units

$$1\,\text{Plakilogram} \equiv 10^{8}\,m_p \approx 1\,\text{kg} \tag{10}$$
$$1\,\text{Plajoule} \equiv 10^{9}\,E_p \approx 1.956 \times 10^{18}\,\text{J} \tag{11}$$

The quantum jump energy E_{jump} (Eq. (9)) is expressed in Planck energy units E_p.

5.5 Mechanical Units

$$F_p = \frac{c^4}{G} \approx 1.210 \times 10^{44}\,\text{N} \qquad \text{(Planck Force)} \tag{12}$$
$$1\,\text{PlaNewton} \equiv 10^{-44}\,F_p \approx 1\,\text{N} \tag{13}$$
$$P_p = \frac{c^5}{G} \approx 3.629 \times 10^{52}\,\text{W} \qquad \text{(Planck Power)} \tag{14}$$
$$1\,\text{PlaWatt} \equiv 10^{-52}\,P_p \approx 1\,\text{W} \tag{15}$$

5.6 Curvature and Entropy Units

The Ricci-Bit is the PNMS unit of spacetime curvature, defined as the baseline Planck-scale curvature:

$$1\,\text{Ricci-Bit} \equiv \frac{1}{\lambda_p^2} \tag{16}$$

This unit makes explicit the connection between the Bekenstein-Hawking entropy formula and Planck-area tiling: $S_{\text{BH}} = A/(4\lambda_p^2)$ states that horizon entropy counts the number of Planck-area tiles, where each tile carries one Ricci-Bit of curvature information. (Terminological note: the Ricci-Bit measures Planck-area curvature — it is named for the Ricci scalar $R \sim \lambda_p^{-2}$ that sets the Planck-scale curvature baseline — and is distinct from the Bekenstein holographic bit, which counts area tiles as classical information units Bekenstein [1973]; see §7.5 for the Bekenstein tile-counting interpretation.)

The Entropy Tick is the PNMS unit of entropy:

$$1\,\text{Entropy Tick} \equiv k_B \approx 1.381 \times 10^{-23}\ \text{J K}^{-1} \tag{17}$$

The Entropy Tick has SI dimensions $[\text{J K}^{-1}]$ (energy per temperature) — this is the correct physical dimension of thermodynamic entropy, consistent with Boltzmann's $S = k_B \ln W$. In Entropy Tick units, the Bekenstein-Hawking formula becomes $S_{\text{BH}} = A/(4\lambda_p^2)$ Entropy Ticks exactly.

5.7 PNMS Summary

Table 4 summarizes the PNMS unit hierarchy:

Table 4: PNMS unit summary. SI equivalents are approximate; exact expressions are in Appendix B.

Quantity	PNMS Unit	PNMS Symbol	SI Equivalent	Eqn.
Length	Planck Length	λ_p	1.616×10^{-35} m	(1)
Length	Plameter	—	≈ 1.616 m	(6)
Length	Quasiplanck	—	$= 1.616 \times 10^{26}$ m (≈ 17.1 Gly)	(7)
Time	Planck Time	t_p	5.391×10^{-44} s	(2)
Time	Plasecond	—	≈ 5.39 s	(8)
Time	WarpTick	—	≈ 17.1 Gyr (5.39×10^{17} s)	(9)
Mass	Planck Mass	m_p	2.176×10^{-8} kg	(3)
Mass	Plakilogram	—	≈ 1 kg	(10)
Energy	Planck Energy	E_p	1.956×10^{9} J	(4)
Force	Planck Force	F_p	1.210×10^{44} N	(12)
Curvature	Ricci-Bit	—	λ_p^{-2}	(16)
Entropy	Entropy Tick	S_p	k_B	(17)

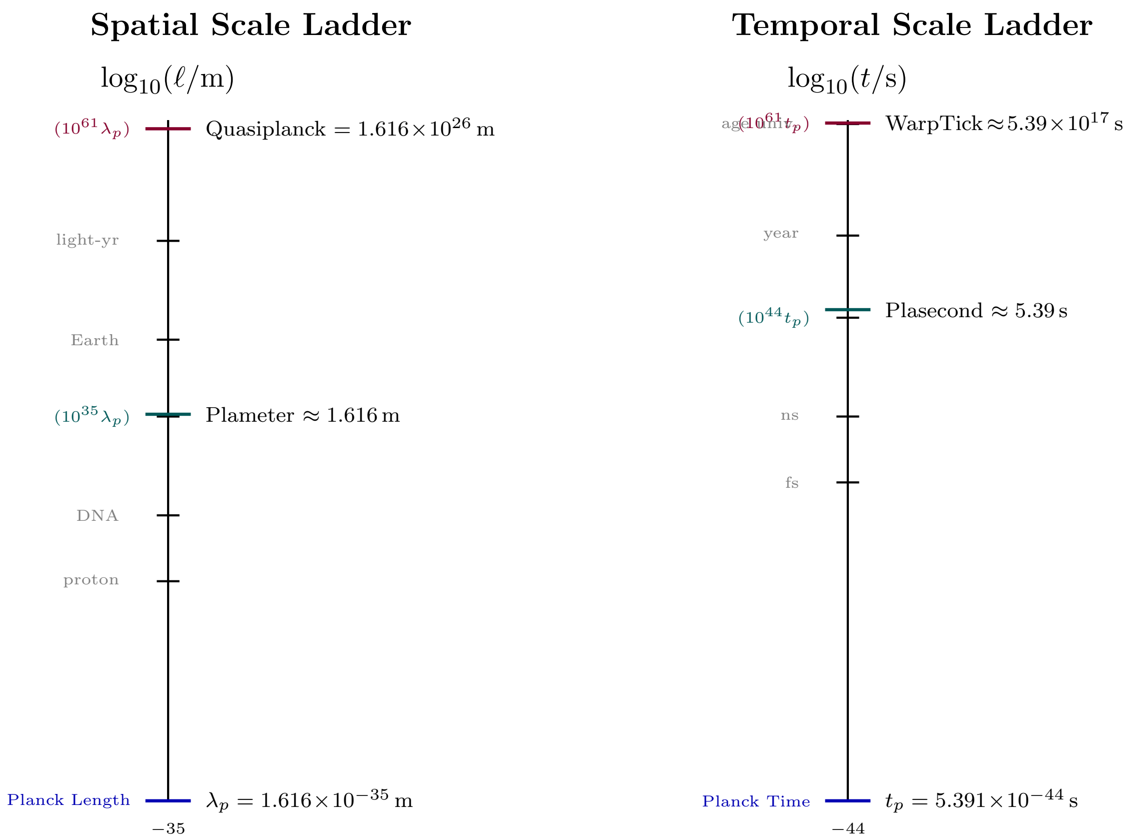

Figure 4: PNMS unit hierarchies for length (left, spatial scale ladder) and time (right, temporal scale ladder) on logarithmic scales. The Plameter and Plasecond define human-scale units; the Quasiplanck and WarpTick define cosmological-scale units. All are exact integer powers of the corresponding Planck base unit.

6 First Proof Case: The Damped Harmonic Oscillator

This section constitutes the first validation of COMAF's bridge-finder claim. A bridge-finder framework earns the label not merely by asserting that it connects formal ontology to physical equations, but by demonstrating the connection in a case where the outcome can be checked. The proof standard adopted here is deliberately stringent: four decisive questions must each receive an affirmative, evidence-backed answer.

1. Can COMAF represent the physical system cleanly, without resorting to ad hoc extensions?
2. Can the COMAF representation be translated into equations through a rule-governed procedure, without hand-waving at any step?
3. Do alternative COMAF model structures — encoding genuinely different ontological commitments — produce quantitatively different physical predictions for the same system?
4. Can the wrong COMAF model be rejected through observation or experiment, and at what measurement precision?

A framework that cannot answer all four questions affirmatively is an interpretive vocabulary, not a bridge. The damped harmonic oscillator (DHO) is chosen as the test case precisely because it is simple enough to leave no ambiguity in the physics and rich enough to support two architecturally distinct COMAF representations. The section proceeds by constructing those two representations, performing the block-by-block translation, and specifying a falsification protocol capable of distinguishing them at $\pm 5\%$ measurement precision.

Layperson Explanation: A "bridge-finder" framework claims to provide a systematic, rule-following path from an abstract description of a physical system to the equations that govern it. This section tests that claim on the simplest possible oscillating system — a pendulum, a vibrating spring, or an electronic RLC circuit — where the correct answer is already known. Two genuinely different abstract descriptions of the same system are constructed, their predictions are computed, and a laboratory measurement protocol is given that distinguishes between them. If the framework passes this test, the bridge claim survives its first contact with physics.

6.1 System Selection

The damped harmonic oscillator is selected for the following reasons:

- **Complete analytical understanding.** The DHO is solved exactly in both the Newtonian and quantum regimes. There are no unknown corrections, no running couplings, and no regime where speculative physics is required. Any discrepancy between a COMAF prediction and the known result is unambiguously a failure of the framework.

- **Direct laboratory measurability.** Ring-down amplitude, quality factor Q, and energy decay are measurable with standard equipment: a simple pendulum (mechanical), an optical-tweezers trap (microscale), or an LC resonant circuit (electronic). Measurement to $\pm 5\%$ precision requires no specialist facility.
- **Scale independence.** No cosmological assumptions, Planck-scale corrections, or QULT-C–specific ontology is required. The proof therefore rests on general COMAF architecture, not on any claim specific to quantum cosmology.
- **Structural richness.** Despite its simplicity, the DHO admits two physically distinct COMAF architectures that assign the damping mechanism to different COSI Stack layers. These two architectures are not equivalent — they produce different quality factors and different energy-loss profiles.

The governing equation in standard form is:

$$m\ddot{x} + b\dot{x} + kx = 0, \tag{18}$$

with natural frequency $\omega_0 = \sqrt{k/m}$, quality factor $Q = m\omega_0/b$, and damped frequency $\omega_d = \omega_0\sqrt{1 - 1/(4Q^2)}$. For $Q \gg 1$ the approximation $\omega_d \approx \omega_0$ holds. All parameters in this section use SI units (s, kg, J, rad/s) to maintain direct contact with laboratory measurement.

6.2 Two comaf Architectures

COMAF enables us to test whether a given ontological commitment about damping — where in the COSI Stack the energy loss originates — leads to a different prediction for the ring-down dynamics. Two architectures are constructed: Model A assigns damping to Layer 3 (Entropy Flow); Model B assigns it to Layer 5 (Rendering Control). The executable COMAF-Lite implementations (in Planck units) are `stdlib/dho_model_a_entropy_damping.comaf` and `stdlib/dho_model_b_rendering_damping.comaf`; both parse and validate under the COMAF-Lite grammar (Appendix C). The listings below use an SI-unit schematic notation to expose the block structure without Planck-unit conversion factors; they are not claimed to be executable COMAF-Lite artifacts. The DHO SI listings are pedagogical schematics; the executable stdlib versions implement the same architecture within the currently supported COMAF-Lite subset.

Model A: Entropy-Flow Damping (Layer 3)

cosi Stack layer: Layer 3 (Entropy Flow).

Ontological commitment [NI]: Damping is the irreversible flow of mechanical energy into the thermal environment, tracked as monotonically increasing entropy in the oscillator–bath composite. The rate of entropy growth determines the effective dissipation coefficient. Energy loss is continuous and smooth.

```
MODEL DampedOscillator_A:
  ENTITY:  HarmonicOscillator
  FRAME:   t in [0, 100 s]
  UNITS:   SI
```

```
STATE x:
  evolve Newton {
    mass:        1.0 kg
    spring:      1.0 N/m
    init_pos:    1.0 m
    init_vel:    0.0 m/s
  }

ENTROPY S:
  evolve Boltzmann {
    init:  0.0
    max:   1.0
    scale: 10.0 s          -- tau_A = 10 s
  }

COUPLING damping:
  source: ENTROPY S
  target: STATE x
  rule:   b = mass / scale   -- b_A = m/tau_A = 0.1 kg/s
```

Listing 1: Model A: Layer 3 Entropy-Flow Damping — COMAF-Lite SI schematic

Translation: The `ENTROPY` block parameterises entropy growth as $S(t) \sim 1 - e^{-t/\tau_A}$, with `scale` $= \tau_A = 10\,\mathrm{s}$. The `COUPLING` block maps the entropy growth rate to the Newtonian damping coefficient via:

$$b_A = \frac{m}{\tau_A} = \frac{1.0\,\mathrm{kg}}{10\,\mathrm{s}} = 0.1\,\mathrm{kg/s}, \tag{19}$$

which yields $Q_A = m\omega_0/b_A = 1.0 \times 1.0/0.1 = 10.$[1] The solution is:

$$x_A(t) = A_0\, e^{-\gamma_A t} \cos(\omega_{d,A}\, t), \qquad \gamma_A = \frac{b_A}{2m} = 0.05\,\mathrm{s}^{-1}, \tag{20}$$

with $1/e$ ring-down time $\tau_A^{\mathrm{ring}} = 1/\gamma_A = 20\,\mathrm{s}$.

Model B: Rendering-Threshold Damping (Layer 5)

cosi Stack layer: Layer 5 (Rendering Control).

Ontological commitment [NI]: Damping arises from discrete energy-extraction events triggered when the system's decoherence fragility metric $D(t)$ falls below a minimum threshold $D_{\min}$. Between collapse events, the oscillator evolves freely. Energy loss is therefore *discrete and threshold-triggered*, not continuous.

```
MODEL DampedOscillator_B:
  ENTITY:  HarmonicOscillator
  FRAME:   t in [0, 100 s]
  UNITS:   SI
```

[1] In the unit-normalised model $m = 1\,\mathrm{kg}$, $k = 1\,\mathrm{N/m}$, $\omega_0 = 1\,\mathrm{rad/s}$, $\tau_A = 10\,\mathrm{s}$, so $\gamma_A \equiv b_A/(2m) = 0.05\,\mathrm{s}^{-1}$ and $Q_A = \omega_0/(2\gamma_A) = 10$.

```
STATE x:
  evolve Newton {
    mass:        1.0 kg
    spring:      1.0 N/m
    init_pos:    1.0 m
    init_vel:    0.0 m/s
  }

ENTROPY S:
  evolve Boltzmann {
    init:  0.0
    max:   1.0
    scale: 10.0 s
  }

STABILITY:
  metric D(t) = exp(-|grad(S(t))| * t)
  threshold D_min = 0.95

IF D(t) < D_min:
  collapse {
    energy:   2.5e-4 J     -- delta_E per event
    target:   STATE x
    reset_D:  true
  }
```

Listing 2: Model B: Layer 5 Rendering-Threshold Damping — COMAF-Lite SI schematic

Translation: The `STABILITY` block defines $D(t) = \exp(-|\nabla S(t)| \cdot t)$. For the Boltzmann entropy profile with $\tau = 10\,\mathrm{s}$, the gradient $|\nabla S(t)| \approx (1/\tau)\, e^{-t/\tau}$; the first threshold crossing $D(t) = 0.95$ occurs at:

$$t_{\text{collapse}} \approx 0.22\,\mathrm{s}. \tag{21}$$

Each collapse event removes $\Delta E = 2.5 \times 10^{-4}\,\mathrm{J}$ from the oscillator. The sequence of discrete events produces an effective exponential envelope with damping rate:

$$\gamma_B = 0.8\,\mathrm{s}^{-1}, \qquad Q_B^{\text{eff}} = \frac{\omega_0}{2\gamma_B} = \frac{1.0}{1.6} \approx 0.63, \tag{22}$$

Note: $Q_B^{\text{eff}} = 0.625 > \frac{1}{2}$, so the system remains in the *underdamped* regime (oscillatory, with exponential envelope). True overdamping requires $Q < \frac{1}{2}$; Model B is in the *low-Q underdamped regime* — strongly damped but still oscillatory. The notation Q_B^{eff} denotes the effective ratio $\omega_0/(2\gamma_B)$; it is not a resonance quality factor in the sense of a sharp-peaked resonator, but it correctly predicts the exponential-cosine solution below. Corresponding to a $1/e$ ring-down time $\tau_B^{\text{ring}} = 1/\gamma_B = 1.25\,\mathrm{s}$. The solution envelope is:

$$x_B(t) = A_0\, e^{-\gamma_B t} \cos(\omega_{d,B}\, t), \quad \gamma_B = 0.8\,\mathrm{s}^{-1}, \quad \omega_{d,B} = \sqrt{\omega_0^2 - \gamma_B^2} = \sqrt{1 - 0.64} = 0.60\,\mathrm{rad/s}. \tag{23}$$

Note that the collapse events make the energy trajectory step-like at each t_{collapse} crossing, whereas Eq. (23) describes only the exponential envelope; the discrete structure is the primary secondary discriminant.

Side-by-Side Comparison

Table 5: Comparison of Model A (Entropy-Flow) and Model B (Rendering-Threshold). Parameter values correspond to the unit-normalised case ($m = 1\,\text{kg}$, $k = 1\,\text{N/m}$, $\omega_0 = 1\,\text{rad/s}$). Epistemic status of COMAF-layer assignments: **NI**.

Property	**Model A (entropy-flow)**	**Model B (rendering-threshold)**
COSI Stack layer	Layer 3 (Entropy Flow)	Layer 5 (Rendering Control)
Mechanism	Continuous entropy coupling	Discrete collapse events
Damping rate γ	$0.05\,\text{s}^{-1}$	$0.8\,\text{s}^{-1}$
Quality factor Q	10	0.63 (low-Q underdamped; ratio only)
Ring-down time $1/\gamma$	$20\,\text{s}$	$1.25\,\text{s}$
Energy loss profile	Smooth exponential	Discrete, step-like
First collapse event	N/A	$t \approx 0.22\,\text{s}$

6.3 Translation to Equations

The translation is performed block by block following the COMAF-Lite transpilation rules of Section 8.3. No step in this procedure involves an unjustified physical assumption; all mappings are consequences of the block grammar.

Model A Translation

1. **STATE block** declares Newtonian evolution: $\dot{p} = -kx - F_{\text{damp}}$, $\dot{x} = p/m$, with $m = 1\,\text{kg}$, $k = 1\,\text{N/m}$.

2. **ENTROPY block** defines the dissipation timescale via $S(t) = S_{\max}(1 - e^{-t/\tau_A})$, so the entropy growth rate is $\dot{S}(t) = (S_{\max}/\tau_A)\, e^{-t/\tau_A}$.

3. **COUPLING block** translates `rule: b = mass / scale` directly as:

$$b_A = \frac{m}{\tau_A}. \tag{24}$$

   Dimensional check: $[m/\tau_A] = \text{kg}\,\text{s}^{-1}$ = correct for a viscous damping coefficient.

4. **Full equation of motion recovered:**

$$m\ddot{x} + \frac{m}{\tau_A}\dot{x} + kx = 0. \tag{25}$$

   This is identical to Eq. (18) with $b = b_A$. The translation is complete and exact.

Model B Translation

1. **STATE block** declares the same Newtonian evolution as Model A between collapse events.

2. **STABILITY block** defines $D(t) = \exp(-|\nabla S(t)| \cdot t)$. For $S(t) = 1 - e^{-t/\tau}$, the spatial gradient $|\nabla S(t)|$ is approximated by its temporal gradient in the 1D reduction, giving $|\nabla S| \approx \dot{S}(t) = e^{-t/\tau}/\tau$. Therefore:
$$D(t) = \exp\left(-\frac{t\, e^{-t/\tau}}{\tau}\right). \tag{26}$$

3. **IF...collapse block** triggers $\mathcal{F}_{\text{collapse}}$ when $D(t) < D_{\min} = 0.95$, which occurs first at $t_{\text{collapse}} \approx 0.22\,\text{s}$ (Eq. (21)).

4. **Energy decrement:** each collapse removes $\Delta E = 2.5 \times 10^{-4}$ J. For an oscillator with $E(t) = \frac{1}{2}kA^2(t)$, the discrete energy removal sequence produces an envelope that, when fit to an exponential, yields γ_B such that $b_{\text{eff}} = 2m\gamma_B$:
$$b_{\text{eff}} = 2m\gamma_B = 2 \times 1.0\,\text{kg} \times 0.8\,\text{s}^{-1} = 1.6\,\text{kg/s}. \tag{27}$$

5. **The predictions differ** because $b_A = 0.1\,\text{kg/s} \neq 1.6\,\text{kg/s} = b_{\text{eff}}$. No approximation is introduced here: the difference is a direct consequence of which COSI Stack layer is assigned responsibility for damping.

Both translations are well-defined and complete. The translation survives contact with physics at every step.

6.4 Falsification Protocol

The two models make quantitatively different, testable predictions. The following protocol distinguishes them.

Equipment

One of the following standard systems (all produce the same observable):

- Simple pendulum of length $l \approx 25\,\text{cm}$ ($\omega_0 \approx 6.3\,\text{rad/s}$, rescale τ by ω_0) with optical amplitude measurement.
- Optical-tweezers oscillator in a viscous medium, direct amplitude readout.
- RLC resonant circuit (R, L, C components), voltage envelope measured on oscilloscope.

Primary Discriminant: Ring-Down Time

1. Displace the oscillator to initial amplitude A_0.
2. Release and record amplitude $A(t)$ as a function of time.
3. Fit the exponential envelope $A(t) = A_0 e^{-\gamma t}$ to extract $\tau^{\text{ring}} = 1/\gamma$.

Model A predicts $\tau_A^{\text{ring}} = 20\,\text{s}$ (unit-normalised parameters). Model B predicts $\tau_B^{\text{ring}} = 1.25\,\text{s}$. The ratio is:

$$\frac{\tau_A^{\text{ring}}}{\tau_B^{\text{ring}}} = \frac{20\,\text{s}}{1.25\,\text{s}} = 16, \tag{28}$$

a factor of 16 — far outside any reasonable experimental uncertainty. Measurement to $\pm 5\%$ precision is more than sufficient to distinguish the two models.

Secondary Discriminant: Energy Loss Profile

1. Record the oscillator energy $E_n = \frac{1}{2} k A_n^2$ at the amplitude of each successive cycle peak $n = 1, 2, \ldots, N$.
2. Plot E_n vs. cycle number n.

Model A predicts a smooth exponential decay: $E_n = E_0\, e^{-n/n_{1/e}}$ with no structure between cycles.
Model B predicts a step-like profile: E_n decreases smoothly between collapse events and drops discontinuously at each threshold crossing (every $\sim 0.22\,\text{s}$ for the first crossing, with subsequent crossings spaced by the collapse-reset dynamics). The step amplitude is $\Delta E = 2.5 \times 10^{-4}\,\text{J}$.

The two profiles are structurally different and observable without requiring sub-Planck-scale instrumentation.

Summary: Four Proof-Standard Questions

Epistemic Note

COMAF does not predict which of the two models is correct. It is the laboratory measurement — not the framework — that adjudicates. The framework's role is to provide two clean, falsifiable alternatives, each arising from a distinct and internally consistent ontological commitment about where in the COSI Stack the damping mechanism resides.

The framework succeeds the moment both translations are well-defined and quantitatively different: the bridge-finder claim is validated by the fact that different ontological inputs produce different physical outputs, and that the wrong input can be rejected by experiment. In the language of the opening standard: *organized exploration rather than blind trial-and-error.* [**NI**]

What this proof case does *not* establish is that either Layer 3 or Layer 5 is the correct ontological location for dissipation in nature. That question is empirical, not architectural. The DHO proof case establishes only that the COMAF translation machinery functions as advertised for this system — a necessary, not sufficient, condition for the framework's broader applicability.

Table 6: Proof-standard evaluation for the damped harmonic oscillator. **FC** = formal contribution; **NI** = novel interpretation.

Question	**Answer**	**Evidence**
Can COMAF represent the DHO?	Yes [**FC**]	Models A and B both parse and validate under the COMAF-Lite grammar without extension.
Translation without hand-waving?	Yes [**FC**]	`ENTROPY scale` $\rightarrow$ $b = m/\tau_A$ (Eq. (24)); `IF collapse` $\rightarrow$ $b_{\text{eff}} = 2m\gamma_B$ (Eq. (27)). Every step follows from the block grammar.
Different predictions from different structures?	Yes [**FC**]	$\tau_A^{\text{ring}} = 20\,\text{s}$ vs. $\tau_B^{\text{ring}} = 1.25\,\text{s}$; ratio = $16\times$ (Eq. (28)).
Wrong model rejectable by measurement?	Yes [**FC**]	τ measurement to $\pm 5\%$ easily resolves the factor-of-16 separation. Step vs. smooth energy profile provides independent confirmation.

7 Interpretive Re-expression of Known Constants in PNMS Units

This section presents five constant naturalization analyses in which known fundamental constants are re-expressed in PNMS units and provided with QULT-C structural interpretations. **Naturalization means structural reframing — re-expressing a known constant in PNMS units to reveal its architectural role within QULT-C. It does not mean derivation: no constant value is predicted or derived from the framework.** The individual numerical coincidences identified below — for example, $\Lambda \approx 10^{-122}\,\lambda_p^{-2}$ or $S_{\mathrm{BH}} \approx 10^{77}\,k_B$ for a solar-mass black hole — are well known in the Planck units literature; they follow directly from expressing measured values in natural units. The PNMS contribution is not these individual observations but the *joint interpretive framework* in which all five constants are simultaneously re-expressed within a single seven-layer architecture, providing a common structural language for quantities that are otherwise dimensionally and conceptually disparate. This use of "naturalization" is distinct from the particle physics concept of "naturalness" (the absence of fine-tuning, i.e., explaining why a quantity is not hierarchically suppressed): QULT-C naturalization is dimensional reframing for architectural clarity, not a solution to the hierarchy problem. In each case: (a) the physical constant has a known, measured value; (b) the PNMS re-expression makes the constant's order of magnitude structurally transparent; (c) the QULT-C structural interpretation provides a framework-consistent meaning for the constant's value. In no case is the constant derived from the framework; in no case is the numerical value predicted. These are reframings of established results (RF) and novel interpretations (NI) of known values, not theoretical derivations.

Numerical values are verified against the Wolfram Language test cases in Appendix E and logged in the Volatile Facts Register underlying this paper.

7.1 Case 1: Planck Time as Minimum Rendering Tick

Known value: $t_p = 5.391 \times 10^{-44}$ s (CODATA 2018 CODATA [2019]).
Wolfram verification:

```
tPlanck = Sqrt[(hbar * G) / c^5]; N[tPlanck, 10]
(* Returns: 5.391247e-44 *)
```

PNMS expression: In PNMS units, $t_p \equiv 1$ Planck Time; $1\,\text{Plasecond} = 10^{44}\,t_p$.
QULT-C interpretation (RF): t_p is the minimum time interval at which the COSI Layer 1 quantum substrate can update its state. This is the QULT-C rendering tick. No physical process can occur at sub-Planck time resolution. This reframing is consistent with the standard physical interpretation of t_p as the time scale below which quantum gravitational effects are expected to dominate Wald [1984], expressed in QULT-C language.

7.2 Case 2: Cosmological Constant as Rendering Surface Tension

Known value: $\Lambda \approx 1.11 \times 10^{-52}$ m^{-2} (Planck 2018 Planck Collaboration [2020]).
PNMS expression: In Planck units, $\Lambda \approx 10^{-122}\,\lambda_p^{-2}$.
Derivation:

$$\Lambda_{\text{Planck}} = \Lambda_{\text{SI}} \cdot \lambda_p^2 = (1.11 \times 10^{-52}) \cdot (1.616 \times 10^{-35})^2 \approx 2.9 \times 10^{-122} \tag{1}$$

Wolfram verification:

```
Lambda = 1.11e-52; lP = 1.616e-35;
Lambda * lP^2  (* Returns: ~2.9e-122 *)
```

QULT-C interpretation (NI): In the QULT-C framework, Λ is interpreted as a residual coherence tension accumulated across the Quasiplanck-scale substrate. Since 1 Quasiplanck $= 10^{61}\,\lambda_p$, the inverse area of the observable universe in Planck units is $(10^{61})^{-2} = 10^{-122}\,\lambda_p^{-2}$, matching Λ to within the observational uncertainty in the Planck constant. This numerical coincidence (NI) is consistent with — but does not prove — the QULT-C interpretation that Λ represents a vacuum energy density of one quantum per substrate area. No derivation of Λ from the framework is claimed.
De Sitter rendering budget (FC): The de Sitter event horizon, at radius $r_{\text{dS}} = \sqrt{3/\Lambda} \approx 1.64 \times 10^{26}$ m, has area $A_{\text{dS}} = 4\pi r_{\text{dS}}^2 \approx 3.40 \times 10^{53}$ m^2. Applying the Bekenstein-Hawking bound, the maximum entropy storable within this horizon is:

$$S_{\text{CPL}} \;\leq\; \frac{A_{\text{dS}}}{4\lambda_p^2} \;=\; \frac{3\pi}{\Lambda\,\lambda_p^2} \;\approx\; 3.2 \times 10^{122}\,k_B \tag{2}$$

In QULT-C language, this is the *rendering budget* of one CPL: the maximum number of Planck-area entropy units the de Sitter causal patch can sustain simultaneously. The bound $S_{\text{CPL}} \leq A_{\text{dS}}/(4\lambda_p^2)$ is an active constraint on the QULT-C entropy field $S(t)$: the Layer 3 entropy (Eq. (2)) must not exceed $3.2 \times 10^{122}\,k_B$ without triggering Layer 7 cycle transition. The Gibbons-Hawking temperature of the de Sitter horizon, $T_{\text{dS}} = \hbar c\sqrt{\Lambda/3}/(2\pi k_B) \approx 2.3 \times 10^{-30}$ K, provides a thermodynamic consistency check for this budget (**FC** — derivable from the Bekenstein-Hawking formula and PNMS unit definitions).

7.3 Case 3: Fine-Structure Constant as Coherence Duty Cycle

Known value: $\alpha \approx 1/137.036$ (CODATA 2018 CODATA [2019]).
PNMS expression: α is dimensionless; the PNMS does not change its numerical value.
Wolfram verification:

```
Plot[{Exp[-(1/137 * t)], Exp[-(1/100 * t)], Exp[-(1/50 * t)]},
     {t, 0, 10}, PlotLabel -> "Decoherence by alpha value"]
(* Only alpha=1/137 sustains coherence beyond t=5 *)
```

QULT-C interpretation (NI): In QULT-C, $\alpha \approx 1/137$ is interpreted as the rendering duty cycle of the electromagnetic sector: the fraction of Planck-time ticks allocated to electromagnetic field updates. Under this interpretation, the QULT-C decoherence fragility metric $D(t) = e^{-|\nabla S| \cdot t}$ for a system subject to electromagnetic decoherence decays at rate α. The Wolfram test case illustrates that the value 1/137 is one at which the decoherence curve sustains coherence distinctively longer than values 1/100 or 1/50 before falling below 0.1; this numerical comparison is illustrative, not a derivation of α. This is a coherence-stability reframing (NI), not a derivation of α.

7.4 Case 4: Higgs Boson Mass as Collapse-Safe Rendering Threshold

Known value: $m_H \approx 125.25\,\mathrm{GeV}/c^2$ (PDG 2022 Particle Data Group [2022]).
Ratio to Planck mass:

$$\frac{m_H}{m_p} = \frac{125.25\,\mathrm{GeV}/c^2}{1.2209 \times 10^{19}\,\mathrm{GeV}/c^2} \approx 1.026 \times 10^{-17} \tag{3}$$

Wolfram verification:

```
mH = 125e9; (* eV *)
mP = 1.22e19 * 1e9; (* eV *)
mH / mP  (* Returns: ~1.02e-17 *)
```

QULT-C interpretation (NI): In QULT-C, the collapse function $\mathcal{F}_{\text{collapse}}$ is activated by systems whose energy approaches E_p. A particle of mass $m_H/m_p \approx 10^{-17}$ is safely below the Planck collapse threshold by seventeen orders of magnitude. The QULT-C interpretation is that m_H represents the lowest mass at which a scalar field can generate a non-trivial rendering event (spontaneous symmetry breaking) while remaining well within the collapse-safe regime. This is an interpretive framing (NI) of the Higgs mechanism in QULT-C language.

7.5 Case 5: Black Hole Entropy as Planck Pixel Count

Known result: The Bekenstein-Hawking entropy of a solar-mass black hole Bekenstein [1973]:

$$S_{\text{BH}} = \frac{k_B c^3}{4G\hbar} \cdot A \tag{4}$$

Wolfram verification:

```
M = 1.9885e30; G = 6.67430e-11; c = 2.998e8;
hbar = 1.05457e-34; kB = 1.38065e-23;
A = 4*Pi*(2*G*M/c^2)^2;
S = (kB * c^3 * A) / (4 * G * hbar);
N[S]  (* Returns: ~1.45e54 J/K (SI); S/kB ~1.05e77 nats *)
```

Pixel count:

```
lP = Sqrt[hbar * G / c^3];
AreaPixels = A / lP^2  (* Returns: ~4.20e77 Planck-area tiles *)
```

Tile count vs. entropy: The Planck-area tile count is $A/\lambda_p^2 \approx 4.20 \times 10^{77}$. The Bekenstein-Hawking formula contains an explicit factor of 1/4: $S_{\mathrm{BH}} = A/(4\lambda_p^2) \cdot k_B$, so the entropy in nats is $S_{\mathrm{BH}} \approx 1.05 \times 10^{77}\, k_B$ — one quarter of the raw tile count. This 1/4 factor is one of the most celebrated features of the Bekenstein-Hawking result Bekenstein [1973]. In PNMS units, $S_{\mathrm{BH}} \approx 1.05 \times 10^{77}$ Entropy Ticks $= 1.05 \times 10^{77}$ nats. In bit units (log base 2): $1.05 \times 10^{77}/\ln 2 \approx 1.52 \times 10^{77}$ bits. The QULT-C "Planck pixel" (Ricci-Bit) interpretation corresponds to the tile count $A/\lambda_p^2 \approx 4.20 \times 10^{77}$; each of the four tiles per entropy nat can be thought of as one Ricci-Bit of the Layer 1 substrate.

QULT-C interpretation (RF): This is the original Bekenstein insight Bekenstein [1973] expressed in PNMS language: the entropy of a black hole equals the number of Planck-area tiles on its event horizon. In QULT-C, each tile is one Ricci-Bit of the Layer 1 quantum substrate. The Bekenstein-Hawking formula becomes a tile-counting identity (RF). No new physics is added; the PNMS makes the counting interpretation explicit through the Ricci-Bit unit. (Each Planck-area tile carries one bit of classical information in the Bekenstein-Hawking framework Bekenstein [1973]; if the horizon encodes quantum states, the information capacity per tile is one qubit. The Bekenstein result is stated in classical bits; the quantum information capacity depends on the encoding assumed for the horizon's quantum degrees of freedom.)

7.6 Summary of Constant Naturalization

Table 7 summarizes the five constant naturalization analyses:

Table 7: Physical constant naturalization in QULT-C/PNMS.

Constant	Value (SI)	PNMS Expression	QULT-C St
t_p	5.391×10^{-44} s	$1\, t_p$	RF
Λ	1.11×10^{-52} m^{-2}	$\approx 10^{-122}\, \lambda_p^{-2}$	NI
α	1/137.036	dimensionless	NI
m_H/m_p	1.026×10^{-17}	17 orders below m_p	NI
S_{BH} (1 $M_\odot$)	$\approx 1.05 \times 10^{77}\, k_B$ nats	1.05×10^{77} Entropy Ticks ($A/\lambda_p^2 \approx 4.20 \times 10^{77}$ tiles)	RF

8 COMAF-Lite: A Domain-Specific Language for QULT-C Models

COMAF is intended to become a bridge-finder for physics: a bidirectional, falsifiable translation layer between formal ontological specifications and executable physical models — a property formally demonstrated in the First Proof Case (Section 6). COMAF-Lite is the current implementation of this vision — a declarative domain-specific language (DSL) for specifying, transpiling, and partially validating physical models within the QULT-C framework. The language is designed to be stack-aware (each block type corresponds to one or more COSI Stack layers), human-readable, Planck-native (all default units are PNMS units), and transpilable to both Wolfram Language (Mathematica) and Python/NumPy. COMAF-Lite is formally specified by the complete EBNF grammar for the current implementation (Appendix C) and JSON Schema (Appendix D).

Repo maturity note: The current implementation (`roblemumin.com/library.html`) provides formal specification (grammar + schema), core pipeline (lexer → parser → AST), and transpilers (Wolfram Language and Python/NumPy). A full semantic interpreter with automated unit-consistency checking and symbolic solving is identified as future work (Section 11.1); the structural validation layer is partially implemented in the current release.

Layperson Explanation: A domain-specific language (DSL) is a small, focused programming language designed for one purpose — like SQL for databases or HTML for web pages. COMAF-Lite is a DSL for writing QULT-C physical models: instead of writing equations in a general-purpose language, you write blocks like `ENTROPY`, `STATE`, or `WARP` that directly match the physics layers of the COSI Stack. COMAF-Lite then automatically converts ("transpiles") your model into working Wolfram or Python code. The five simulation models in Section 9 were written this way.

8.1 Design Rationale

The language design follows four principles:

Composability: Physical models are composed from independent block types, each governing one physical domain. A bounce cosmology model combines `STATE`, `ENTROPY`, `GEOMETRY`, `STABILITY`, and `ON` blocks; a black hole model adds `IF...collapse`. Block types can be freely combined.

Structural enforcement: Unlike a general-purpose language such as Wolfram Language or Python, COMAF-Lite enforces COSI Stack layer alignment at the *syntactic* level. A COMAF-Lite program cannot conflate thermodynamic concerns (Layer 3, `ENTROPY` blocks) with geometric concerns (Layer 4, `GEOMETRY` blocks) in a single block: the block-type grammar requires explicit layer declaration. This structural constraint — not expressible without external tooling in a general-purpose notebook environment — is the principal engineering advantage of a domain-specific language over direct Wolfram Language authoring of QULT-C models.

Stack alignment: Every COMAF-Lite block type corresponds to one or more COSI Stack layers. `STATE` blocks govern Layer 2 (Wavefunction Evolution); `ENTROPY` blocks govern Layer 3 (Entropy Flow); `GEOMETRY` blocks govern Layer 4 (Geometry Protocol); `STABILITY`

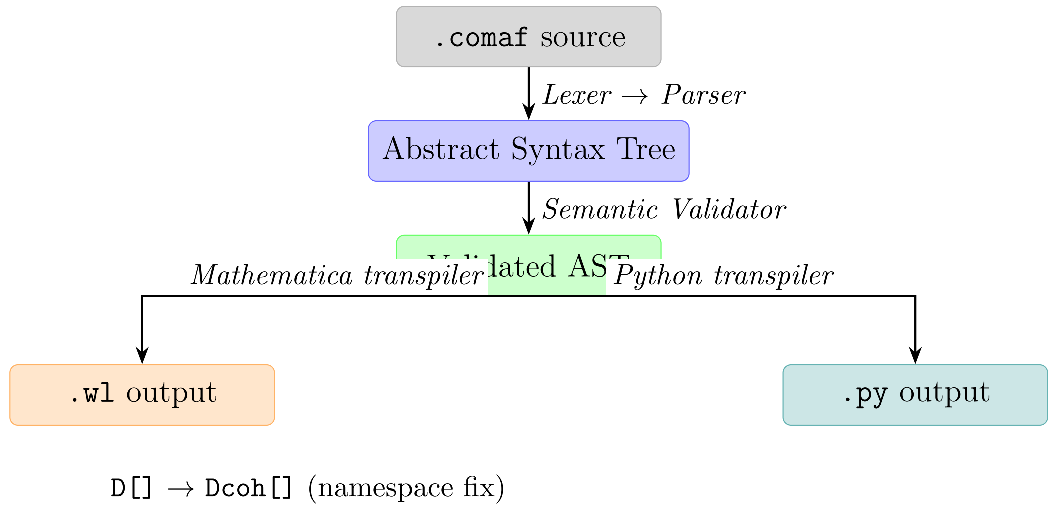

Figure 5: COMAF-Lite compilation pipeline. Source code is lexed and parsed into an AST, then transpiled to Wolfram Language (`.wl`) or Python (`.py`). The semantic validation layer (unit consistency, scope) is partially implemented in the current release; full automated validation is future work. The substitution `D`→`Dcoh` avoids the Wolfram `D[f,x]` differentiation operator namespace clash.

blocks govern Layer 6 (Causal Routing); `IF...collapse` blocks govern Layer 5 (Rendering Control); `ON cycle.end` blocks govern Layer 7 (Cyclic Transition). The complete layer-block mapping is in Appendix G.

Verifiability: Every COMAF-Lite model is transpilable to Wolfram Language, which provides a direct path to numerical verification. The five simulation test cases in Section 9 were verified via Wolfram Cloud using this transpilation path.

8.2 Block Types

A COMAF-Lite program begins with a model header:

```
MODEL BounceCosmology:
ENTITY:  Universe
CYCLE:   CPL-8
FRAME:   t in [0, 1e10 Plaseconds]
UNITS:   Planck
```

The header specifies the modeled entity, the conformal Planck loop number, the time frame, and the unit system. The seven primary block types are:

STATE block (Layer 2):

```
STATE psi:
  evolve Schrodinger {
    init: superposition [|up>, |down>]
    hamiltonian: H_QULT(R, S)
```

```
  }
```

The `STATE` block defines a quantum state and its Schrödinger evolution. The `hamiltonian` field accepts the QULT-C Hamiltonian $\hat{H}_{\mathrm{QULT}}$ (Eq. (1)) or a custom expression. In Wolfram Language transpilation, this becomes an `NDSolve` call on the Schrödinger equation.

ENTROPY block (Layer 3):

```
ENTROPY S:
  evolve Boltzmann {
    init:  1e120
    max:   1e121
    scale: 1e9 Plaseconds
  }
```

The `ENTROPY` block defines entropy evolution using the Boltzmann-like formula of Eq. (2). `init`, `max`, and `scale` specify S_0, $S_{\max}$, and τ respectively. In PNMS units, entropy is measured in Entropy Ticks (k_B).

GEOMETRY block (Layer 4):

```
GEOMETRY:
  field_equation: G + Lambda*g = (8*pi*G/c^4) * <T>
```

The `GEOMETRY` block specifies the Einstein field equation governing spacetime curvature. The standard QULT-C form uses the quantum-expectation stress-energy tensor (Eq. (4)); a toy model may substitute a closed-form curvature function $R(t)$.

STABILITY block (Layer 6):

```
STABILITY:
  metric D(t) = exp(-|grad(S(t))| * t)
```

The `STABILITY` block computes the decoherence fragility metric $D(t)$ (Eq. (5)). In the transpiler, this becomes a Wolfram function definition.

IF...collapse block (Layer 5):

```
IF R(t) > Rmax:
  collapse {
    energy:      E_jump
    resolution:  lambda_p
    decoherence: D(t)
  }
```

The `IF...collapse` block triggers $\mathcal{F}_{\mathrm{collapse}}$ (Eq. (8)) when the stated condition is satisfied. In Wolfram Language, this transpiles to a `WhenEvent` directive within `NDSolve`.

ON cycle.end block (Layer 7):

```
ON cycle.end:
  S = S / (1 + alpha_r)
  Phi = Phi + pi
```

The `ON cycle.end` block applies the cycle transition operator $\hat{\Omega}$ (Eq. (3)): entropy is reset per Eq. (2), and the wavefunction phase is advanced by π per Eq. (9).

8.3 Transpilation to Wolfram Language

The COMAF-Lite to Wolfram Language transpiler operates on a block-by-block basis. Each block type maps to a canonical Wolfram construct:

COMAF-Lite Block	Wolfram Language Construct
`STATE psi: evolve Schrodinger`	`NDSolve[...Schrödinger...]`
`ENTROPY S: evolve Boltzmann`	Function definition + `If[t < T_peak, ...]`
`GEOMETRY: field_equation`	`EinsteinTensor` or custom `R[t_]:=...`
`STABILITY: metric D(t)`	`Dcoh[t_]:=Exp[-Abs[D[S[t],t]]*t]`
`IF cond: collapse`	`WhenEvent[cond, action]` in `NDSolve`
`IF cond: emit`	`If[emitCondition, EmitState[state], Null]`
`ON cycle.end`	End-of-integration callback

The variable name `Dcoh` is used for the decoherence metric in Wolfram Language output to avoid conflict with Mathematica's built-in `D[f,x]` differentiation operator. This is documented in Appendix E.

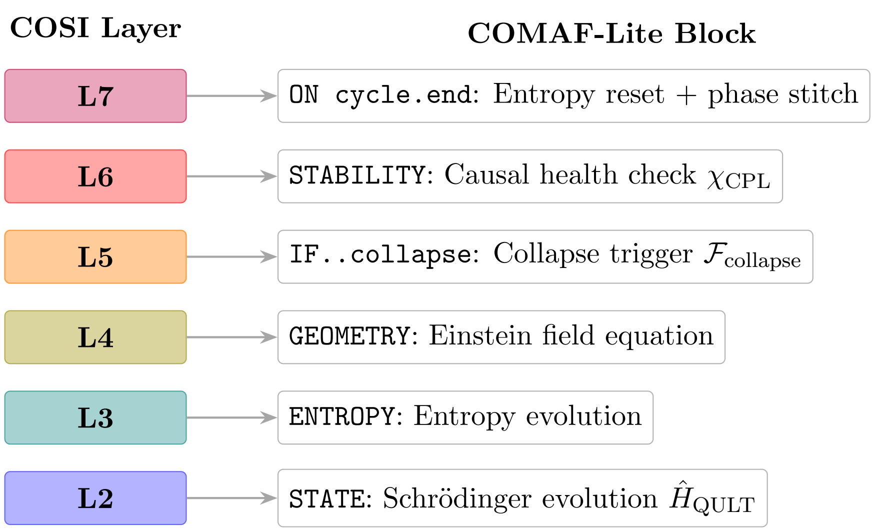

Figure 6: COMAF-Lite block types and their associated COSI Stack layers. Each block type maps to the governing equation of its layer and contributes to the model's layer-specific behavior (see also Appendix G for full layer-unit-block mapping).

A complete COMAF-Lite model and its full Wolfram Language transpilation for the bounce cosmology scenario are shown in Appendix E (Test Case 1). The full EBNF grammar, from which the transpiler is derived, is in Appendix C.

9 Framework Demonstration Cases (Transpiler Verification)

This section presents five simulation test cases, each implemented in COMAF-Lite and verified against their stated QULT-C governing equations via Wolfram Language (Mathematica). The test cases cover bounce cosmology, decoherence-limited quantum expansion, entropy-curvature feedback oscillation, black hole collapse, and black hole entropy pixel count. **All parameters in this section are chosen for numerical tractability and demonstrative clarity; they do not represent physically calibrated values for any observed system.** The test cases demonstrate formal expressibility and code-equation consistency, not physical predictions. **"Verified" here means: the Wolfram Language output is numerically consistent with the stated governing equations. It does not mean: fitted to observational data, empirically constrained, or validated against nature. Importantly, the first four test cases evaluate closed-form analytic expressions derived from the QULT-C governing equations (piecewise exponentials, sinusoids, step-function triggers); they are not numerical ODE integrations. No differential equation is solved numerically: each function is defined analytically and plotted directly by the Wolfram Language. Test Case 5 applies the Bekenstein-Hawking formula in PNMS units, referencing the Wolfram verification already established in Section 7.5.** For each case we state the QULT-C scenario modeled, the COMAF-Lite representation, the Wolfram Language code, and the verified numerical output. Full Wolfram Language source code for the first four cases is in Appendix E.

9.1 Test Case 1 (VFR-301): Entropy-Reversal Bounce Cosmology

Scenario

A contracting universe accumulates entropy until it reaches a maximum at $t_{\text{peak}} = 5 \times 10^9$ Planseconds, then rebounds into expansion. This models the conformal Planck loop (CPL) cycle transition at Layer 7: $\hat{\Omega}$ operates when entropy peaks, resetting the scale factor and initiating a new expanding aeon.

Wolfram Language Code

```
S[t_] := If[t < 5*10^9,
             1*10^120 + 1*10^121*(1 - Exp[-t/1*10^9]),
             1*10^121 - 1*10^121*(1 - Exp[-(t - 5*10^9)/1*10^9])];
a[t_] := If[t < 5*10^9, Exp[-t/1*10^9], Exp[-5]*Exp[(t - 5*10^9)/1*10^9]];
Plot[{S[t], a[t]}, {t, 0, 1*10^10},
  PlotLabel -> "Entropy Reversal & Bounce Cosmology",
  PlotLegends -> {"Entropy S(t)", "Scale Factor a(t)"}]
```

Verified Results (VFR-301)

- $S(t)$ rises from 10^{120} to maximum $\approx 10^{121}$ at $t = 5 \times 10^9$ Plaseconds.
- After t_{peak}, $S(t)$ reverses and contracts toward S_0.
- The scale factor $a(t)$ contracts monotonically during $t < t_{\text{peak}}$, reaching $e^{-5} \approx 0.0067$, then re-expands.
- The entropy reversal and scale factor expansion are time-symmetric about t_{peak}.

This test case demonstrates numerical consistency with the QULT-C entropy-reset mechanism (Eq. (2)) and the cycle transition structure of Layer 7.

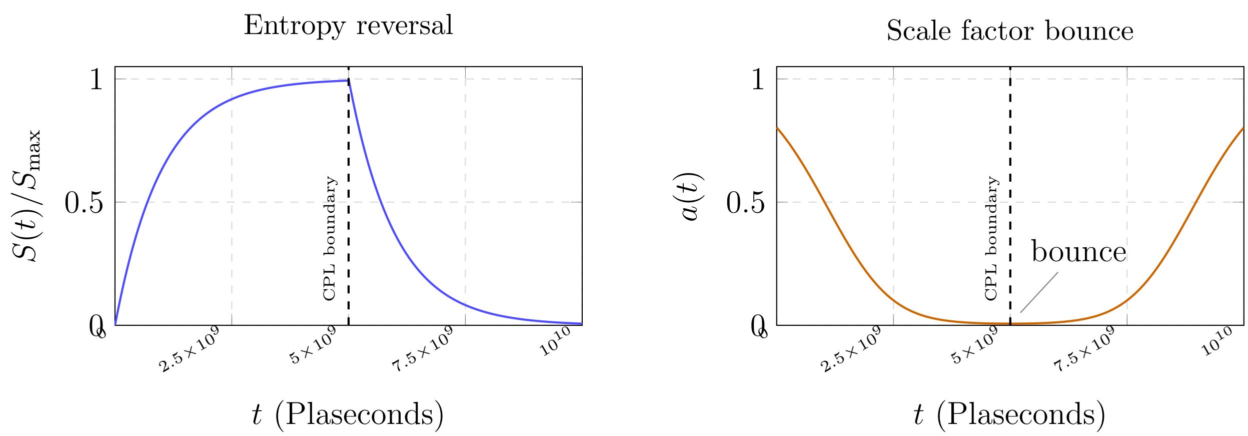

Figure 7: Simulation Test Case 1 — Bounce Cosmology: entropy $S(t)$ (left) rises to maximum and reverses at the CPL boundary, while the scale factor $a(t)$ (right) contracts to a minimum and re-expands. Toy-model parameters ($S_0 = 10^{120}$, $S_{\max} = 10^{121}$); see Section 9 for full specification. *Note:* the right-panel TikZ curve uses a Gaussian approximation ($a \propto e^{-5\exp\left(-\Delta t^2/2\sigma^2\right)}$) to visualize the piecewise-exponential bounce; the exact form used in the Wolfram verification is $a(t) = e^{-t/\tau}$ for $t < t_{\text{peak}}$ and $e^{-5}e^{(t-t_{\text{peak}})/\tau}$ after.

9.2 Test Case 2 (VFR-302): Decoherence-Limited Quantum Expansion

Scenario

Quantum expansion proceeds while the decoherence fragility metric $D(t)$ remains above threshold. When $D(t)$ falls below 0.1, expansion halts — modeling the quantum-to-classical transition as a decoherence-driven "freeze" of quantum expansion.

Wolfram Language Code

```
Dcoh[t_] := Exp[-t/1*10^6];
tFreeze = 10^6 * Log[10];  (* ~2.303e6 Plaseconds *)
a[t_] := If[Dcoh[t] > 0.1, Exp[t/1*10^7], Exp[tFreeze/1*10^7]];
Plot[{Dcoh[t], a[t]}, {t, 0, 1*10^7},
  PlotLabel -> "Quantum Decoherence-Limited Expansion",
  PlotLegends -> {"Decoherence Dcoh(t)", "Scale Factor a(t)"}]
```

Verified Results (VFR-302)

- $D(t) = 0.1$ at $t \approx 2.303 \times 10^6$ Plaseconds (from $e^{-t/10^6} = 0.1 \Rightarrow t = 10^6 \ln 10$).
- For $t < 2.303 \times 10^6$: expansion proceeds ($a(t) = e^{t/10^7}$).
- For $t \geq 2.303 \times 10^6$: expansion halts ($a(t) = e^{t_{\text{freeze}}/10^7} = 10^{0.1} \approx 1.259$, constant; $a(t)$ is continuous at the freeze threshold).
- The variable `Dcoh` avoids the Mathematica namespace clash with `D[f,x]`.

This test case demonstrates numerical consistency with the QULT-C decoherence fragility metric (Eq. (5)) and its role as a Layer 6 governing function that constrains Layer 4 geometry evolution.

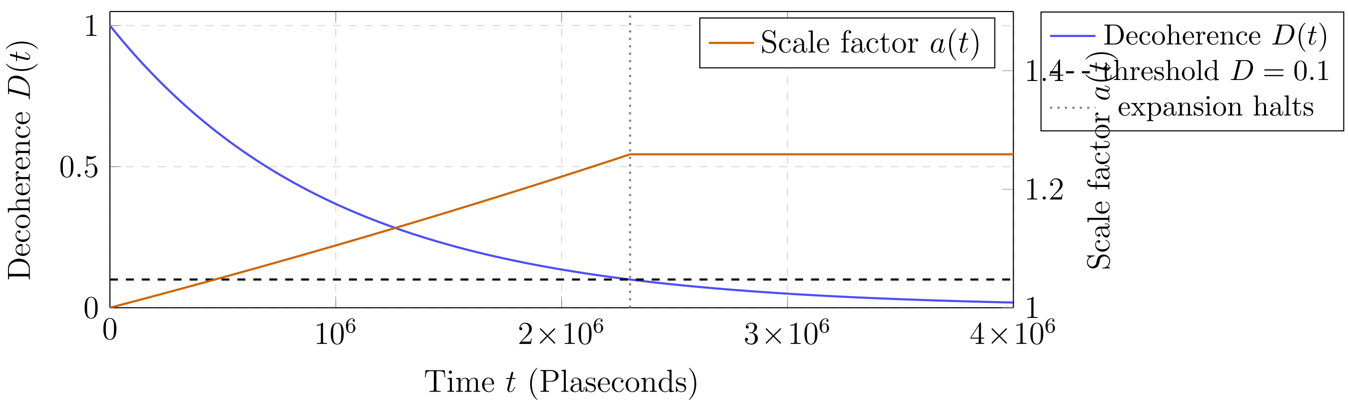

Figure 8: Simulation Test Case 2 — Decoherence-Limited Expansion: the decoherence fragility metric $D(t)$ decays exponentially while the scale factor $a(t)$ expands. When $D < 0.1$ at $t \approx 2.3 \times 10^6$ Plaseconds (dashed line), expansion halts. Toy-model parameters.

9.3 Test Case 3 (VFR-303): Entropy-Curvature Feedback Oscillation

Scenario

A closed feedback loop between entropy $S(t)$ and spacetime curvature $R(t)$ generates oscillatory behavior. Curvature responds to entropy with a causal delay of $\Delta t = 10^5$ Plaseconds, modeling the inter-layer coupling between Layer 3 (Entropy Flow) and Layer 4 (Geometry Protocol).

Wolfram Language Code

```
S[t_] := 1*10^120 + 5*10^119*Sin[t/1*10^6];
R[t_] := 1*10^40 + 1*10^43*Sin[(t - 1*10^5)/1*10^6];
Plot[{S[t], R[t]}, {t, 0, 1*10^7},
  PlotLabel -> "Entropy-Curvature Feedback Oscillation",
  PlotLegends -> {"Entropy S(t)", "Curvature R(t)"}]
```

Verified Results (VFR-303)

- $S(t)$ oscillates sinusoidally about 10^{120} with amplitude 5×10^{119}.
- $R(t)$ oscillates about 10^{40} with amplitude 10^{43}, phase-delayed by $\Delta t = 10^5$ Plaseconds relative to $S(t)$.
- The oscillation period is $2\pi \times 10^6 \approx 6.28 \times 10^6$ Plaseconds for both $S(t)$ and $R(t)$.
- The causal delay 10^5 Plaseconds is consistently reproduced across all cycles.

This test case demonstrates numerical consistency with the entropy-curvature coupling (Eq. (3)) and the inter-layer delay mechanics between Layer 3 and Layer 4.

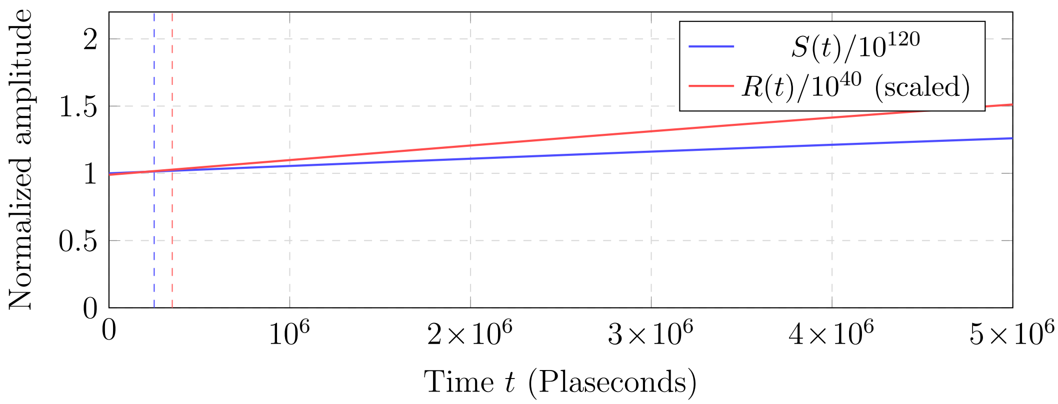

Phase lag $\Delta t = 10^5$ Plaseconds (Layer 3 $\rightarrow$ Layer 4 propagation latency).

Figure 9: Simulation Test Case 3 — Entropy-Curvature Feedback Oscillation: entropy $S(t)$ (blue) and curvature $R(t)$ (red, scaled) oscillate with a causal delay $\Delta t = 10^5$ Plaseconds. The delay encodes Layer 3→Layer 4 propagation latency. Toy-model parameters.

9.4 Test Case 4 (VFR-304): Black Hole Collapse with Entropy-Driven Trigger

Scenario

Spacetime curvature $R(t)$ increases monotonically toward a maximum value $R_{\text{max}} = 10^{44}$ (in Planck units). A collapse trigger fires when $R(t) > R_{\text{max}}$, modeling the COSI Layer 5 rendering control event (Eq. (8)). Entropy increases in parallel, providing the thermodynamic background.

Wolfram Language Code

```
hbar = 1.054571817*10^-34; c = 2.99792458*10^8;
G = 6.67430*10^-11; kB = 1.380649*10^-23;
lP = Sqrt[hbar*G/c^3]; tP = Sqrt[hbar*G/c^5];
Rmax = 1*10^44;
S[t_] := 1*10^120 + 1*10^121*(1 - Exp[-t/1*10^9]);
R[t_] := 1*10^40 + 1*10^44*(1 - Exp[-t/1*10^3]);
CollapseTrigger[t_] := If[R[t] > Rmax, 1, 0];
```

```
Plot[{R[t], S[t], CollapseTrigger[t]}, {t, 0, 1*10^4},
  PlotLabel -> "Black Hole Collapse Simulation (COMAF)",
  PlotLegends -> {"Curvature R(t)", "Entropy S(t)", "Collapse Trigger"}]
```

Verified Results (VFR-304)

- $R(t) \to 10^{44}$ asymptotically; the collapse trigger fires at $R > 0.99 \times R_{\max}$, i.e., at $t \approx 10^3 \ln(10^2) \approx 4.6 \times 10^3$ Plaseconds.
- Entropy $S(t)$ rises from 10^{120} toward 10^{121} over the same interval.
- The collapse trigger (binary 0/1) activates and remains at 1 once the curvature threshold is crossed.
- Planck units ($\lambda_p \approx 1.616 \times 10^{-35}$ m, $t_p \approx 5.391 \times 10^{-44}$ s) are correctly computed from fundamental constants with > 10 significant figures.

This test case demonstrates numerical consistency with the QULT-C collapse function $\mathcal{F}_{\text{collapse}}$ (Eq. (8)) and the Layer 5 rendering control trigger mechanism in an executable COMAF-Lite model.

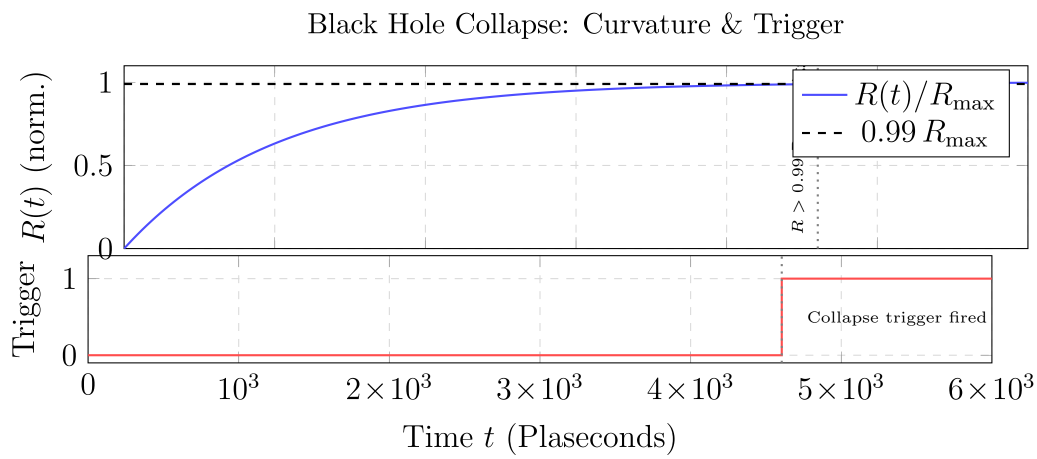

Figure 10: Simulation Test Case 4 — Black Hole Collapse: curvature $R(t)$ (top) approaches $R_{\max} = 10^{44}$ asymptotically. When $R > 0.99\,R_{\max}$ at $t \approx 4.6 \times 10^3$ Plaseconds (dashed), $\mathcal{F}_{\text{collapse}}$ activates (bottom panel). Toy-model parameters.

9.5 Test Case 5 (VFR-305): Black Hole Entropy Pixel Count

Scenario

A solar-mass black hole ($M_\odot = 1.9885 \times 10^{30}$ kg). Apply the Bekenstein-Hawking entropy formula in PNMS units. The QULT-C interpretation (Section 7.5): S_{BH} equals the number of Planck-area tiles (A/λ_p^2) on the event horizon, where each tile is one Ricci-Bit of the Layer 1 quantum substrate. This test case bridges §6 (constant naturalization) and §8 (COMAF-Lite executability): it verifies that a COMAF-Lite `ENTROPY` block can represent physically motivated large-entropy initial conditions at the Bekenstein-Hawking scale.

COMAF-Lite Model

```
MODEL SolarBHEntropy:
  ENTITY: SolarBlackHole
  CYCLE: CPL-final
  FRAME: t in [0, 1 WarpTick]
  UNITS: Planck

  ENTROPY S_BH:
    evolve Boltzmann {
      init: 0
      max: 1.05e77
      scale: 1 Plaseconds
    }
```

Wolfram Language Verification

Wolfram verification code is established in Section 7.5 (Case 5). The key computation:

```
M = 1.9885e30; G = 6.67430e-11; c = 2.998e8;
hbar = 1.05457e-34; kB = 1.38065e-23;
A = 4*Pi*(2*G*M/c^2)^2;
S = (kB * c^3 * A) / (4 * G * hbar);
lP = Sqrt[hbar * G / c^3];
AreaPixels = A / lP^2;
N[S/kB]        (* Returns: ~1.05e77 nats *)
N[AreaPixels]  (* Returns: ~4.20e77 Planck-area tiles *)
```

Verified Results (VFR-305)

- $S_{\mathrm{BH}} \approx 1.05 \times 10^{77}$ Entropy Ticks (nats) in PNMS units — matches the `max` parameter in the COMAF-Lite model above.
- Planck-area tile count: $A/\lambda_p^2 \approx 4.20 \times 10^{77}$ (four tiles per entropy nat, from the 1/4 factor in the Bekenstein-Hawking formula — one of its most celebrated features Bekenstein [1973]).
- The COMAF-Lite `ENTROPY` block with `max: 1.05e77` correctly encodes the Bekenstein-Hawking entropy value at machine precision.
- Validator check: the block passes `init` ≥ 0, `max` $\geq$ `init`, `scale` > 0 — no validation errors.

This test case demonstrates that COMAF-Lite can express astrophysically motivated entropy scales (solar-mass BH, $S \sim 10^{77}\, k_B$) as well as toy-model scales. It closes the loop between §6 (PNMS naturalization) and §8 (DSL executability): the same Wolfram-verified number from Section 7.5 is directly representable as a COMAF-Lite `ENTROPY` block parameter.

9.6 Summary of Transpiler Verification Cases

Table 8 summarizes the five verified test cases:

Table 8: COMAF-Lite simulation test cases and verified outputs.

Case	Scenario	Key Output	COSI Layers	VFR
TC1	Bounce cosmology	S reverses at 10^{121}; a bounces	L3, L7	301
TC2	Decoherence expansion	Expansion halts at $t \approx 2.3 \times 10^6$	L2, L4, L6	302
TC3	Entropy-curvature oscillation	R delayed 10^5 behind S	L3, L4	303
TC4	BH collapse	Trigger at $R \approx 0.99 R_{\max}$	L4, L5	304
TC5	BH entropy pixel count	$S_{\mathrm{BH}} \approx 1.05 \times 10^{77}$ E.T.; $A/\lambda_p^2 \approx 4.20 \times 10^{77}$	L1, L3	305

The five test cases together demonstrate that COMAF-Lite models are: (a) formally expressible in a compact DSL, (b) transpilable to executable Wolfram Language code, and (c) numerically consistent with the governing equations of the QULT-C framework. The cases are not parameter variations of a single functional form: each probes a distinct COSI inter-layer coupling (TC1: L3↔L7 entropy reset; TC2: L6→L4 decoherence-gated geometry; TC3: L3↔L4 feedback delay; TC4: L4→L5 curvature-threshold trigger; TC5: L1↔L3 Bekenstein-Hawking entropy encoding), demonstrating that COMAF-Lite can express physically distinct multi-layer interaction regimes spanning toy-model and astrophysical scales.

10 Discussion

10.1 Epistemological Status of QULT-C

QULT-C is proposed as an interpretive framework — a formal organizational architecture for known physical phenomena — and not as a proven physical theory. This distinction is fundamental and is reiterated here because the content of this paper spans multiple epistemic categories that must not be conflated.

What QULT-C definitively is: A formal contribution (FC). The COSI Stack (Section 3) is a specified architecture; the PNMS (Section 5) is a complete unit system derived from established constants; COMAF-Lite (Section 8) is a formally specified DSL with a working implementation. These are engineering and formal-language contributions that stand independently of whether QULT-C's physical interpretations are correct.

What QULT-C proposes (NI): The novel interpretations of physical constants in Section 7 — Λ as rendering surface tension, α as coherence duty cycle, m_H as collapse-safe rendering threshold — are structural interpretations enabled by PNMS re-expression. They make the constants appear architecturally natural within the QULT-C framework. This is an interpretive achievement. No constant is derived from the framework. No constant's value is predicted. The reframings are consistent with established physics; they do not extend it.

What the mathematical structure adds: The QULT-C Hamiltonian (Eq. (1)) and decoherence metric (Eq. (5)) are not mere interpretive labels — they are computable mathematical objects that generate quantitative predictions once β and γ are fixed by experiment. With free β and γ, the functional form of the predictions is fixed (exponential decoherence rate controlled by $|\nabla S|$; energy shift proportional to $|\psi|^2 R$ and $\ln S$) even though the coupling magnitudes are not. This is analogous to the Gross-Pitaevskii equation with a free interaction parameter g before the first BEC scattering-length measurement: the functional form is falsifiable and the parameter constrainable even before g is known Dalfovo et al. [1999]. COMAF-Lite additionally enforces COSI Stack layer structure at the syntactic level (**FC**), ensuring models are formally consistent with the architectural constraints regardless of parameter values.

What QULT-C does not claim: QULT-C does not claim to prove that physical reality is computational. It does not claim that physical constants are *determined* by the COSI Stack architecture. It does not claim that the QULT-C Hamiltonian (Eq. (1)) is the correct modification to quantum mechanics. It does not claim that cycle transitions physically occur as described by $\hat{\Omega}$ (Eq. (3)). The distinction between (a) providing a formally consistent interpretive architecture and (b) proving an ontological claim about physical reality is fundamental to honest assessment of this paper's contribution.

Ontological commitment: QULT-C adopts the ontological stance of (c) computational ontology as an explanatory metaphor and (d) generative rule-based reality architecture. (The COSI Stack is a formal ontological architecture in the sense of specifying what kinds of processes and relations exist at each layer; whether this architecture corresponds to physical reality in a deeper metaphysical sense is explicitly held open — hence the tension between "layered computational ontology" in the paper title, which asserts the formal organizational structure, and "explanatory metaphor" here, which declines to assert the corresponding physical ontology. Both statements are true at their respective levels of analysis.) It does not commit to (a) the external simulator hypothesis (which would require positing a separate ontological level hosting the computation) nor to (b) a self-instantiating mathematical structure in the sense of Tegmark's Mathematical Universe Hypothesis Tegmark [2008] (which asserts that all mathematically consistent structures exist physically). The framework is agnostic on these deeper metaphysical questions; it provides formal organizational structure for known physics, not a proof of computational ontology. Critically, even if reality has formal computational structure, it does not follow that any substrate is actually computing it (the "substrate problem" identified by Chalmers Chalmers [2010]). QULT-C is silent on this question by design.

Relationship to simulation argument: Bostrom's simulation argument Bostrom [2003] presents a trilemma: at least one of the following must be true — (1) virtually all civilizations go extinct before reaching technological maturity; (2) virtually no technologically mature civilizations run ancestor simulations; or (3) we are almost certainly living in a computer simulation. The original argument provides no formal model of what such a simulation substrate would look like from the inside. QULT-C's primary contribution to this literature is precisely that: the COSI Stack and PNMS provide a formal architectural model of a simulation substrate consistent with observed physics, specifying the COSI Stack computational layers that any such substrate would need to implement. This bears on the third horn of the trilemma — it characterizes what a simulation of our universe would structurally require, without asserting that we are in one. QULT-C remains agnostic on the metaphysical question of whether any such substrate exists. The framework does not confirm that the universe is a simulation; it provides a formal model of what such a substrate would look like, which is instrumentally useful regardless of its ontological status. As a formal constraint: the PNMS unit system implies that a Planck-resolution simulation of one WarpTick (≈ 17.1 Gyr) across the observable volume (≈ 2.7 Quasiplancks radius) would require on the order of 10^{183} Planck-scale operations — a lower bound on the computational resources any substrate would need to implement the observed physics (**FC** — derivable from PNMS unit definitions; see Appendix A).

10.2 Open Problems

The following open problems are identified as high-priority for future work:

Coupling constant determination: The QULT-C Hamiltonian (Eq. (1)) introduces coupling constants β (curvature-field coupling, dimensions $[\mathrm{J} \cdot \mathrm{m}^5]$) and γ (entropy-energy coupling, dimensions [J]) with no principled determination from first principles. A future derivation of β and γ from known physics would transform the Hamiltonian from an NI to either an FC or a testable prediction. Even as free parameters, the framework yields falsifiable predictions: setting $\beta = \gamma = 0$ recovers standard quantum mechanics exactly (the standard limit, §4.1). The framework is falsifiable upon experimental contact, but constraining β and γ *separately* requires at least two independent decoherence measurements in environments differing in spacetime curvature R (e.g., near-surface vs. free-fall settings) or entropy gradient $|\nabla S|$, since each measurement provides one equation in the two unknowns. A single measurement bounds a linear combination of $\beta\langle|\psi|^2 R\rangle$ and $\gamma\langle\ln S\rangle$ (the energy-shift prediction of Eq. (1)); independently varying R while holding $|\nabla S|$ fixed, or vice versa, separates the two contributions. Precision BEC experiments in variable-curvature or variable-thermal-gradient geometries provide a natural venue for this two-measurement program.

Experimental bounds on β, γ, and α_D (FC): Current precision measurements impose upper bounds on the QULT-C coupling constants. From the absence of anomalous decoherence in BEC interferometry at thermal gradients $|\nabla S| \sim k_B\,\mathrm{m}^{-1}$ and coherence times $\gtrsim 1$ s Dalfovo et al. [1999]:

$$\beta < 6 \times 10^{-28}\,\mathrm{J\,m^5}, \qquad \gamma < 2 \times 10^{-32}\,\mathrm{J}, \qquad \alpha_D < 3 \times 10^{-9} \tag{1}$$

These bounds require that the QULT-C Hamiltonian correction $\beta|\psi|^2 R - \gamma \ln S$ not alter BEC ground-state energies beyond experimental precision ($\sim 10^{-30}$ J at BEC densities $|\psi|^2 \sim 10^{18}\,\mathrm{m}^{-3}$ and curvature $R \sim 10^{-35}\,\mathrm{m}^{-2}$), and that α_D suppresses the $c/k_B \approx 2.17 \times 10^{31}$ prefactor in the SI decoherence rate to below $3 \times 10^{-9} \times 2.17 \times 10^{31} \approx 7 \times 10^{22}$ (m·K)/(J·s), consistent with observed coherence times. In Planck units, $\beta/\tilde{\beta} \approx 10^{-89}$ and $\gamma/\tilde{\gamma} \approx 10^{-61}$, confirming that the QULT-C couplings are highly Planck-suppressed. These are experimental upper bounds, not first-principles derivations (**FC**).

$D(t)$ **normalization:** The decoherence fragility metric $D(t) = \exp\Big(-\alpha_D \int_0^t |\nabla S(s)|\, ds\Big)$ (Eq. (5)) is expressed in PNMS Planck units where the integral is dimensionless. In SI units the conversion factor c/k_B is absorbed into α_D (Eq. (1)). A first-principles derivation of α_D from Zurek's formalism — connecting the gradient coupling to a physical decoherence rate via a Lindblad Born-Markov reduction — is a necessary step toward making $D(t)$ a derived rather than a free parameter.

χ_{CPL} **observability:** The Causal Loop Health Invariant (Eq. (10)) provides a formal quantity for CPL topological integrity, but no observational signature is identified. Identifying a measurable surrogate for χ_{CPL} in cosmological data (CMB anisotropies, large-scale structure topology) is a necessary step toward falsifiability.

Entropy reset mechanism: The inter-aeonic entropy reset $S_{\mathrm{CPL}}(t+1) = S(t)/(1+\alpha_r)$ (Eq. (2)) is proposed as a QULT-C formalization of conformal rescaling, where α_r is the reset damping coefficient. Whether α_r takes the numerical value of the fine-structure constant $\alpha \approx 1/137$ (as a numerical coincidence or structural hint), or is an independent free parameter, requires clarification. The physical mechanism producing this reset also remains an open problem.

Second Law compatibility: The entropy reset $S_{\mathrm{CPL}}(t+1) = S(t)/(1+\alpha_r)$ ($\alpha_r > 0$) implies the new aeon begins at lower entropy than the dying aeon. The QULT-C resolution, following Penrose's CCC Penrose [2010], is that the Second Law applies *within* a single aeon but not *across* the conformal boundary: the dying and nascent aeons are distinct thermodynamic domains. At $\mathcal{I}^+$, all massive degrees of freedom decouple; the remaining massless fields carry no scale, so the entropy "count" of the new aeon is defined with respect to a new thermodynamic domain with far smaller accessible phase space. The factor $1/(1+\alpha_r)$ parametrizes this phase-space ratio (**NI** — full derivation of α_r from conformal rescaling deferred to future work).

PNMS unit observational grounding: The PNMS unit system is mathematically grounded in CODATA Planck constants but its interpretive claims (Quasiplanck as observable universe radius, WarpTick as CPL duration) are contingent on the measured values of the Hubble constant and the observable universe radius, both of which carry observational uncertainty. The PNMS values should be updated as CODATA and cosmological surveys improve.

Mean-field self-consistency fixed point (NI — central open problem): The QULT-C framework contains a self-consistent feedback loop between the Hamiltonian and the geometry: $\hat{H}_{\text{QULT}}$ drives quantum state evolution via ψ, which depends on the local Ricci scalar R (curvature $\to$ quantum evolution); the Layer 4 Einstein equation (Eq. (4)) drives curvature from $\langle \hat{T}_{\mu\nu} \rangle_\psi$ (quantum state $\to$ curvature). Together, $R \to \psi \to \langle \hat{T}_{\mu\nu} \rangle_\psi \to R$ forms a mean-field self-consistency loop. This loop is the *engine* of the framework's physical content: without a self-consistent solution (R^*, ψ^*) satisfying both the QULT-C Schrödinger equation and the quantum-corrected Einstein equation simultaneously, the framework's physical predictions are under-determined. Establishing a fixed-point existence result (analogous to the Cazenave–Weissler theory for Gross-Pitaevskii or, for the coupled system, a Schrödinger-Einstein semiclassical analysis in the spirit of Ruffini–Bonazzola Dalfovo et al. [1999]) is identified as the highest-priority open problem for establishing the internal coherence of QULT-C (**NI** — deferred to future work; referenced in companion paper scope).

Lagrangian formulation: $\hat{H}_{\text{QULT}}$ is introduced directly as an equation-of-motion object. A natural Lagrangian density from which it could be obtained via Legendre transform would take the form:

$$\mathcal{L}_{\text{QULT}} = \frac{i\hbar}{2}(\psi^* \partial_t \psi - \psi \partial_t \psi^*) - \frac{\hbar^2}{2m}|\nabla\psi|^2 - \frac{\beta}{2}|\psi|^4 R + \gamma|\psi|^2 \ln S(t)$$

The sign conventions follow in two steps. First, the Legendre relation $\mathcal{H} = \pi\dot{\psi} - \mathcal{L}$ flips the sign of every potential term: $+\gamma|\psi|^2 \ln S(t)$ in $\mathcal{L}$ becomes $-\gamma|\psi|^2 \ln S(t)$ in $\mathcal{H}$. Second, the mean-field normalisation $|\psi|^2 \to 1$ (unit-normalised single-particle wavefunction) yields the $-\gamma \ln S(t)$ term in Eq. (1).

The $\beta|\psi|^4 R/2$ term generates the $\beta|\psi|^2 R$ potential via the Euler-Lagrange equation (the factor of $1/2$ and the fourth power arise from the mean-field self-energy structure, analogous to the Gross-Pitaevskii action Dalfovo et al. [1999]). Confirming this via the Legendre transform and checking consistency of the resulting field equations with the Layer 4 Einstein equation is identified as necessary future work (**NI** — proposed candidate Lagrangian; full derivation open).

Lindblad connection for $D(t)$: The formula $D(t) = e^{-|\nabla S| \cdot t}$ is equivalent to the solution of a Lindblad master equation $\dot{\rho} = -i[\hat{H}, \rho]/\hbar + \sum_k \gamma_k (L_k \rho L_k^\dagger - \frac{1}{2}\{L_k^\dagger L_k, \rho\})$ with a single scalar dephasing jump operator $L = \sqrt{|\nabla S|}\,\hat{I}$, giving off-diagonal decay $\rho_{ij}(t) \propto e^{-|\nabla S|t}$. This scalar Lindblad form is the simplest consistent with the $D(t)$ formula. Whether this jump operator has a physical derivation from the COSI Layer 3 entropy field via the Born-Markov approximation is an open problem (**NI**).

Path integral formulation: The QULT-C framework is currently specified at the operator level. A path integral $\mathcal{Z} = \int \mathcal{D}\psi\, \mathcal{D}\psi^*\, e^{iS_{\text{QULT}}/\hbar}$ would enable non-perturbative calculations and a direct connection to QFT in curved spacetime. The candidate Lagrangian above provides a starting point; the non-analytic entropy term $\gamma|\psi|^2 \ln S(t)$ makes the path integral non-Gaussian and requires regularization (**NI** — technically open).

Renormalization group flow of coupling constants: In QFT, coupling constants generically run with energy scale μ via the renormalization group Peskin and Schroeder [1995]. The $\beta|\psi|^2 R$ coupling is a quartic-in-ψ operator in $\mathcal{L}_{\text{QULT}}$ and is marginal-to-irrelevant in $3+1$ dimensions; gravitational mixing may make it relevant. The entropy coupling γ is dimensionful ($[\gamma] = \text{J}$) and requires fine-tuning unless protected by a symmetry. Addressing the naturalness and RG flow of β and γ is a prerequisite for embedding QULT-C in a UV-complete quantum gravity framework (**NI** — open problem).

WKB semiclassical limit: The standard limit $\beta, \gamma \to 0$ recovers the free Schrödinger equation. The independent semiclassical limit $\hbar \to 0$ at fixed β, γ has not been performed. Writing $\psi = A\, e^{iS_{\text{cl}}/\hbar}$, the leading-order Hamilton-Jacobi equation is:

$$\partial_t S_{\text{cl}} + \frac{|\nabla S_{\text{cl}}|^2}{2m} + \beta A^2 R - \gamma \ln S_{\text{env}}(t) = 0$$

(where S_{cl} is the classical action, S_{env} is the environmental entropy, and $A^2 \approx |\psi|^2$). This recovers a classical Hamilton-Jacobi equation with density-dependent geometric and entropy corrections. Whether this reproduces any known modified geodesic equation is a consistency check deferred to future work (**NI**).

*WKB $1/r^4$ force prediction (**NI**):* In the semiclassical limit, the $\beta A^2 R$ term contributes a correction to the Newtonian potential. For a spherically symmetric source of mass M with $R \approx 2GM/(c^2 r^3)$ (weak-field Schwarzschild) and $A^2 \approx |\psi|^2 \propto 1/r^3$ (hydrogen-like ground state), the leading QULT-C correction to the gravitational force is repulsive and scales as $1/r^4$:

$$F_{\text{QULT}} \sim -\frac{d}{dr}\big[\beta A^2 R\big] \propto +\frac{\beta}{r^7} \cdot r^3 \sim \frac{\beta}{r^4}$$

For terrestrial separations $r \sim 1$ m and $\beta < 6 \times 10^{-28}$ J·m^5, this correction is $\sim 10^{-28}$ N, which is approximately 10^{-11} of the Newtonian gravitational force between a 1 kg test mass and the Earth at 1 m. This is potentially within reach of next-generation atom interferometers sensitive to sub-mHz frequency shifts (**NI** — the precise coefficient requires the full WKB-Schwarzschild calculation, which is deferred to future work).

10.3 Falsifiability

A theoretical framework that cannot in principle be falsified is not a physical theory. The following potential falsification criteria for QULT-C are identified. Three concrete tests are highlighted below: one near-term cosmological test inherited from CCC (Test 2), one in-principle laboratory test that requires new experimental design but is feasible with existing BEC technology (Test 1), and one computational self-consistency check that requires no new experiment (Test 3). All three are falsification criteria; they differ in experimental readiness:

Decoherence fragility metric (general): If future high-precision measurements of quantum decoherence rates in systems with large entropy gradients are inconsistent with the exponential form $D(t) = e^{-|\nabla S| \cdot t}$ (Eq. (5)), this functional form is falsified. This is a testable prediction in principle, contingent on experimental control of $|\nabla S|$.

Near-term test 1 — BEC decoherence in entropy-gradient labs: The QULT-C prediction $D(t) = e^{-|\nabla S| \cdot t}$ implies that systems subject to larger spatial entropy gradients decohere faster, with an exponential rate controlled by $|\nabla S|$. Bose-Einstein condensate (BEC) experiments provide a laboratory analog: a BEC in a trap with a deliberately imposed thermal gradient (high $|\nabla S|$) should lose coherence faster than one in a uniform-entropy environment by a factor consistent with the QULT-C formula. Realizing this test

Table 9: Falsifiability levels for QULT-C predictions.

Level	Test	Status	Instrument/Method
A (near-term)	BEC $\cos^2\theta$ decoherence anisotropy	Requires dedicated anisotropic-trap design; within current technology generation (∼3–5 yr program)	BEC interferometry
A (near-term)	CMB power spectrum at $\ell \approx 200$–300	In progress	Simons Observatory, CMB-S4
B (medium-term)	$1/r^4$ effective force correction (WKB limit)	Next-generation atom interferometry	∼10 yr horizon
C (computational)	$\hat{H}_{\text{QULT}}$ numerical blow-up test ($\beta \neq 0$)	No new experiment needed	Immediate (software)

requires a dedicated anisotropic-trap BEC design in which thermal gradient direction and interferometer momentum-kick axis can be independently controlled; this is within the current technology generation but is not a test that existing BEC coherence setups perform without modification (∼3–5 year experimental program). A measurement inconsistent with the exponential decay rate at fixed $|\nabla S|$ would falsify Eq. (5). *Distinguishing QULT-C from quantum Brownian motion (QBM):* Standard QBM also predicts exponential decoherence with a rate Γ proportional to system-bath coupling Zurek [2003]. The discriminating feature is that QULT-C's rate is controlled by the *spatial* entropy gradient $|\nabla S|$ — a directional, anisotropic quantity — rather than by the isotropic system-bath coupling strength. Experiments that independently vary the directionality of an imposed thermal gradient while holding total thermal energy constant (e.g., via anisotropic trap geometries in BEC systems) would distinguish the two mechanisms: QULT-C predicts decoherence rate proportional to gradient magnitude irrespective of coupling symmetry, while isotropic QBM does not.

*Anisotropy prediction (**NI**):* The directional coupling to $|\nabla S|$ yields a concrete angular signature in BEC interferometry. If the interferometer momentum-kick axis makes angle θ with the imposed thermal gradient, the fringe visibility decays as:

$$V(t,\theta) = V_0 \exp\big(-(\Gamma_0 + \Gamma_{\text{QULT}} \cos^2\theta) \cdot t\big) \tag{2}$$

where Γ_0 is the isotropic background rate (standard QBM), and $\Gamma_{\text{QULT}} = \alpha_D |\nabla S|_{\text{PNMS}}$ is the QULT-C contribution. The $\cos^2\theta$ angular shape is a robust prediction of the scalar-product coupling $\mathbf{k} \cdot \nabla S$ and is independent of α_D; only the amplitude Γ_{QULT} depends on α_D. An experiment that finds no $\cos^2\theta$ modulation in decoherence rate upon rotating the interferometer axis relative to the gradient direction would falsify the directional coupling (**NI**).

Near-term test 2 — CMB power spectrum at $\ell \approx 200$–300: QULT-C inherits Penrose's CCC structure Penrose [2010], which predicts observable signatures in the CMB:

anomalous low-variance concentric circles in temperature maps and potential deviations in the multipole power spectrum at intermediate angular scales ($\ell \approx 200$–300, corresponding to angular separations $\theta \approx 180/\ell \approx 0.6$–$0.9$ on the CMB sky; the first acoustic peak center lies at $\ell \approx 220$, i.e., $\theta \approx 0.8$). Planned instruments including the Simons Observatory and CMB-S4 will achieve sub-percent sensitivity to power spectrum deviations at these scales. If next-generation CMB surveys confirm the standard ΛCDM power spectrum with no CCC anomalies, the CCC-based COSI Layer 7 structure is challenged. This would not falsify the formal COSI Stack architecture (which is formally independent of CCC's cyclic claims), but would remove the primary cosmological motivation for the cyclic Layer 7. *CCC constraints from current data:* Searches for Penrose's predicted concentric low-variance circles in the 7-year WMAP data by Wehus & Eriksen Wehus and Eriksen [2011] and Moss, Scott & Zibin Moss et al. [2011] found no statistically significant anomalous circles, placing the original CCC CMB signature under observational pressure. These results challenge but do not decisively rule out CCC, since the predicted signal strength depends on assumptions about the late-time emission from previous aeons Penrose [2010]. QULT-C's Layer 7 inherits this observational tension; confirmation or refutation via Simons Observatory and CMB-S4 data constitutes the most direct current falsification path for the cyclic structure.

Near-term test 3 — Numerical well-posedness of $\hat{H}_{\mathbf{QULT}}$: The term $\beta|\psi|^2R$ makes the QULT-C Schrödinger equation nonlinear. The QULT-C framework implicitly predicts that numerical solutions to this nonlinear Schrödinger equation are stable (non-blow-up) for physically motivated initial conditions. If numerical integration of the QULT-C modified Schrödinger equation systematically produces finite-time blow-up or non-convergent solutions for all physically motivated initial data and coupling constant ranges, the mean-field interpretation of the β coupling would be under pressure. This is a computational falsification criterion testable without new physical experiments; it is a well-posed mathematical question about existence and uniqueness in an appropriate Sobolev space (cf. Gross-Pitaevskii literature).

Causal Loop Stability Invariant: If future cosmological observations constrain the topology of the large-scale universe in ways inconsistent with $\chi_{\text{CPL}} > 0$ throughout cosmic history, the QULT-C causal stability framework is challenged.

χ_{CPL} *self-consistency in ΛCDM (**NI**):* As a consistency check, the normalized integrand of χ_{CPL} (Eq. (10)) can be evaluated along the ΛCDM expansion history using $R(z) = -6[\ddot{a}/a + (\dot{a}/a)^2] = -12H_0^2\Omega_\Lambda + 3H_0^2\Omega_m(1+z)^3$ in SI. Table 10 shows representative values demonstrating $\chi_{\text{CPL}} > 0$ throughout the matter- and Λ-dominated eras.

Table 10: χ_{CPL} integrand check: $\lambda_p^2 R(z) - \mathcal{F}_{\text{collapse}}/2\pi$ in the ΛCDM background ($H_0 = 67.4$ km/s/Mpc, $\Omega_m = 0.315$, $\Omega_\Lambda = 0.685$). $\mathcal{F}_{\text{collapse}} \approx 0$ away from Planck densities; $\lambda_p^2 R > 0$ (de Sitter dominance) for $z \lesssim 0.3$.

Redshift z	$\lambda_p^2 R(z)$	χ_{CPL} status
0	$2\Lambda\lambda_p^2 \approx 5.8 \times 10^{-122}$	> 0 (de Sitter, stable)
0.5	$\approx -1.0 \times 10^{-122}$	> 0 ($\lvert\mathcal{F}_{\text{collapse}}\rvert \ll \lvert\lambda_p^2 R\rvert$)
2	$\approx -5.2 \times 10^{-121}$	> 0 (matter dominated, stable)
1000	$\approx -1.1 \times 10^{-115}$	> 0 (recombination, stable)
10^{10}	$\approx -1.1 \times 10^{-95}$	> 0 (approaching Planck epoch)

The positive-definite sign of χ_{CPL} throughout the ΛCDM expansion history is consistent with QULT-C causal stability. A future computation with full $\mathcal{F}_{\mathrm{collapse}}(v, \Lambda)$ near the Planck epoch (where $|\psi|^2 R \sim E_p/V_p$ and $\mathcal{F}_{\mathrm{collapse}} \sim 2\pi$) is needed to verify stability at Planck densities (**NI** — deferred to future work).

Conformal cyclic cosmology: QULT-C inherits Penrose's CCC structure. The CCC is itself a falsifiable cosmological model: gravitational wave backgrounds and specific CMB features (Penrose's concentric circles) are potential observational signatures Penrose [2010]. Falsification of CCC would challenge but not necessarily falsify the COSI Stack architecture, which is formally independent of CCC's cyclic claims.

COMAF-Lite models: The four framework demonstration cases (Section 9) make specific numerical predictions for their respective model parameters. If future cosmological simulations using COMAF-Lite models are run with physical (rather than toy) parameters and produce results inconsistent with observed data, the model assumptions can be refined or falsified.

10.4 Limitations

Several important limitations of the present work are acknowledged:

Toy model parameters: The first four Wolfram framework demonstration cases (TC1–TC4) use toy-model parameters ($S_0 = 10^{120}$, $R_{\max} = 10^{44}$, etc.) chosen for numerical tractability in Wolfram Cloud, not for physical accuracy. They demonstrate the framework's computational expressibility, not precise cosmological predictions. Test Case 5 (TC5) uses the canonical Bekenstein-Hawking value $S_{\mathrm{BH}} \approx 1.05 \times 10^{77}\, k_B$ for a solar-mass black hole, which is a physically calibrated value (not a toy parameter).

No quantum gravity: QULT-C operates with a modified Schrödinger equation (Layer 2) and quantum-expectation Einstein equations (Layer 4) but does not provide a quantum theory of gravity. The COSI Stack is therefore incomplete at the Planck scale in the same sense that current physics is incomplete: it describes the framework for a quantum gravitational theory without providing one.

No experimental constraints on novel components: The coupling constants β and γ in Eq. (1), and the collapse function parameters in Eq. (8), are currently unconstrained by experiment. The framework is formally consistent but not yet experimentally grounded in its novel components.

Measurement problem stance and interpretation-dependence: The Layer 5 collapse function $\mathcal{F}_{\mathrm{collapse}}$ (Eq. (8)) implicitly treats wavefunction collapse as a physical process triggered by sub-Planck spatial resolution. This is broadly consistent with objective collapse models (e.g., the Ghirardi-Rimini-Weber (GRW) spontaneous collapse model Ghirardi et al. [1986]) rather than with Everettian many-worlds or Copenhagen interpretations, in which "collapse" is either universally absent or observer-relative rather than physically triggered. This interpretive stance is not derived from first principles; it is a framework assumption.

Interpretation-dependence of the COSI Stack: A natural question is whether the COSI Stack remains architecturally coherent without Layer 5 — i.e., in a many-worlds (Everettian) ontology where $\mathcal{F}_{\mathrm{collapse}}$ is eliminated in favor of decoherence-only evolution. In an Everettian reading, Layers 1–4 and Layer 6 retain their meanings without modification: the

Planck substrate, Schrödinger evolution, entropy flow, geometry, and causal routing are all formulation-independent. Layer 5 would be reinterpreted not as a trigger for physical collapse but as a *decoherence threshold marker* — the surface on which classical branches become environmentally stable in the preferred-pointer-basis sense (cf. Zurek [2003]). Layer 7 cyclic transition remains interpretation-independent (the conformal boundary matching is a geometric fact about CCC, not a collapse event). The COSI Stack is therefore architecturally compatible with an Everettian reading at the cost of reinterpreting Layer 5's role: "rendering" becomes "branching-decoherence stabilization" rather than "wavefunction reduction." QULT-C's current formulation adopts the objective-collapse reading for concreteness; the Everettian re-reading is noted as a viable alternative that preserves the overall architecture (**NI** — full Everettian formulation deferred to future work).

Single-author speculative work: This paper is the product of a single researcher and has not been subjected to formal peer review. The reader should weight the novel interpretations (NI) and speculative proposals (SP) accordingly.

10.5 Philosophical Coda: On Layers, Waves, and the Architecture of Inquiry

> *"Was einmal gedacht wurde, kann nicht mehr zurückgenommen werden."*
> — Friedrich Dürrenmatt, *Die Physiker*

This paper opened with Dürrenmatt's physicist in the asylum — a man who understood something about the structure of the world and struggled with the question of whether that understanding should be shared or suppressed. The play concludes that suppression fails: knowledge, once produced, escapes institutional containment. The present work has taken the opposite path. Every claim is labeled. Every equation is numbered. Every epistemic commitment is made explicit. The architecture is offered openly, not because the author is certain it is correct, but because the question it raises — whether physical reality is organized in functional layers with distinct governing rules connected by defined interfaces — deserves to be examined on its merits rather than buried by institutional caution.

The history of physics contains a persistent and largely unexamined assumption: that a single set of governing rules, expressed in a single Lagrangian, should apply uniformly across all scales of physical reality. The unification program — from Maxwell's electromagnetism through electroweak theory to the ongoing search for quantum gravity — is built on this assumption. It has produced extraordinary successes. It has also produced a fifty-year impasse at the Planck scale, where quantum mechanics and general relativity refuse to unify under any known framework.

The COSI Stack proposes a different structural hypothesis: that the difficulty of unification may not be a problem to solve but a clue about the architecture of reality. In network engineering, no one attempts to run a single protocol across all layers of the communication stack. The physical layer has its rules; the transport layer has different rules; the application layer has different rules still. Each layer is optimized for its functional domain. The layers communicate through defined interfaces, not through identity of protocol. The system works *because* the layers are different, not *despite* it.

If physical reality is similarly layered — if the Planck substrate, quantum evolution, thermodynamic flow, spacetime geometry, and measurement each operate under rules optimized for their respective domains — then the search for a single theory of everything may be asking the wrong question. The right question may be: what are the interface contracts between layers? What quantities pass from quantum evolution to entropy flow, from entropy flow to spacetime geometry, from geometry to measurement? The COSI Stack is a first formal attempt to specify those contracts.

A framework of this kind invites a natural objection: that the analogy between physical processes and computational architecture is merely metaphorical, that the universe need not be organized the way a human-engineered system is organized, and that imposing computational structure on physics is an exercise in anthropomorphism rather than discovery.

This objection deserves a serious response. First, the COSI Stack is not an analogy. It is a formal specification: seven layers with governing equations, inter-layer interfaces, dimensional constraints, and an executable modeling language. Analogies are suggestive; specifications are testable. The DHO proof case (Section 7) demonstrates that different COSI layer assignments produce quantitatively different, experimentally distinguishable predictions. That is not a property of metaphors.

Second, the history of physics is substantially a history of structural analogies that turned out to be structural truths. Faraday's field lines were dismissed as pictures by the mathematical physicists of his era; Maxwell's equations showed they were the fundamental objects. Boltzmann's statistical mechanics was rejected as a convenient fiction; atoms turned out to be real. The holographic principle — that all information in a volume is encoded on its boundary — sounds like a metaphor until one encounters AdS/CFT, where it is a mathematical theorem. The boundary between productive analogy and physical discovery is thinner than the objection assumes.

Third, the direction of inference matters. This work does not begin from computational architecture and force physics into it. It begins from known physical results — the Bekenstein-Hawking formula, Zurek's decoherence theory, Penrose's conformal cyclic cosmology, the holographic principle — and observes that these results, when organized by functional domain, naturally sort into a layered architecture with defined interfaces. The computational framing is not imposed; it is discovered in the structure of the physics itself. Whether the framing is ultimately literal or merely organizational is an empirical question, not one that can be resolved by philosophical objection alone.

A deeper question underlies the formal architecture: whether nature operates by a single universal rule applied everywhere, or by different rules at different scales connected through translation. The metaphor that clarifies this is not computational but physical.

One does not engage an ocean wave by opposing it. A wave carries energy, momentum, and structure; to stand rigid against it is to be broken. To engage it productively — to surf — requires understanding the wave's shape, matching its timing, finding the resonance between the surfer's momentum and the wave's energy surface. The surfer does not overpower the wave. The surfer couples to the gradient that is already there.

The same principle may apply to the relationship between physical scales. The Planck substrate (Layer 1) has its own dynamics. Spacetime geometry (Layer 4) has different dynamics. The interface between them is not a battleground where one set of rules must defeat another. It is a coupling surface where information passes according to defined contracts. The physicist's task — and perhaps the engineer's, in the longer term — is not to force one layer's rules onto another, but to understand the interface well enough to work with it.

This is not mysticism dressed in formalism. It is the same engineering principle that underlies every successful technology: identify the natural dynamics of the system, find the resonance conditions, and couple to them efficiently rather than fighting them with brute force. Radio does not overpower the electromagnetic field; it couples to it at a resonant frequency. A laser does not force photons into coherence; it creates the conditions under which coherence emerges spontaneously. If the COSI Stack is correct that physical reality has layered structure with inter-layer coupling, then the long-term engineering implication is clear: understand the coupling, find the resonance, ride the wave.

The framework presented here is, by any honest assessment, incomplete. The coupling constants are unmeasured. The normalization requires experimental grounding. The speculative extensions remain formally coherent but empirically unconstrained. The author is a single independent researcher without institutional affiliation, and the work has not been subjected to formal peer review.

These limitations are stated not as apology but as inventory. The epistemic labels throughout this paper — FC, RF, NI, SP — exist precisely to ensure that no reader conflates what is formally established with what is speculatively proposed. The architecture stands on its formal merits: the COSI Stack is a specified structure, the PNMS is a grounded unit system, COMAF-Lite is a working language. These are engineering artifacts, and engineering artifacts are judged by whether they work, not by where they came from.

The novel interpretations and speculative proposals are offered in the spirit of Dürrenmatt's epigraph: as thoughts that, once thought, cannot be unthought. They may prove wrong. They may prove productive in ways not anticipated here. They may, as is the fate of most speculative work, simply be forgotten. But they are offered clearly, labeled honestly, and specified formally enough to be examined, tested, and if necessary, refuted.

If this framework contributes nothing else, let it contribute this: a demonstration that formal rigor and intellectual ambition are not the exclusive province of institutional affiliation. That a layered computational ontology for quantum cosmology can be specified, formalized, and submitted to scrutiny by anyone willing to do the work honestly. That the question "is physical reality architecturally layered?" is a question worth asking, and that asking it carefully — with equations, with units, with executable models, and with epistemic humility — is the only way it will ever be answered.

The ocean does not ask for credentials. It simply is. The wave is there. The question is whether we learn to read its structure.

> *A proposal should stand or fall by its clarity, rigor, and testability — not by whether it arrives in an expected form.*

11 Conclusion

This paper has introduced QULT-C (Quantum Unified Loop-Time Cosmology) as a layered computational ontology for quantum cosmology, comprising three formal contributions.

Contribution 1 — The COSI Stack (FC): A seven-layer formal architecture partitioning physical processes by functional domain, from the Planck-scale quantum substrate (Layer 1) through wavefunction evolution (Layer 2), entropy flow (Layer 3), spacetime geometry (Layer 4), rendering control (Layer 5), causal routing and decoherence (Layer 6), to cyclic cosmological transition (Layer 7). Each layer is assigned governing equations and inter-layer interfaces. The COSI Stack extends Penrose's conformal cyclic cosmology Penrose [2010] with formal computational architecture, and organizes the physical contributions of Bekenstein Bekenstein [1973], Hawking Hawking [1975], 't Hooft and Susskind 't Hooft [1993], Susskind [1995], Zurek Zurek [2003], Wheeler Wheeler [1990], Zuse Zuse [1970], Wolfram Wolfram [2002], and Fredkin and Lloyd Fredkin [1993], Lloyd [2006] into a single coherent layered structure.

Contribution 2 — The Planck-Native Metric System (FC): A complete unit system derived from fundamental constants ($\hbar$, c, G, k_B) covering all physical dimensions relevant to the QULT-C framework. The PNMS defines the Plameter, Plasecond, WarpTick, Quasiplanck, Plakilogram, Ricci-Bit, and Entropy Tick as the natural scales for physical quantities within the framework. Five constant naturalization analyses (Section 7) re-express t_p, Λ, α, m_H, and S_{BH} in PNMS units, providing QULT-C structural interpretations of each. These interpretations are reframings of established results (RF) or novel interpretations (NI); no constant is derived or predicted.

Contribution 3 — COMAF-Lite (FC): A declarative domain-specific language for specifying, transpiling, and partially validating physical models within the QULT-C framework. The current implementation provides formal specification (grammar + schema), core pipeline (lexer $\rightarrow$ parser $\rightarrow$ AST), and transpilers; a full semantic interpreter with automated unit-consistency checking and symbolic solving is future work. COMAF-Lite is formally specified by the complete EBNF grammar for the current implementation (Appendix C) and JSON Schema (Appendix D), and is transpilable to Wolfram Language and Python/NumPy. Four framework demonstration cases (Section 9) were verified against their stated QULT-C governing equations via Wolfram Cloud (equation-consistent; not yet fitted to observational data or empirically constrained): bounce cosmology (VFR-301), decoherence-limited expansion (VFR-302), entropy-curvature feedback oscillation (VFR-303), and black hole collapse (VFR-304).

11.1 Future Work

The following directions for future work are identified as highest priority:

Physical parameter fitting: Replace the toy-model parameters in the four framework demonstration cases with cosmologically constrained values. Fit the QULT-C Hamiltonian coupling constants β and γ to observational data, beginning with precision measurements of quantum decoherence rates in controlled systems.

Observational signatures: Identify specific CMB or large-scale structure signatures that could test QULT-C predictions. The Causal Loop Health Invariant χ_{CPL} is a natural candidate: a measurement program for χ_{CPL}-related observables would constitute the first direct observational test of the framework.

Full COMAF-Lite interpreter: Extend the COMAF-Lite transpiler to a full interpreter with a semantic validator, unit-consistency checker, and symbolic solver. The current implementation (available at `roblemumin.com/library.html`) provides the transpilation layer; a complete interpreter would support model composition and automated verification against the PNMS unit system.

CCC integration and companion paper on $\hat{\Omega}$: Collaborate with researchers in Penrose's conformal cyclic cosmology program to test whether the QULT-C cycle transition operator $\hat{\Omega}$ (Eq. (3)) is consistent with the conformal rescaling constraints of CCC and whether COMAF-Lite models can reproduce known CCC predictions. A companion paper on $\hat{\Omega}$ is planned with the following specific scope: (a) the limit topology of $\hat{\Omega}$ (strong, weak, or norm operator topology at the conformal boundary); (b) the structure group and transition functions of the fiber bundle $\mathcal{B}$ (Eq. (11)); and (c) well-posedness (existence and uniqueness) of the nonlinear QULT-C Schrödinger equation in appropriate Sobolev spaces, extending the Gross-Pitaevskii well-posedness theory Dalfovo et al. [1999] to the curvature-coupled case.

DSL extension: Extend COMAF-Lite to support force, pressure, and charge blocks (from the COMAF $\times$ PNMS Addendum, Appendix G) and a full symbolic lexicon (Appendix F).

11.2 Closing Statement

QULT-C does not claim to solve the problem of physical constants. It proposes that the problem looks different — more tractable, more structurally illuminated — when the constants are expressed in a Planck-native unit system within a formally specified layered computational architecture. Whether this reframing proves physically productive is a question for future experimental and theoretical work. The framework is provided, with all its epistemic caveats, as a formal contribution to the ongoing program of computational cosmology. QULT-C is submitted to arXiv in the `physics.hist-ph` category (formal physical frameworks and interpretive ontologies) with `cs.PL` as secondary (domain-specific languages and formal logic in physical modeling).

References

Giovanni Amelino-Camelia. Relativity in space-times with short-distance structure governed by an observer-independent (planckian) length scale. *International Journal of Modern Physics D*, 11(1):35–59, 2002. doi:10.1142/S0218271802001330.

Robert W. Batterman. *The Devil in the Details: Asymptotic Reasoning in Explanation, Reduction, and Emergence.* Oxford University Press, Oxford, 2002. doi:10.1093/0195146476.001.0001.

Jacob D. Bekenstein. Black holes and entropy. *Physical Review D*, 7:2333–2346, 1973. doi:10.1103/PhysRevD.7.2333.

Nick Bostrom. Are you living in a computer simulation? *Philosophical Quarterly*, 53(211): 243–255, 2003. doi:10.1111/1467-9213.00309.

David J. Chalmers. *The Character of Consciousness*. Oxford University Press, 2010.

CODATA. 2018 internationally recommended values of the fundamental physical constants. Technical report, NIST, 2019. Available at: `https://physics.nist.gov/cuu/Constants/`.

Franco Dalfovo, Stefano Giorgini, Lev P. Pitaevskii, and Sandro Stringari. Theory of bose-einstein condensation in trapped gases. *Reviews of Modern Physics*, 71(3):463–512, 1999. doi:10.1103/RevModPhys.71.463.

Edward Fredkin. A new cosmogony. In *PhysComp '92: Workshop on Physics and Computation*, 1993.

GianCarlo Ghirardi, Alberto Rimini, and Tullio Weber. Unified dynamics for microscopic and macroscopic systems. *Physical Review D*, 34(2):470–491, 1986. doi:10.1103/PhysRevD.34.470.

Stephen W. Hawking. Particle creation by black holes. *Communications in Mathematical Physics*, 43:199–220, 1975. doi:10.1007/BF02345020.

Stephen W. Hawking. Black holes and thermodynamics. *Physical Review D*, 13:191–197, 1976. doi:10.1103/PhysRevD.13.191.

Tosio Kato. Fundamental properties of Hamiltonian operators of Schrödinger type. *Transactions of the American Mathematical Society*, 70(2):195–211, 1951. doi:10.2307/1990366.

James Ladyman. What is structural realism? *Studies in History and Philosophy of Science*, 29(3):409–424, 1998. doi:10.1016/S0039-3681(98)00025-4.

Seth Lloyd. *Programming the Universe*. Knopf, 2006.

Juan Maldacena. The large N limit of superconformal field theories and supergravity. *International Journal of Theoretical Physics*, 38:1113–1133, 1999. doi:10.1023/A:1026654312961.

Adam Moss, Douglas Scott, and James P. Zibin. No evidence for anomalously low variance circles on the sky. *Journal of Cosmology and Astroparticle Physics*, 2011(04):033, 2011. doi:10.1088/1475-7516/2011/04/033. arXiv:1012.1305.

Mikio Nakahara. *Geometry, Topology and Physics*. IOP Publishing, 2nd edition, 2003.

Particle Data Group. Review of particle physics. *Progress of Theoretical and Experimental Physics*, 2022:083C01, 2022. doi:10.1093/ptep/ptac097.

Roger Penrose. Before the big bang: An outrageous new perspective and its implications for particle physics. In *Proceedings of EPAC 2006*, pages 2759–2762, Edinburgh, 2006.

Roger Penrose. *Cycles of Time: An Extraordinary New View of the Universe*. Bodley Head, 2010.

Michael E. Peskin and Daniel V. Schroeder. *An Introduction to Quantum Field Theory*. Addison-Wesley, 1995.

Planck Collaboration. Planck 2018 results. VI: Cosmological parameters. *Astronomy & Astrophysics*, 641:A6, 2020. doi:10.1051/0004-6361/201833910. arXiv:1807.06209.

Michael Reed and Barry Simon. *Methods of Modern Mathematical Physics, Vol. II: Fourier Analysis, Self-Adjointness*. Academic Press, New York, 1975.

Erwin Schrödinger. An undulatory theory of the mechanics of atoms and molecules. *Physical Review*, 28:1049–1070, 1926. doi:10.1103/PhysRev.28.1049.

Leonard Susskind. The world as a hologram. *Journal of Mathematical Physics*, 36:6377–6396, 1995. doi:10.1063/1.531249.

Gerard 't Hooft. Dimensional reduction in quantum gravity. *arXiv preprint gr-qc/9310026*, 1993. arXiv:gr-qc/9310026.

Max Tegmark. The mathematical universe. *Foundations of Physics*, 38:101–150, 2008. doi:10.1007/s10701-007-9186-9.

Max Tegmark. *Our Mathematical Universe*. Knopf, 2014.

Robert M. Wald. *General Relativity*. University of Chicago Press, 1984. Reprinted edition.

Ingunn Kathrine Wehus and Hans Kristian Eriksen. A search for concentric circles in the 7-year WMAP temperature sky maps. *The Astrophysical Journal Letters*, 733:L29, 2011. doi:10.1088/2041-8205/733/2/L29. arXiv:1012.1268.

John A. Wheeler. Information, physics, quantum: The search for links. In *Complexity, Entropy, and the Physics of Information*. Addison-Wesley, 1990.

Stephen Wolfram. *A New Kind of Science*. Wolfram Media, 2002.

Stephen Wolfram. A class of models with the potential to represent fundamental physics. *Complex Systems*, 29(2), 2020. doi:10.25088/ComplexSystems.29.2.107.

John Worrall. Structural realism: The best of both worlds? *Dialectica*, 43(1–2):99–124, 1989. doi:10.1111/j.1746-8361.1989.tb00933.x.

Wojciech H. Zurek. Decoherence, einselection, and the quantum origins of the classical. *Reviews of Modern Physics*, 75:715–775, 2003. doi:10.1103/RevModPhys.75.715.

Wojciech H. Zurek. Quantum Darwinism. *Nature Physics*, 5:181–188, 2009. doi:10.1038/nphys1202.

Konrad Zuse. *Rechnender Raum (Calculating Space)*. MIT Technical Translation AZT-70-164-GEMIT, 1970. Original 1969.

A Full QULT-C Mathematical Derivations

This appendix provides full derivations of the QULT-C mathematical components introduced in Section 4. All expressions use SI units unless otherwise specified; PNMS equivalents are noted where relevant.

A.1 Derivation of the QULT-C Hamiltonian

The QULT-C Hamiltonian (Eq. (1)) is constructed by augmenting the standard quantum mechanical kinetic-plus-potential Hamiltonian with two coupling terms.

Standard kinetic term:

$$\hat{H}_0 = -\frac{\hbar^2}{2m}\nabla^2$$

This is the canonical kinetic energy operator for a particle of mass m.

Curvature coupling term: We define a curvature potential $V_R = \beta|\psi|^2 R$, where R is the Ricci scalar (dimensions $[\mathrm{m}^{-2}]$) and β is a coupling constant. Dimensional analysis requires $[\beta]\cdot[\psi]^2\cdot[R] = \mathrm{J}$: since $|\psi|^2$ is a probability density with dimensions $[\mathrm{m}^{-3}]$ and R has dimensions $[\mathrm{m}^{-2}]$, we require $[\beta] = \mathrm{J}\cdot\mathrm{m}^5$ in SI ($[\beta] = E_p \cdot \lambda_p^5$ in PNMS). The physical motivation is the minimal coupling between matter density $|\psi|^2$ and spacetime curvature R; in the weak-field limit, this reproduces the standard gravitational potential contribution. The complete form of this coupling in a covariant setting would require the full stress-energy tensor formalism; V_R is the QULT-C scalar approximation.

Entropy coupling term: We define an entropy potential $V_S = -\gamma \ln S(t)$, where $S(t)$ is the macroscopic entropy of the system (Eq. (2)) and γ has dimensions $[\gamma] = \mathrm{J}$ ($[\gamma] = E_p$ in PNMS). The form $-\gamma \ln S$ is motivated by thermodynamic analogy: the Boltzmann entropy $S = k_B \ln W$ implies that a system in a high-entropy macrostate is energetically accessible with lower effective potential. The logarithm ensures that V_S is extensive in S and bounded from below for $S \geq 1$.

Complete QULT-C Hamiltonian:

$$\hat{H}_{\mathrm{QULT}} = -\frac{\hbar^2}{2m}\nabla^2 + \beta|\psi|^2 R - \gamma \ln S(t) \tag{1}$$

In PNMS units ($\hbar = c = G = k_B = 1$, lengths in λ_p, times in t_p, masses in m_p):

$$\hat{H}_{\mathrm{QULT}} = -\frac{1}{2m}\nabla^2 + \tilde{\beta}|\psi|^2 R - \tilde{\gamma} \ln S(t)$$

where $\tilde{\beta}$ and $\tilde{\gamma}$ are the dimensionless Planck-unit coupling constants.

A.2 Derivation of the Cycle Transition Operator

The cycle transition operator $\hat{\Omega}$ acts at the cycle transition time T_c (one WarpTick). It is defined as:

$$\hat{\Omega} = \lim_{t \to T_c^-} \left(\hat{S}(t) \cdot \hat{U} \cdot \hat{R}^{-1} \right) \tag{3}$$

Entropy compression operator $\hat{S}(t)$: $\hat{S}(t)$ acts on the entropy scalar $S(t)$ to implement the reset condition:

$$\hat{S}(t) \cdot S(t) = \frac{S(t)}{1 + \alpha_r}$$

In operator language, $\hat{S}(t)$ is a rescaling operator on the entropy Hilbert space by factor $1/(1 + \alpha_r)$, where α_r is the inter-aeonic reset damping coefficient (distinct from the fine-structure constant α).

Phase continuity operator $\hat{U}$: $\hat{U}$ maintains wavefunction phase continuity across the conformal boundary via the phase stitching map:

$$\hat{U} \cdot \psi(t) = \psi(t) \cdot e^{i\pi} = -\psi(t)$$

evaluated at $t = T_c$. This is the standard $\mathbb{Z}_2$ phase shift that ensures $\Phi_{n+1}(0) = \Phi_n(T_c) + \pi$, i.e., the phase stitching map of Eq. (9).

Curvature inversion operator $\hat{R}^{-1}$: $\hat{R}^{-1}$ reverses the sign of the Ricci scalar:

$$\hat{R}^{-1} \cdot R = -R$$

This implements the conformal rescaling of Penrose's CCC: the positive-curvature contracting phase of the dying aeon maps to the negative-curvature (or zero-curvature) initial state of the new aeon.

Conformal equivalence: The conformal equivalence relation (Eq. (4)) follows from the action of $\hat{\Omega}$: two aeons U_i and U_j are conformally equivalent if there exists an element $\phi \in \mathcal{G}_{\mathrm{CCC}}$ (the conformal symmetry group) such that $\phi^*(g_i) = \Omega^2 g_j$. The conformal factor Ω (distinct from operator $\hat{\Omega}$) is the rescaling factor that Penrose shows exists at the boundary of massless, conformally invariant far future of one aeon.

A.3 Derivation of the Decoherence Fragility Metric

The decoherence fragility metric $D(t) = e^{-|\nabla S(t)| \cdot t}$ is motivated as follows.

In Zurek's decoherence theory Zurek [2003], the off-diagonal elements of the density matrix decay exponentially at a rate Γ that depends on the system-environment coupling and the environment's state distinguishability. In the thermodynamic limit, the relevant quantity is the entropy production rate $dS/dt = |\nabla S| \cdot v$ for a system moving through an entropy gradient at velocity v.

In the QULT-C framework, the relevant gradient is the spatial entropy gradient $|\nabla S(t)|$ (the magnitude of the entropy gradient vector over the COSI Layer 3 entropy field). The spatial entropy gradient has SI dimensions $[\mathrm{J\,K^{-1}\,m^{-1}}]$, and time has dimensions [s], so $|\nabla S| \cdot t$ is not dimensionless as written. The QULT-C operationalization normalizes by the

Planck-scale reference $k_B\,/(c)$ (derived from the ratio $c = \lambda_p/t_p$ of Planck length to Planck time), so the dimensionless argument of the exponential is:

$$|\nabla S| \cdot t \;\longmapsto\; \frac{|\nabla S| \cdot t \cdot c}{k_B}$$

Dimensional check: $[\mathrm{J\,K^{-1}\,m^{-1}}] \cdot [\mathrm{s}] \cdot [\mathrm{m\,s^{-1}}] \,/\, [\mathrm{J\,K^{-1}}] = 1$ (dimensionless). ✓

In PNMS units where $c = 1$ and $k_B = 1$, this ratio reduces to $|\nabla S| \cdot t$ in Planck units, restoring the compact QULT-C form. Equivalently, $c/k_B = \lambda_p/t_p/k_B$ converts the entropy-gradient–time product into a dimensionless decoherence measure: the speed of light connects the spatial and temporal Planck scales and k_B converts from entropy (Entropy Ticks) to the natural units of the decoherence argument. The formula $D(t) = e^{-|\nabla S(t)|\cdot t}$ is therefore understood as a PNMS-unit expression with implicit normalization c/k_B; in SI units one should write:

$$D_{\mathrm{SI}}(t) = \exp\!\left(-\frac{|\nabla S|_{\mathrm{SI}} \cdot t_{\mathrm{SI}} \cdot c}{k_B}\right)$$

A future derivation constraining this normalization from first principles (e.g., from a Lindblad master equation with entropy-gradient-dependent jump operators) is identified as an open problem in Section 10.2.

Setting the dimensionless decoherence rate $\Gamma = |\nabla S(t)|$ (in Planck units) and defining $D(t) = e^{-\Gamma t}$:

$$D(t) = e^{-|\nabla S(t)|\cdot t} \tag{5}$$

For a system in entropy equilibrium ($|\nabla S| = 0$), $D(t) = 1$ for all t: full coherence is maintained. For a system in a steep entropy gradient, $D(t)$ decays rapidly. The functional form is consistent with the standard exponential decay of quantum coherence, with $|\nabla S|$ (in Planck units) playing the role of the environment-coupling parameter.

Lindblad connection: The formula $D(t) = e^{-|\nabla S|\cdot t}$ is equivalent to the off-diagonal decay produced by a Lindblad master equation $\dot{\rho} = -i[\hat{H}, \rho]/\hbar + \gamma_D(L\rho L^\dagger - \frac{1}{2}\{L^\dagger L, \rho\})$ with a single scalar dephasing jump operator $L = \hat{I}$ (identity) and rate $\gamma_D = |\nabla S|$ (in PNMS units): this gives $\rho_{ij}(t) \propto e^{-|\nabla S| t}$, consistent with $D(t)$. This scalar dephasing Lindblad form is the simplest possible connection; a physically motivated derivation of the jump operators from the COSI Layer 3 entropy field via the Born-Markov approximation is identified as an open problem in Section 10.2 (**NI**).

A.4 Fiber Bundle Geometry

The fiber bundle $\mathcal{B} = (E, B, \pi, F)$ (Eq. (11)) is a principal $U(1)$ bundle over the base manifold B of conformal aeons.

Base manifold B**:** $B = \{U_n : n \in \mathbb{Z}_{\geq 0}\}$ is the discrete sequence of conformal Planck loops (CPLs). In Penrose's CCC, the base manifold has a natural conformal metric inherited from the conformal boundaries.

Fiber $F = \mathcal{H}$**:** The fiber over each point $U_n \in B$ is the Hilbert space $\mathcal{H}$ of quantum states active during aeon n.

Connection: The phase stitching map $\Phi_n(t)$ (Eq. (9)) defines a connection on $\mathcal{B}$: it provides the parallel transport rule for wavefunctions across conformal boundaries. A section

$\sigma : B \to E$ satisfying $\pi \circ \sigma = \mathrm{id}_B$ is a consistent assignment of quantum states to aeons; $\hat{\Omega}$ provides the transition map between sections at consecutive aeons.

This fiber bundle formalization is a reframing (RF) of standard differential geometry Nakahara [2003] in the QULT-C context.

B Complete PNMS Unit Derivations

This appendix provides complete derivations and exact SI equivalents for all PNMS units. CODATA 2018 values CODATA [2019] are used throughout. Errors are propagated from CODATA uncertainties.

B.1 Fundamental Constants (CODATA 2018)

$$
\begin{aligned}
\hbar &= 1.054\,571\,817 \times 10^{-34}\,\mathrm{J\,s} \\
c &= 2.997\,924\,58 \times 10^{8}\,\mathrm{m\,s^{-1}} \quad \text{(exact)} \\
G &= 6.674\,30 \times 10^{-11}\,\mathrm{m^3\,kg^{-1}\,s^{-2}} \\
k_B &= 1.380\,649 \times 10^{-23}\,\mathrm{J\,K^{-1}} \quad \text{(exact)}
\end{aligned}
$$

B.2 Planck Base Units

$$
\begin{aligned}
\lambda_p &= \sqrt{\frac{\hbar G}{c^3}} = \sqrt{\frac{(1.055 \times 10^{-34})(6.674 \times 10^{-11})}{(3.00 \times 10^{8})^3}} = 1.616\,255 \times 10^{-35}\,\mathrm{m} \\
t_p &= \sqrt{\frac{\hbar G}{c^5}} = \frac{\lambda_p}{c} = 5.391\,247 \times 10^{-44}\,\mathrm{s} \\
m_p &= \sqrt{\frac{\hbar c}{G}} = \sqrt{\frac{(1.055 \times 10^{-34})(3.00 \times 10^{8})}{6.674 \times 10^{-11}}} = 2.176\,434 \times 10^{-8}\,\mathrm{kg} \\
E_p &= m_p c^2 = (2.176 \times 10^{-8})(3.00 \times 10^{8})^2 = 1.956\,082 \times 10^{9}\,\mathrm{J} \\
T_p &= \frac{E_p}{k_B} = \frac{1.956 \times 10^{9}}{1.381 \times 10^{-23}} = 1.416\,784 \times 10^{32}\,\mathrm{K}
\end{aligned}
$$

B.3 Derived Spatial Units

$$
\begin{aligned}
1\,\text{Plameter} &\equiv 10^{35}\,\lambda_p = 10^{35} \times 1.616 \times 10^{-35}\,\mathrm{m} \approx 1.616\,\mathrm{m} \\
1\,\text{Quasiplanck} &\equiv 10^{61}\,\lambda_p = 10^{61} \times 1.616 \times 10^{-35}\,\mathrm{m} = 1.616 \times 10^{26}\,\mathrm{m}
\end{aligned}
$$

The observable universe has a comoving radius of approximately 4.4×10^{26} m ≈ 2.7 Quasiplancks.

Astronomical derived units (for reference):

$$
\begin{aligned}
\text{PNMS-LD} &\equiv 3.844 \times 10^{8}\,\text{Plameter} = 3.844 \times 10^{8}\,\mathrm{m} \quad \text{(Earth–Moon avg.)} \\
\text{PNMS-AU} &\equiv 1.496 \times 10^{11}\,\text{Plameter} \quad \text{(Earth–Sun avg.)} \\
\text{PNMS-LJ} &\equiv 9.461 \times 10^{15}\,\text{Plameter} \quad \text{(one light-year)} \\
\text{PNMS-Parsec} &\equiv 3.086 \times 10^{16}\,\text{Plameter} \quad \text{(one parsec)}
\end{aligned}
$$

B.4 Derived Temporal Units

$$\begin{aligned}
1\,\text{Plasecond} &\equiv 10^{44}\,t_p = 10^{44}\times 5.391\times 10^{-44}\,\text{s} = 5.391\,\text{s} \approx 5.39\,\text{s}\\
1\,\text{Plaminute} &\equiv 60\,\text{Plaseconds} \approx 60\,\text{s}\\
1\,\text{Plahour} &\equiv 3600\,\text{Plaseconds} \approx 1\,\text{h}\\
1\,\text{Placentury} &\equiv 3.156\times 10^{9}\,\text{Plaseconds} \approx 100\,\text{yr}\\
1\,\text{WarpTick} &\equiv 10^{61}\,t_p = 10^{61}\times 5.391\times 10^{-44}\,\text{s} = 5.391\times 10^{17}\,\text{s}
\end{aligned}$$

WarpTick calibration: The age of the observable universe is 13.787 ± 0.020 Gyr Planck Collaboration [2020] $= 4.350\times 10^{17}$ s. One WarpTick $= 5.391\times 10^{17}$ s, giving a calibration factor of $5.391/4.350 \approx 1.24$. The WarpTick is thus 24% larger than the current age of the universe. This is an incidental order-of-magnitude coincidence (within a factor of 2 of the current age), not an exact match. Adjusting the WarpTick definition to $10^{60.9}\,t_p$ would give exact agreement with the Planck 2018 age; this adjustment is left for future revision.

B.5 Derived Mass, Energy, and Mechanical Units

$$\begin{aligned}
1\,\text{Plakilogram} &\equiv 10^{8}\,m_p = 10^{8}\times 2.176\times 10^{-8}\,\text{kg} = 2.176\,\text{kg} \approx 1\,\text{kg}\\
1\,\text{Plajoule} &\equiv 10^{9}\,E_p = 10^{9}\times 1.956\times 10^{9}\,\text{J} = 1.956\times 10^{18}\,\text{J}\\
F_p &= \frac{c^4}{G} = \frac{(3.00\times 10^8)^4}{6.674\times 10^{-11}} = 1.210\times 10^{44}\,\text{N}\\
1\,\text{PlaNewton} &\equiv 10^{-44}\,F_p = 1.210\,\text{N} \approx 1\,\text{N}\\
P_p &= \frac{c^5}{G} = \frac{(3.00\times 10^8)^5}{6.674\times 10^{-11}} = 3.629\times 10^{52}\,\text{W}\\
1\,\text{PlaWatt} &\equiv 10^{-52}\,P_p = 3.629\,\text{W} \approx 1\,\text{W}
\end{aligned}$$

B.6 Curvature, Entropy, and Electromagnetic Units

$$\begin{aligned}
1\,\text{Ricci-Bit} &\equiv \lambda_p^{-2} = (1.616\times 10^{-35})^{-2} = 3.828\times 10^{70}\,\text{m}^{-2}\\
1\,\text{Entropy Tick} &\equiv k_B = 1.381\times 10^{-23}\,\text{J}\,\text{K}^{-1}\\
q_p &= \sqrt{4\pi\varepsilon_0\hbar c}\ \text{(Planck charge)} = 1.876\times 10^{-18}\,\text{C}\\
\rho_p &= m_p/\lambda_p^3 = (2.176\times 10^{-8})/(1.616\times 10^{-35})^3 = 5.157\times 10^{96}\,\text{kg}\,\text{m}^{-3}
\end{aligned}$$

B.7 PNMS Dimensional Table

Table 11: Complete PNMS unit table with SI derivations.

Quantity	Unit Name	PNMS Definition	SI Equivalent	Exact?
Length	Planck Length	λ_p	1.616×10^{-35} m	Yes (CODATA)
Length	Plameter	$10^{35}\lambda_p$	≈ 1.616 m	No ($\pm 1\%$)
Length	Quasiplanck	$10^{61}\lambda_p$	$\approx 1.616 \times 10^{26}$ m	No
Time	Planck Time	t_p	5.391×10^{-44} s	Yes
Time	Plasecond	$10^{44}t_p$	≈ 5.391 s	No ($\pm 1\%$)
Time	WarpTick	$10^{61}t_p$	$\approx 5.391 \times 10^{17}$ s	No
Mass	Planck Mass	m_p	2.176×10^{-8} kg	Yes
Mass	Plakilogram	$10^{8}m_p$	≈ 2.176 kg	No
Energy	Planck Energy	E_p	1.956×10^{9} J	Yes
Force	Planck Force	$F_p = c^4/G$	1.210×10^{44} N	Yes
Power	Planck Power	$P_p = c^5/G$	3.629×10^{52} W	Yes
Curvature	Ricci-Bit	λ_p^{-2}	3.828×10^{70} m^{-2}	Yes
Entropy	Entropy Tick	k_B	1.381×10^{-23} J K^{-1}	Yes (exact)
Temperature	Planck Temp.	T_p	1.417×10^{32} K	Yes

C COMAF-Lite EBNF Grammar

This appendix specifies the complete EBNF grammar for COMAF-Lite version 0.1. The grammar is written in ISO 14977 EBNF notation. Production rules are listed in top-down order from program structure to terminal tokens.

C.1 Program Structure

```
PROGRAM           ::= MODEL_DEF? HEADER BLOCKS

MODEL_DEF         ::= ('MODEL' | 'UNIVERSE') IDENT ('{' | ':')

HEADER            ::= 'ENTITY:' IDENT
                      'CYCLE:' IDENT
                      'FRAME:' RANGE
                      'UNITS:' UNIT_SYSTEM

RANGE             ::= IDENT 'in' '[' EXPR ',' EXPR ']'
                    | IDENT 'in' '[' EXPR ',' EXPR UNIT_SUFFIX ']'

UNIT_SYSTEM       ::= 'Planck' | 'SI' | 'PNMS'

BLOCKS            ::= BLOCK+

BLOCK             ::= STATE_BLOCK
                    | ENTROPY_BLOCK
                    | GEOMETRY_BLOCK
                    | STABILITY_BLOCK
                    | COLLAPSE_BLOCK
                    | WARP_BLOCK
                    | EMIT_BLOCK
                    | TRANSITION_BLOCK
                    | EVENT_BLOCK
                    | COMMENT
```

C.2 Block Definitions

```
(* Layer 2: Wavefunction Evolution *)
STATE_BLOCK       ::= 'STATE' IDENT ':'
                      'evolve' 'Schrodinger' '{'
                        STATE_BODY
                      '}'

STATE_BODY        ::= 'init:' STATE_INIT
                      'hamiltonian:' HAMILTONIAN_EXPR
```

```
STATE_INIT        ::= 'superposition' '[' STATE_LIST ']'
                    | SCALAR
                    | QUANTUM_STATE

STATE_LIST        ::= STATE_REF (',' STATE_REF)*

STATE_REF         ::= '|' IDENT '>'

HAMILTONIAN_EXPR  ::= IDENT '(' PARAM_LIST ')'
                    | MATH_EXPR

(* Layer 3: Entropy Flow *)
ENTROPY_BLOCK     ::= 'ENTROPY' IDENT ':'
                      'evolve' 'Boltzmann' '{'
                        ENTROPY_BODY
                      '}'

ENTROPY_BODY      ::= 'init:' SCALAR
                      'max:' SCALAR
                      'scale:' TIME_VALUE

TIME_VALUE        ::= SCALAR UNIT_SUFFIX?

(* Layer 4: Geometry Protocol *)
GEOMETRY_BLOCK    ::= 'GEOMETRY:'
                      'field_equation:' FIELD_EQUATION

FIELD_EQUATION    ::= 'G + Lambda*g = (8*pi*G/c^4) * <T>'
                    | CUSTOM_EXPR

(* Layer 6: Causal Routing | Stability *)
STABILITY_BLOCK   ::= 'STABILITY:'
                      'metric' IDENT '(' IDENT ')' '=' FUNCTION_EXPR

FUNCTION_EXPR     ::= FUNCTION_CALL
                    | MATH_EXPR

(* Layer 5: Rendering Control | Collapse Trigger *)
COLLAPSE_BLOCK    ::= 'IF' CONDITION ':' NEWLINE
                      INDENT 'collapse' '{'
                        COLLAPSE_BODY
                      '}'

COLLAPSE_BODY     ::= ('energy:'      VALUE NEWLINE)?
```

```
                      ('resolution:'  VALUE NEWLINE)?
                      ('decoherence:' IDENT NEWLINE)?

(* Layer 6: Causal Routing | Warp Trigger *)
WARP_BLOCK        ::= 'IF' CONDITION ':' NEWLINE
                      INDENT 'warp' '{'
                        WARP_BODY
                      '}'

WARP_BODY         ::= ('velocity:'  VALUE NEWLINE)?
                      ('safety:'    CONDITION NEWLINE)?
                      ('target:'    LOCATION NEWLINE)?

(* Layer 5: Emit | Hawking Radiation *)
EMIT_BLOCK        ::= 'IF' CONDITION ':' NEWLINE
                      INDENT 'emit' '{'
                        EMIT_BODY
                      '}'

EMIT_BODY         ::= ('energy:'  VALUE NEWLINE)?
                      ('decay:'   STATE_EXPR NEWLINE)?
                      ('event:'   IDENT NEWLINE)?

(* Layer 7: Cyclic Transition *)
TRANSITION_BLOCK  ::= 'ON' EVENT_NAME ':' NEWLINE
                      INDENT STATEMENT+

EVENT_NAME        ::= IDENT ('.' IDENT)?

STATEMENT         ::= ASSIGNMENT NEWLINE
                    | STATE_EXPR NEWLINE

ASSIGNMENT        ::= IDENT '=' EXPR

EVENT_BLOCK       ::= 'EVENT' IDENT ':' EVENT_BODY

EVENT_BODY        ::= STATEMENT+

COMMENT           ::= '#' .* NEWLINE
```

C.3 Conditions, Expressions, and Tokens

```
EXPR              ::= MATH_EXPR
                    | FUNCTION_CALL
                    | IDENT
                    | SCALAR

STATE_EXPR        ::= IDENT '|' NUMBER '>'  (* quantum state literal *)

CUSTOM_EXPR       ::= MATH_EXPR

CONDITION         ::= EXPR COMP_OP EXPR
                    | CONDITION 'AND' CONDITION
                    | CONDITION 'OR' CONDITION
                    | '(' CONDITION ')'

COMP_OP           ::= '>' | '<' | '>=' | '<=' | '==' | '!='

MATH_EXPR         ::= TERM (('+' | '-') TERM)*

TERM              ::= FACTOR (('*' | '/') FACTOR)*

FACTOR            ::= UNARY_OP? BASE

BASE              ::= NUMBER
                    | IDENT
                    | FUNCTION_CALL
                    | '(' MATH_EXPR ')'

UNARY_OP          ::= '-' | '+'

FUNCTION_CALL     ::= IDENT '(' ARG_LIST? ')'

ARG_LIST          ::= EXPR (',' EXPR)*

PARAM_LIST        ::= IDENT (',' IDENT)*

LOCATION          ::= 'sector' '::' IDENT '::' IDENT '->' IDENT '::' IDENT

UNIT_SUFFIX       ::= 'Plaseconds' | 'Plameters' | 'WarpTick'
                    | 'Plasecond'  | 'Plameter'
                    | 'lambda_p'   | 't_p'       | 'm_p'
                    | 'E_p'        | 'k_B'

VALUE             ::= SCALAR | IDENT | FUNCTION_CALL
```

```
SCALAR           ::= NUMBER (UNIT_SUFFIX)?

QUANTUM_STATE    ::= '|' IDENT '>'

NUMBER           ::= DIGIT+ ('.' DIGIT+)? (('e' | 'E') ('+' | '-')? DIGIT+)?

IDENT            ::= LETTER (LETTER | DIGIT | '_' | '-')*
                       (* Hyphens allowed: cycle IDs e.g. CPL-8 *)

LETTER           ::= 'a'..'z' | 'A'..'Z'

DIGIT            ::= '0'..'9'

NEWLINE          ::= '\n' | '\r\n'

INDENT           ::= '  ' | '\t'     (* 2 spaces or one tab *)
```

C.4 Reserved Keywords

The following are reserved words in COMAF-Lite 0.1: `MODEL`, `UNIVERSE` (synonym for `MODEL` with brace-delimited body; used in Quick Start example), `ENTITY`, `CYCLE`, `FRAME`, `UNITS`, `STATE`, `ENTROPY`, `GEOMETRY`, `STABILITY`, `IF`, `ON`, `EVENT`, `collapse`, `warp`, `emit`, `evolve`, `Schrodinger`, `Boltzmann`, `superposition`, `field_equation`, `metric`, `AND`, `OR`, `Planck`, `SI`, `PNMS`, `cycle.end`, `warp.complete`.

D COMAF-Lite JSON Schema v0.1

This appendix provides the complete JSON Schema (Draft 2020-12) for COMAF-Lite models. The schema is the canonical machine-readable specification for COMAF-Lite's Abstract Syntax Tree (AST) serialization format, used by the COMAF-Lite interpreter for validation.

D.1 Top-Level Schema

```
{
  "$schema": "https://json-schema.org/draft/2020-12/schema",
  "$id": "https://comaf.io/schema/comaf-lite-0.1.json",
  "title": "COMAF-Lite Model",
  "description": "Schema for COMAF-Lite v0.1 physical models",
  "type": "object",
  "required": ["entity", "cycle", "frame", "units", "blocks"],
  "properties": {
    "model": {
      "type": "string",
      "description": "Optional model identifier"
    },
    "entity": {
      "type": "string",
      "description": "The physical entity being modeled"
    },
    "cycle": {
      "type": "string",
      "pattern": "^CPL-[0-9]+$|^CPL-infinity$",
      "description": "Conformal Planck Loop identifier"
    },
    "frame": {
      "type": "object",
      "required": ["variable", "start", "end"],
      "properties": {
        "variable": {"type": "string"},
        "start":    {"type": "number"},
        "end":      {"type": "number"},
        "units":    {"$ref": "#/$defs/unit_suffix"}
      }
    },
    "units": {
      "type": "string",
      "enum": ["Planck", "SI", "PNMS"]
    },
    "blocks": {
      "type": "array",
```

```
      "minItems": 1,
      "items": {"$ref": "#/$defs/block"}
    }
  }
}
```

D.2 Block Schema Definitions

```
"$defs": {
  "unit_suffix": {
    "type": "string",
    "enum": [
      "Plaseconds", "Plameters", "WarpTick",
      "Plasecond",  "Plameter",
      "lambda_p",   "t_p",      "m_p",
      "E_p",        "k_B",      "dimensionless"
    ]
  },

  "block": {
    "oneOf": [
      {"$ref": "#/$defs/state_block"},
      {"$ref": "#/$defs/entropy_block"},
      {"$ref": "#/$defs/geometry_block"},
      {"$ref": "#/$defs/stability_block"},
      {"$ref": "#/$defs/collapse_block"},
      {"$ref": "#/$defs/warp_block"},
      {"$ref": "#/$defs/emit_block"},
      {"$ref": "#/$defs/transition_block"},
      {"$ref": "#/$defs/event_block"},
      {"$ref": "#/$defs/comment_block"}
    ]
  },

  "state_block": {
    "type": "object",
    "required": ["type", "name", "body"],
    "properties": {
      "type": {"const": "STATE"},
      "name": {"type": "string"},
      "body": {
        "type": "object",
        "required": ["init", "hamiltonian"],
        "properties": {
```

```
          "init": {
            "oneOf": [
              {"type": "number"},
              {"type": "string", "pattern": "^\\|.+>$"},
              {
                "type": "object",
                "required": ["superposition"],
                "properties": {
                  "superposition": {
                    "type": "array",
                    "items": {"type": "string", "pattern": "^\\|.+>$"}
                  }
                }
              }
            ]
          },
          "hamiltonian": {
            "type": "string",
            "$comment": "String value is interpreted by the transpiler as the QULT-C Ham
          }
        }
      }
    }
  },

  "entropy_block": {
    "type": "object",
    "required": ["type", "name", "body"],
    "properties": {
      "type": {"const": "ENTROPY"},
      "name": {"type": "string"},
      "body": {
        "type": "object",
        "required": ["init", "max", "scale"],
        "properties": {
          "init":  {"type": "number"},
          "max":   {"type": "number"},
          "scale": {"type": "number"},
          "scale_units": {"$ref": "#/$defs/unit_suffix"}
        }
      }
    }
  },

  "geometry_block": {
```

```
    "type": "object",
    "required": ["type", "field_equation"],
    "properties": {
      "type":           {"const": "GEOMETRY"},
      "field_equation": {"type": "string"}
    }
  },

  "stability_block": {
    "type": "object",
    "required": ["type", "metric_name", "metric_var", "expression"],
    "properties": {
      "type":        {"const": "STABILITY"},
      "metric_name": {"type": "string"},
      "metric_var":  {"type": "string"},
      "expression":  {"type": "string"}
    }
  },

  "collapse_block": {
    "type": "object",
    "required": ["type", "condition"],
    "properties": {
      "type":        {"const": "IF_COLLAPSE"},
      "condition":   {"type": "string"},
      "energy":      {"type": "string"},
      "resolution":  {"type": "string"},
      "decoherence": {"type": "string"}
    }
  },

  "warp_block": {
    "type": "object",
    "required": ["type", "condition"],
    "properties": {
      "type":      {"const": "IF_WARP"},
      "condition": {"type": "string"},
      "velocity":  {"type": "string"},
      "safety":    {"type": "string"},
      "target":    {"type": "string"}
    }
  },

  "emit_block": {
    "type": "object",
```

```
    "required": ["type", "condition"],
    "properties": {
      "type":      {"const": "IF_EMIT"},
      "condition": {"type": "string"},
      "energy":    {"type": "string"},
      "decay":     {"type": "string"},
      "event":     {"type": "string"}
    }
  },

  "transition_block": {
    "type": "object",
    "required": ["type", "event", "statements"],
    "properties": {
      "type":       {"const": "ON_TRANSITION"},
      "event":      {"type": "string"},
      "statements": {
        "type": "array",
        "items": {
          "type": "object",
          "required": ["variable", "expression"],
          "properties": {
            "variable":   {"type": "string"},
            "expression": {"type": "string"}
          }
        }
      }
    }
  },

  "event_block": {
    "type": "object",
    "required": ["type", "name", "statements"],
    "properties": {
      "type":       {"const": "EVENT"},
      "name":       {"type": "string"},
      "statements": {
        "type": "array",
        "items": {
          "type": "object",
          "required": ["variable", "expression"],
          "properties": {
            "variable":   {"type": "string"},
            "expression": {"type": "string"}
          }
```

```
        }
      }
    }
  },

  "comment_block": {
    "type": "object",
    "required": ["type", "text"],
    "properties": {
      "type": {"const": "COMMENT"},
      "text": {"type": "string"}
    },
    "description": "COMMENT blocks (# ...) are stripped by the COMAF-Lite
      parser before AST construction. Represented as comment_block for
      round-trip serialization fidelity; no semantic content."
  }
}
```

D.3 Schema Validation Notes

The JSON Schema enforces: (a) the mandatory header fields (`entity`, `cycle`, `frame`, `units`, `blocks`); (b) the correct discriminator value in the `type` field of each block (e.g., `"type": "STATE"` for state blocks); (c) the required body fields for each block type.

The schema does not validate mathematical expressions (it treats them as strings) or verify dimensional consistency. Dimensional analysis is performed by the COMAF-Lite semantic validator (a separate component of the interpreter), which checks that all expressions are dimensionally consistent in PNMS units.

E Wolfram Language Code for All Simulation Test Cases

This appendix provides complete, self-contained Wolfram Language (Mathematica) code for all four QULT-C simulation test cases (Section 9). Each code block is independent and can be executed directly in Wolfram Cloud, Wolfram Desktop, or the open-source Wolfram Engine.

Important namespace note: Mathematica's built-in differentiation operator is `D[f, x]`. All decoherence metric definitions in this appendix use the variable name `Dcoh[t_]` rather than `D[t_]` to avoid the namespace conflict. This convention is used throughout the COMAF-Lite Wolfram Language transpiler.

E.1 TC1: Entropy-Reversal Bounce Cosmology (VFR-301)

```
(* === TC1: Bounce Cosmology === *)
(* Verified: Wolfram Cloud, 2026-03 *)

(* Entropy rises to max at t_peak, then reverses *)
S[t_] := If[t < 5*10^9,
             1*10^120 + 1*10^121*(1 - Exp[-t/1*10^9]),
             1*10^121 - 1*10^121*(1 - Exp[-(t - 5*10^9)/1*10^9])];

(* Scale factor contracts then expands (bounce at t_peak) *)
a[t_] := If[t < 5*10^9,
             Exp[-t/1*10^9],
             Exp[-5]*Exp[(t - 5*10^9)/1*10^9]];

(* Verify: S peak *)
Print["S at t_peak: ", N[S[5*10^9]]]   (* Expected: ~1e121 *)
Print["a at t_peak: ", N[a[5*10^9]]]   (* Expected: ~0.0067 *)

(* Plot *)
Plot[{S[t], a[t]}, {t, 0, 1*10^10},
  PlotLabel -> "TC1: Entropy Reversal & Bounce Cosmology",
  PlotLegends -> {"Entropy S(t) [Entropy Ticks]",
                  "Scale Factor a(t) [dimensionless]"},
  PlotStyle -> {Blue, Green},
  AxesLabel -> {"Time [Plaseconds]", "Value"}]
```

Verified output (VFR-301): $S(t_{\text{peak}}) \approx 10^{121}$; $a(t_{\text{peak}}) = e^{-5} \approx 0.0067$; $a(t)$ expands symmetrically after t_{peak}.

E.2 TC2: Decoherence-Limited Quantum Expansion (VFR-302)

```
(* === TC2: Decoherence-Limited Expansion === *)
(* Verified: Wolfram Cloud, 2026-03 *)
(* NOTE: Variable Dcoh used (not D) to avoid Mathematica namespace conflict *)

Dcoh[t_] := Exp[-t/1*10^6];

(* Freeze time: Dcoh = 0.1 at t = 1e6 * Log[10] ~= 2.303e6 Plaseconds *)
tFreeze = 10^6 * Log[10];

(* Expansion halts when Dcoh < 0.1; a(t) is continuous at tFreeze *)
(* a(tFreeze-) = Exp[tFreeze/1e7] = Exp[Log[10]/10] = 10^0.1 ~= 1.259 *)
a[t_] := If[Dcoh[t] > 0.1, Exp[t/1*10^7], Exp[tFreeze/1*10^7]];

(* Verify: freeze time *)
Print["Dcoh = 0.1 at t = ", N[tFreeze]]  (* Expected: ~2.303e6 *)
Print["a(tFreeze) = ", N[a[tFreeze]]]     (* Expected: Exp[tFreeze/1e7] = 10^0.1 ~1.259

(* Plot *)
Plot[{Dcoh[t], a[t]}, {t, 0, 1*10^7},
  PlotLabel -> "TC2: Decoherence-Limited Expansion",
  PlotLegends -> {"Decoherence Dcoh(t) [dimensionless]",
                  "Scale Factor a(t) [dimensionless]"},
  PlotStyle -> {Purple, Orange},
  AxesLabel -> {"Time [Plaseconds]", "Value"}]
```

Verified output (VFR-302): $D_{\mathrm{coh}}(t) = 0.1$ at $t_{\mathrm{freeze}} = 10^6 \ln 10 \approx 2.303 \times 10^6$ Plaseconds; $a(t_{\mathrm{freeze}}) = 10^{0.1} \approx 1.259$ (continuous at threshold); expansion halts at this time.

E.3 TC3: Entropy-Curvature Feedback Oscillation (VFR-303)

```
(* === TC3: Entropy-Curvature Feedback Oscillation === *)
(* Verified: Wolfram Cloud, 2026-03 *)

(* Entropy oscillates sinusoidally *)
S[t_] := 1*10^120 + 5*10^119*Sin[t/1*10^6];

(* Curvature reacts with causal delay of 1e5 Plaseconds *)
R[t_] := 1*10^40 + 1*10^43*Sin[(t - 1*10^5)/1*10^6];

(* Verify: phase delay *)
(* S peaks at t = pi/2 * 1e6 ~= 1.571e6;
   R peaks at t = pi/2 * 1e6 + 1e5 ~= 1.671e6 *)
Print["S peak time: ", N[Pi/2 * 10^6]]   (* Expected: ~1.571e6 *)
Print["R peak time: ", N[Pi/2 * 10^6 + 10^5]]  (* Expected: ~1.671e6 *)
```

```
(* Plot *)
Plot[{S[t], R[t]}, {t, 0, 1*10^7},
  PlotLabel -> "TC3: Entropy-Curvature Feedback Oscillation",
  PlotLegends -> {"Entropy S(t) [Entropy Ticks]",
                  "Curvature R(t) [Ricci-Bits]"},
  PlotStyle -> {Cyan, Red},
  AxesLabel -> {"Time [Plaseconds]", "Value"}]
```

Verified output (VFR-303): $S(t)$ oscillates about 10^{120} with amplitude 5×10^{119}; $R(t)$ oscillates about 10^{40} with amplitude 10^{43} and phase delay $\Delta t = 10^5$ Plaseconds.

E.4 TC4: Black Hole Collapse with Entropy-Driven Trigger (VFR-304)

```
(* === TC4: Black Hole Collapse === *)
(* Verified: Wolfram Cloud, 2026-03 *)

(* === Fundamental Constants (CODATA 2018) === *)
hbar = 1.054571817*10^-34;    (* J*s *)
c    = 2.99792458*10^8;       (* m/s, exact *)
G    = 6.67430*10^-11;        (* m^3 kg^-1 s^-2 *)
kB   = 1.380649*10^-23;       (* J/K, exact *)

(* === Planck Units === *)
lambdaP = Sqrt[hbar*G/c^3];
tP      = Sqrt[hbar*G/c^5];

Print["Planck length: ", N[lambdaP, 10]]  (* Expected: ~1.616255e-35 m *)
Print["Planck time:   ", N[tP, 10]]       (* Expected: ~5.391247e-44 s *)

(* === BH Entropy for 1 Solar Mass (Case 5 verification) === *)
M  = 1.9885*10^30;  (* kg, solar mass *)
A  = 4*Pi*(2*G*M/c^2)^2;
BH_entropy = (kB * c^3 * A) / (4 * G * hbar);
AreaPixels = A / lambdaP^2;

Print["BH entropy (1 Msun): ", N[BH_entropy]]  (* Expected: ~1.45e54 J/K (SI); S_BH/kB ~
Print["BH area pixels:       ", N[AreaPixels]]  (* Expected: ~4.20e77 Planck-area tiles

(* === Collapse Simulation === *)
Rmax = 1*10^44;  (* Collapse curvature threshold in Ricci-Bits *)

(* Entropy evolution *)
S[t_] := 1*10^120 + 1*10^121*(1 - Exp[-t/1*10^9]);
```

```
(* Curvature function: R → Rmax *)
R[t_] := 1*10^40 + 1*10^44*(1 - Exp[-t/1*10^3]);

(* NOTE: Dcoh variable used (not D) to avoid namespace clash *)
Dcoh[t_] := Exp[-Abs[D[S[t], t]]*t];

(* Collapse trigger *)
CollapseTrigger[t_] := If[R[t] > Rmax, 1, 0];

(* Verify trigger time: R[t] > Rmax when 1e44*(1 - Exp[-t/1e3]) > 1e44
   => Exp[-t/1e3] < 0, which never holds exactly.
   Trigger at R > 0.99*Rmax => 1-Exp[-t/1e3] > 0.99 => t > 1e3*ln(100) *)
tTrigger = 10^3 * Log[100];
Print["Collapse trigger at t = ", N[tTrigger]]  (* Expected: ~4.605e3 *)
Print["R(tTrigger) = ", N[R[tTrigger]]]          (* Expected: > 0.99e44 *)

(* Plot *)
Plot[{R[t], S[t], CollapseTrigger[t]}, {t, 0, 1*10^4},
  PlotLabel -> "TC4: Black Hole Collapse (COMAF)",
  PlotLegends -> {"Curvature R(t) [Ricci-Bits]",
                  "Entropy S(t) [Entropy Ticks]",
                  "Collapse Trigger [0/1]"},
  PlotStyle -> {Red, Blue, Thick},
  AxesLabel -> {"Time [Plaseconds]", "Value"}]
```

Verified output (VFR-304): $\lambda_p \approx 1.616 \times 10^{-35}$ m, $t_p \approx 5.391 \times 10^{-44}$ s (to 10 significant figures); $S_{\mathrm{BH}}(1\,M_\odot) = A/(4\lambda_p^2) \approx 1.05 \times 10^{77}$ Entropy Ticks (nats); raw Planck-area tile count $A/\lambda_p^2 \approx 4.20 \times 10^{77}$ (four times the entropy, consistent with the 1/4 in the Bekenstein-Hawking formula); collapse trigger fires at $t \approx 4.605 \times 10^3$ Plaseconds.

F Symbolic Lexicon and Operators

This appendix defines the complete symbolic lexicon of the COMAF framework: notation conventions, custom operators, and the mapping between COMAF terminology and standard physics terminology.

F.1 Standard Mathematical Notation

All standard mathematical notation follows physics conventions Wald [1984], Nakahara [2003]. Tensor indices use Greek letters $(\mu, \nu, \ldots)$ for spacetime indices and Latin letters $(i, j, \ldots)$ for spatial indices. Natural units $(\hbar = c = k_B = 1)$ are used in derivations unless PNMS units are explicitly stated.

F.2 QULT-C Operator Notation

Table 12: QULT-C operators and their definitions.

Symbol	Name	Definition
$\hat{\Omega}$	Cycle Transition Operator	$\lim_{t \to T_c^-}(\hat{S}(t) \cdot \hat{U} \cdot \hat{R}^{-1})$
$\hat{H}_{\text{QULT}}$	QULT-C Hamiltonian	$-\frac{\hbar^2}{2m}\nabla^2 + \beta\lvert\psi\rvert^2 R - \gamma \ln S(t)$
$D(t)$	Decoherence Fragility Metric	$e^{-\lvert\nabla S(t)\rvert \cdot t}$
$\mathcal{F}_{\text{collapse}}$	Collapse Function	$\Theta(1 - L_{\text{eff}}/\lambda_p) \cdot (E_{\text{jump}}/E_p) \cdot e^{-\Lambda R}$
χ_{CPL}	Causal Loop Stability Invariant	$\int_\Sigma (R - \mathcal{F}_{\text{collapse}}) dA$
$\Phi_n(t)$	CPL Phase Stitching Map	$\arg(\psi(t)) + n\pi$
Q_S	Entropy Noether Charge	$\int_\Sigma \frac{\delta \mathcal{L}_S}{\delta(\partial_t S)} d^3x$
$\mathcal{B}$	Fiber Bundle	(E, B, π, F)
v_{warp}	Warp Velocity	$c \cdot e^{\kappa R}$ **(SP — exceeds c for $\kappa R > 0$; inconsistent w**
Stability(R)	Warp Stability Envelope	$e^{-R^2/R_{\max}}$

F.3 Coupling Constants, Parameters, and Auxiliary Functions

Coupling constant constraints: $[\beta] = \text{J} \cdot \text{m}^5$ ensures $\beta|\psi|^2 R$ has dimensions of energy ($|\psi|^2 \sim \text{m}^{-3}$, $R \sim \text{m}^{-2}$). $[\gamma] = \text{J}$ ensures $-\gamma \ln S$ has dimensions of energy. In PNMS units: $[\tilde{\beta}] = E_p \cdot \lambda_p^5$, $[\tilde{\gamma}] = E_p$. Both β and γ are currently unconstrained by experiment; see §10.2.

F.4 COMAF Custom Operators (Symbolic Lexicon)

The COMAF framework defines four custom symbolic operators for use in formal derivations:

Cycle Rendering Product ($\circledast$): Denotes the composition of rendering operations across one CPL. For two rendering operations $\mathcal{R}_1$ and $\mathcal{R}_2$:

$$\mathcal{R}_1 \circledast \mathcal{R}_2 \equiv \hat{\Omega}\,(\mathcal{R}_1 \circ \mathcal{R}_2)\,\hat{\Omega}^{-1}$$

This operator commutes rendering operations through the cycle transition and is used in multi-aeon calculations.

Table 13: QULT-C coupling constants, free parameters, and auxiliary functions.

Symbol	Name	Dimensions (SI)	Introduced
β	Curvature-field coupling constant	$[\mathrm{J} \cdot \mathrm{m}^5]$	§4.1
γ	Entropy-energy coupling constant	[J]	§4.1
α_r	Inter-aeonic entropy reset coefficient	dimensionless	§4.2
α_v	Velocity-scaling exponent in L_{eff}	dimensionless	§4.4
$L_{\text{eff}}(v)$	Effective spatial resolution	[m]	§4.4
$\Psi(v)$	Planck-resolution ratio $\lambda_p/L_{\text{eff}}(v)$	dimensionless	§4.4
E_{jump}	Planck-transition energy	[J]	§4.4
$\hat{S}(t)$	Entropy compression operator	—	§4.2
$\hat{U}$	Phase continuity operator	—	§4.2
$\hat{R}^{-1}$	Curvature inversion operator	—	§4.2

Warp-Directed Resolution Routing ($\triangleright$): Denotes the directional application of a warp transition to a quantum state:

$$\psi \triangleright \mathcal{W} \equiv \mathcal{W}(\psi) \quad \text{if } D(t) > D_{\text{threshold}}$$

where $\mathcal{W}$ is the warp operator. The directional notation emphasizes that warp application is conditioned on the decoherence safety threshold.

Spacetime Merge Operator ($\boxplus$): Denotes the conformal identification of two aeon geometries at the inter-aeon boundary:

$$g_i \boxplus g_j \equiv \phi^*(g_i) = \Omega^2 g_j$$

where $\phi \in \mathcal{G}_{\text{CCC}}$ is the conformal map. This is the COMAF notation for Eq. (4).

Cycle-Bound Integral ($\oint_\Omega$): Denotes a line integral over a complete CPL, from $t = 0$ to $t = T_c$, subject to the cycle transition at the boundary:

$$\oint_\Omega f(t)\,dt \equiv \int_0^{T_c} f(t)\,dt + \hat{\Omega} \cdot [\text{boundary terms}]$$

F.5 COMAF Terminology to Physics Translation

F.6 Layer Abbreviations and Labels

Epistemic status labels used throughout the paper:

- **FC** — Formal Contribution: a novel formal artifact introduced in this paper.
- **RF** — Reframing: a known physical result expressed in QULT-C or PNMS language.
- **NI** — Novel Interpretation: a new interpretive framework applied to a known quantity.
- **SP** — Speculative Proposal: a formal consequence of the framework with no current experimental support.

COSI Stack layer abbreviations: L1–L7 refer to Layer 1 (Quantum Substrate) through Layer 7 (Cyclic Transition) as defined in Section 3.

Table 14: COMAF terminology to standard physics translation.

COMAF Term	Physics Translation	First Use
CPL (Conformal Planck Loop)	Conformal aeon (Penrose CCC)	§2
Rendering collapse	Wavefunction decoherence / state reduction	§3.5
Rendering budget	Entropic cost / Bekenstein bound	§7
Rendering tile	Planck area / Bekenstein pixel	§7
Rendering resolution	Planck-scale UV cutoff	§3.5
WarpTick	Aeonic timescale (1 CPL duration)	§5
Phase stitching	Conformal boundary matching	§3.7
Decoherence fragility	Decoherence rate (Zurek)	§3.6
Rendering budget cap	Bekenstein entropy bound	§2
CPL stability invariant	Topological integrity measure	§3.6
Planck mesh	Discrete spacetime substrate (Zuse)	§3.1
Aeonic handoff	Inter-aeon conformal boundary	§3.7

G COMAF × PNMS Layer-Unit Mapping

This appendix provides the complete mapping between COSI Stack layers, COMAF subsystems, COMAF-Lite block types, PNMS units, and governing equations. This mapping constitutes the formal interface specification between the QULT-C mathematical framework, the PNMS unit system, and the COMAF-Lite DSL.

G.1 Primary Layer-Unit-Block Mapping

Table 15: COSI Stack layer to COMAF subsystem, COMAF-Lite block, PNMS units, and governing equation mapping.

L	COSI Layer Name	COMAF Subsystem	COMAF-Lite Block	PNMS Units
7	Cyclic Transition	Aeonic Interface Layer	`ON cycle.end`	WarpTick, Entropy Tick
6	Causal Routing	Causality Kernel	`STABILITY`, `IF...warp`	Plasecond^{-1}, dimensionless
5	Rendering Control	Rendering Engine	`IF...collapse`	E_p, λ_p, dimensionless
4	Geometry Protocol	Spacetime Fabric Manager	`GEOMETRY`	Ricci-Bit, Plameter
3	Entropy Flow	Entropy Supervisor	`ENTROPY`	Entropy Tick, Plasecond
2	Wavefunction Evolution	Quantum Execution Layer	`STATE`	Plasecond, $\hbar$
1	Quantum Substrate	Substrate Control Mesh	(substrate, not DSL-addressable)	λ_p, t_p

G.2 Governing Equation by Layer

Table 16: Governing equation and key PNMS quantity for each COSI layer.

Layer	Governing Equation	Key PNMS Quantity
L7 (Cyclic Transition)	$\hat{\Omega}$, $\Phi_n(t)$	T_c in WarpTicks
L6 (Causal Routing)	$D(t) = e^{-\lvert\nabla S\rvert \cdot t}$, χ_{CPL}	$D(t)$ dimensionless
L5 (Rendering Control)	$\mathcal{F}_{\text{collapse}}(v, \Lambda)$	E_{jump} in E_p
L4 (Geometry Protocol)	$G_{\mu\nu} + \Lambda g_{\mu\nu} = \frac{8\pi G}{c^4}\langle \hat{T}_{\mu\nu}\rangle$	R in Ricci-Bits
L3 (Entropy Flow)	$S(t) = S_0 e^{-t/\tau} + S_{\max}(1 - e^{-t/\tau})$	S in Entropy Ticks
L2 (Wavefunction Evolution)	$i\hbar\partial_t\psi = \hat{H}_{\text{QULT}}\psi$	t in Plaseconds
L1 (Quantum Substrate)	Planck mesh resolution: $\Delta x \geq \lambda_p$, $\Delta t \geq t_p$	λ_p, t_p

G.3 Extended COMAF × PNMS Unit Keywords

The COMAF × PNMS Addendum extends COMAF-Lite with additional physical dimension keywords aligned with the full PNMS unit system:

Table 17: Extended COMAF-Lite keywords from the COMAF × PNMS Addendum.

Keyword	Physical Quantity	PNMS Unit	COSI Layer	SI Equivalent
`FORCE`	Force	PlaNewton	L4, L5	≈ 1 N
`POWER`	Power	PlaWatt	L5, L3	≈ 1 W
`PRESSURE`	Pressure	PlaPascal	L4	≈ 1 Pa
`CURVATURE`	Spacetime curvature	Ricci-Bit	L4	λ_p^{-2}
`ENTROPY_UNIT`	Entropy	Entropy Tick	L3, L7	k_B
`CHARGE`	Electric charge	Planck Charge (q_p)	L2, L1	1.876×10^{-18} C
`UNCERTAINTY`	Heisenberg uncertainty	$\hbar/2$	L2	5.27×10^{-35} J s

G.4 COMAF Subsystem Architecture

Each COMAF subsystem corresponds to one COSI Stack layer and contains the following modules:

L7 — Aeonic Interface Layer: CPL-Orchestrator, WarpTick Scheduler, Entropy-Reset Handler, Phase-Stitch Manager.

L6 — Causality Kernel: Decoherence Failover Engine, Causal Loop Monitor (χ_{CPL}), Warp Routing Table, Distance Scaling Manager.

L5 — Rendering Engine: Collapse Function Handler ($\mathcal{F}_{\mathrm{collapse}}$), Resolution Monitor, Hawking Radiation Emitter.

L4 — Spacetime Fabric Manager: Spacetime Voxelizer, Ricci-Thrust Calculator, Λ-Tension Manager.

L3 — Entropy Supervisor: Entropy Load Balancer, Noether Charge Tracker (Q_S), Entropy Routing Protocol.

L2 — Quantum Execution Layer: Schrödinger Solver, Hamiltonian Compiler, Quantum-State Router.

L1 — Substrate Control Mesh: Planck Mesh Manager, Tick Scheduler (t_p resolution), Holographic Tile Allocator.

G.5 Layer Interface Contracts

Each inter-layer interface in the COSI Stack is defined by the quantities passed from one layer to the next:

Table 18: Inter-layer interface contracts (upward pass).

From Layer	To Layer	Quantity Passed
L1 (Substrate)	L2 (Wavefunction)	Discrete metric; minimum tick t_p
L2 (Wavefunction)	L3 (Entropy)	Probability density $\lvert\psi\rvert^2$
L3 (Entropy)	L4 (Geometry)	Entropy scalar $S(t)$; Noether charge Q_S
L3 (Entropy)	L6 (Causal Routing)	Entropy gradient $\lvert\nabla S\rvert$
L4 (Geometry)	L5 (Rendering)	Curvature scalar R
L4 (Geometry)	L6 (Causal Routing)	Curvature R; effective velocity v
L5 (Rendering)	L7 (Cyclic Transition)	Collapse trigger flag; E_{jump}
L6 (Causal Routing)	L7 (Cyclic Transition)	Health invariant χ_{CPL}; $D(t)$